Principles and Basics of Pol-InSAR

Irena Hajnsek
*Earth Observation and Remote Sensing,
Institute of Environmental Engineering, ETH Zürich
*Microwaves and Radar Institut,
German Aerospace Center, Oberpfaffenhofen

Earth Observation and Remote Sensing

hajnsek@ifu.baug.ethz.ch
irena.hajnsek@dlr.de

ETH
Eidgenössische Technische Hochschule Zürich
Swiss Federal Institute of Technology Zurich

SAR Polarimetry (PolSAR)

Allows the identification / decomposition of different scattering processes occurring inside the resolution cell

SAR Interferometry (InSAR)

Allows the location of the effective scattering center inside the resolution cell

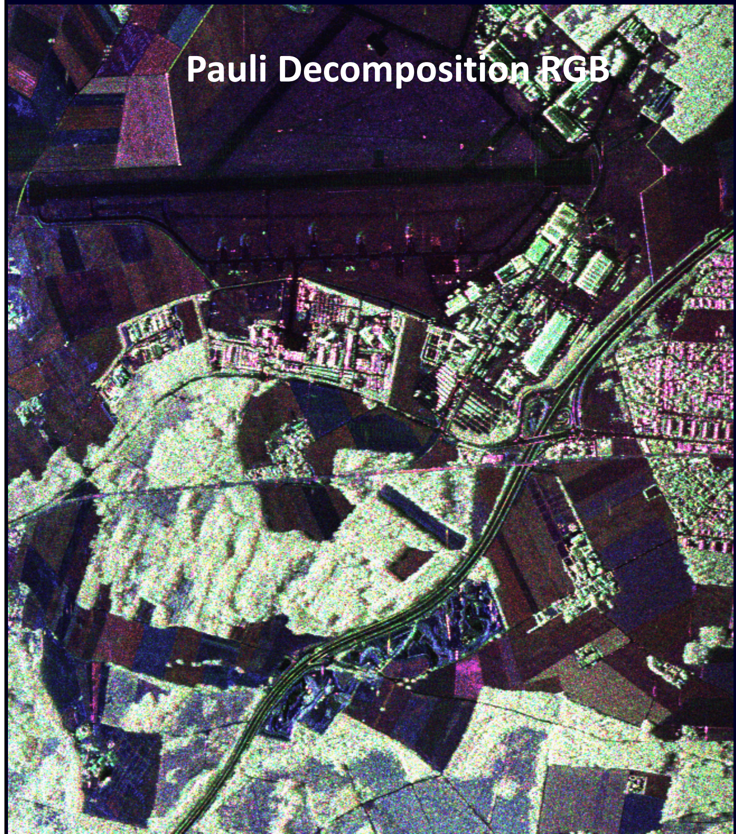

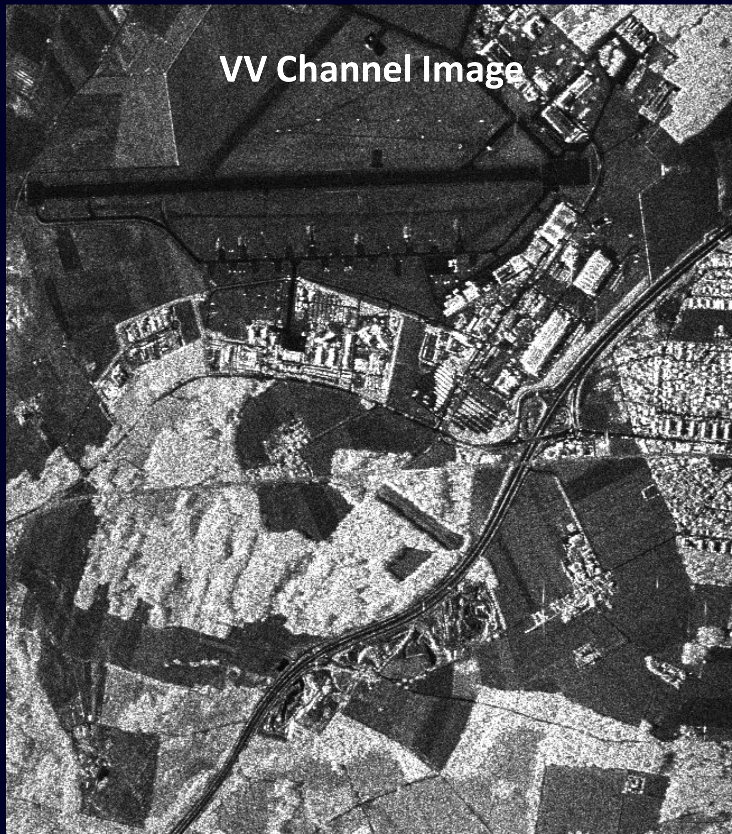

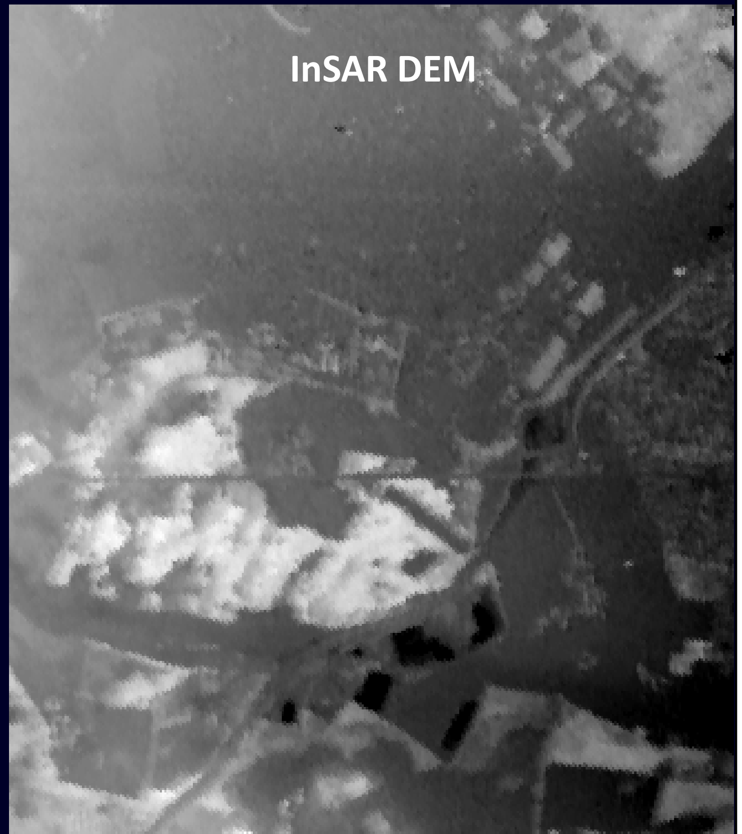

Polarimetric SAR Interferometry (Pol-InSAR)

Potential to separate in height different scattering processes occurring inside the resolution cell

Interferometry vs. Polarimetry

$$S^1_{HH} = A^1_D + A^1_S$$

$$S^2_{HH} = A^2_D + A^2_S$$

$$\varphi = \arg\{\, S^1_{HH} \;\; S^{2*}_{HH} \,\}$$

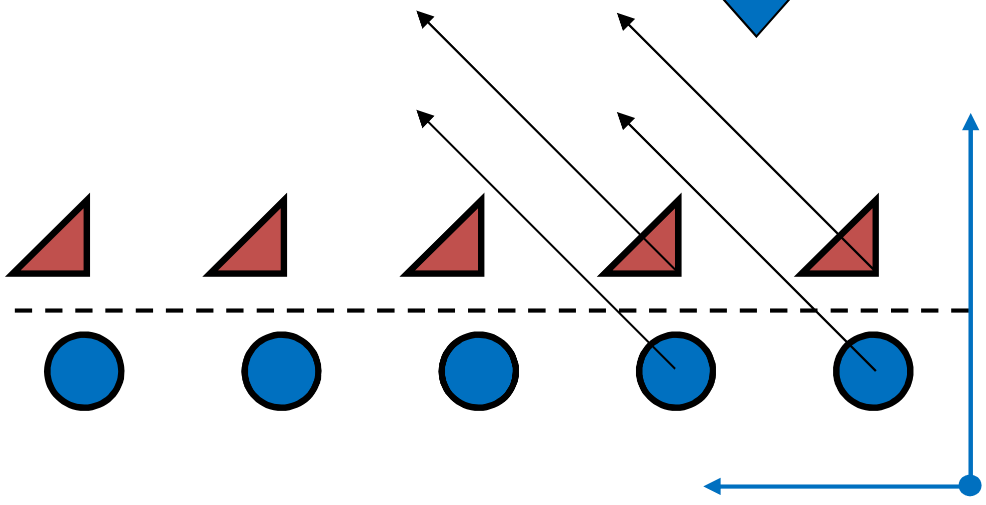

$$[S_D] = A_D \begin{bmatrix} 1 & 0 \\ 0 & -1 \end{bmatrix}$$ Dihedral Reflector

$$[S_S] = A_S \begin{bmatrix} 1 & 0 \\ 0 & 1 \end{bmatrix}$$ Sphere or Triedral Reflector

$$S_{HH} + S_{VV} = 2A_S$$

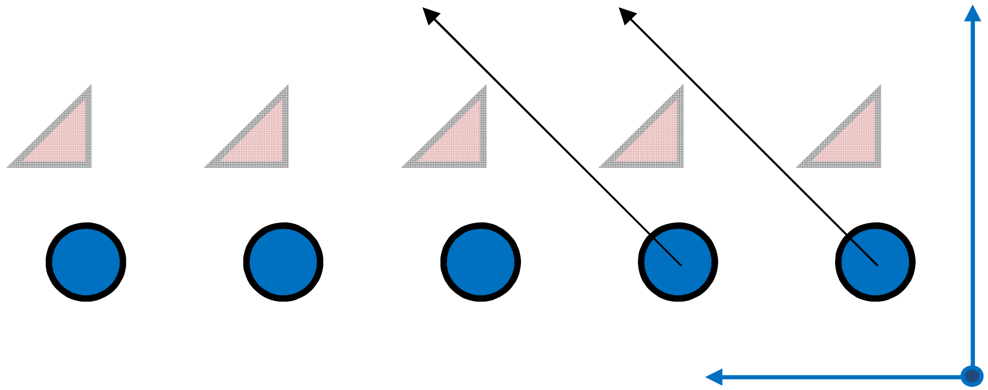

$$S_{HH} - S_{VV} = 2A_D$$

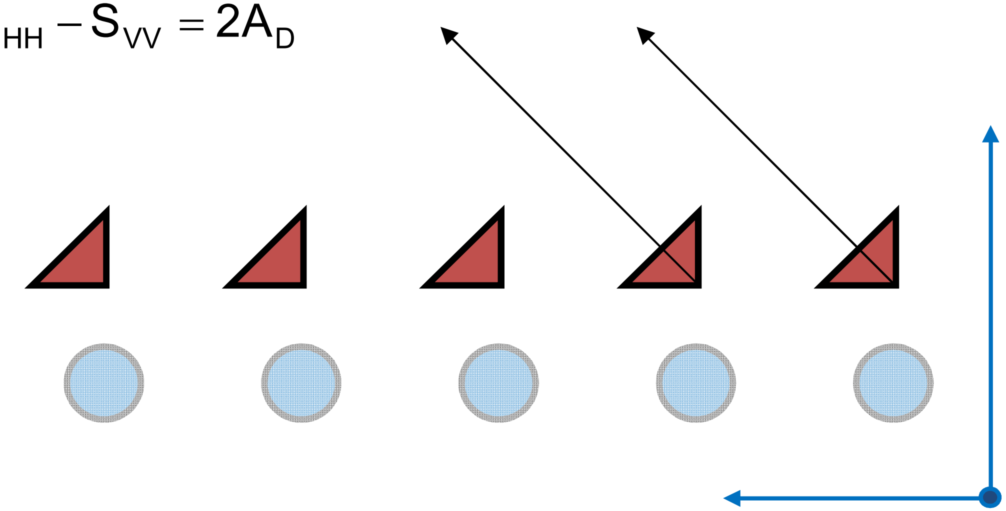

hajnsek@ifu.baug.ethz.ch
irena.hajnsek@dlr.de

Polarimetric Interferometry

$$i_{1S} = S_{HH}^{1} + S_{VV}^{1} = 2A_{S}^{1}$$

$$i_{2S} = S_{HH}^{2} + S_{VV}^{2} = 2A_{S}^{2}$$

$$\varphi_{S} = \arg\{\, i_{1S} \; i_{2S}^{*} \,\}$$

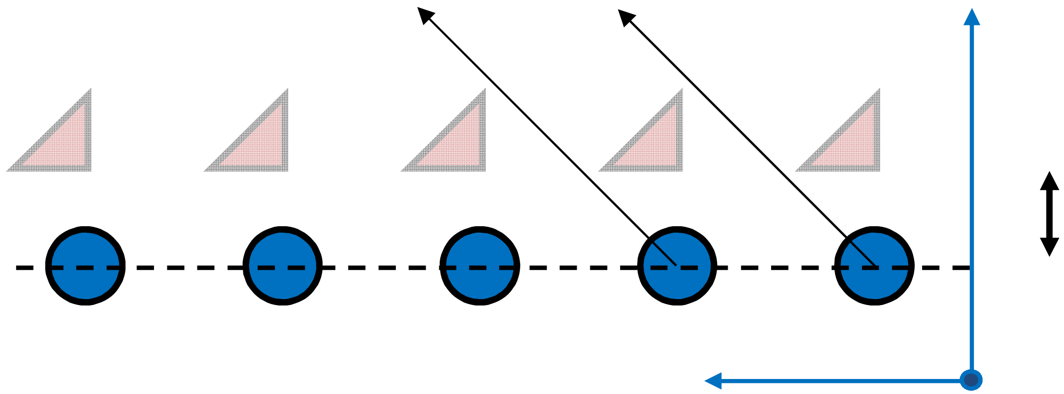

$$i_{1D} = S_{HH}^{1} - S_{VV}^{1} = 2A_{D}^{1}$$

$$i_{2D} = S_{HH}^{2} - S_{VV}^{2} = 2A_{D}^{2}$$

$$\varphi_{D} = \arg\{\, i_{1D} \; i_{2D}^{*} \,\}$$

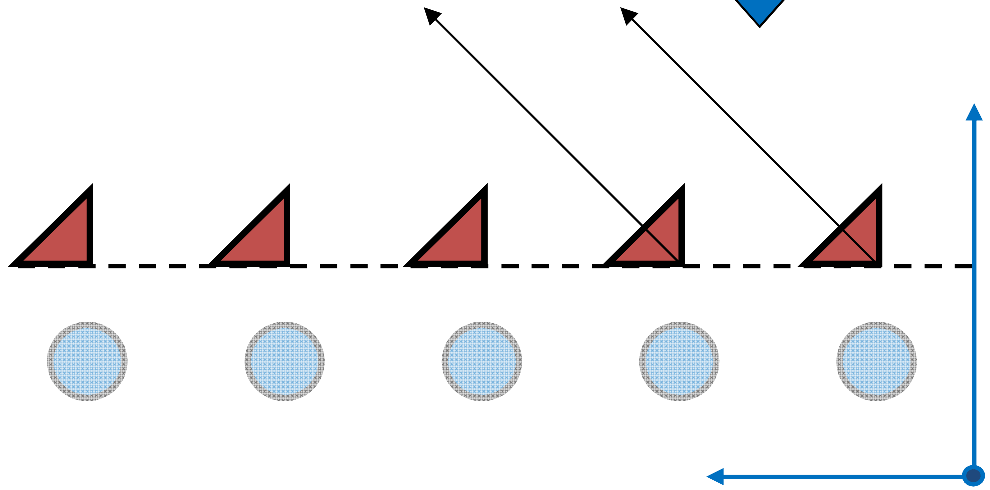

$$[S_{D}] = A_{D}\begin{bmatrix} 1 & 0 \\ 0 & -1 \end{bmatrix}$$ Dihedral Reflector

$$[S_{S}] = A_{S}\begin{bmatrix} 1 & 0 \\ 0 & 1 \end{bmatrix}$$ Sphere or Triedral Reflector

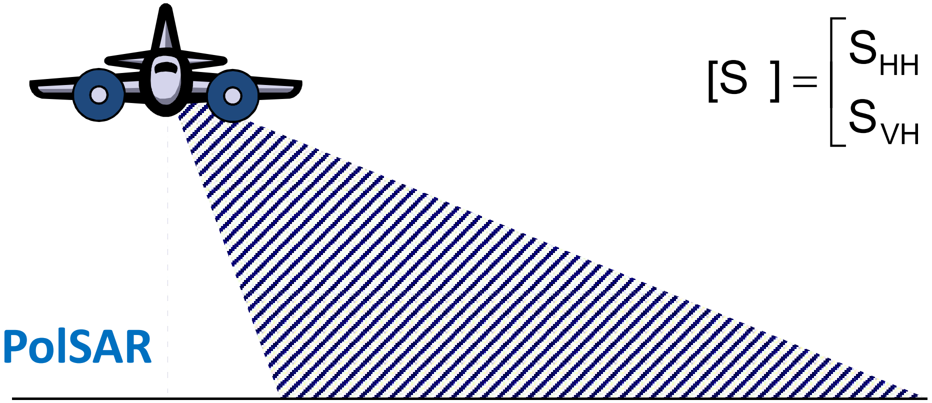

PolSAR

$$[S] = \begin{bmatrix} S_{HH} & S_{HV} \\ S_{VH} & S_{VV} \end{bmatrix}$$

Polarimetric Coherences

$$\tilde{\gamma}(S_{ij}\ S_{mn}) = \frac{< S_{ij}\ S_{mn}^{*} >}{\sqrt{< S_{ij}\ S_{ij}^{*} > < S_{mn}\ S_{mn}^{*} >}}$$

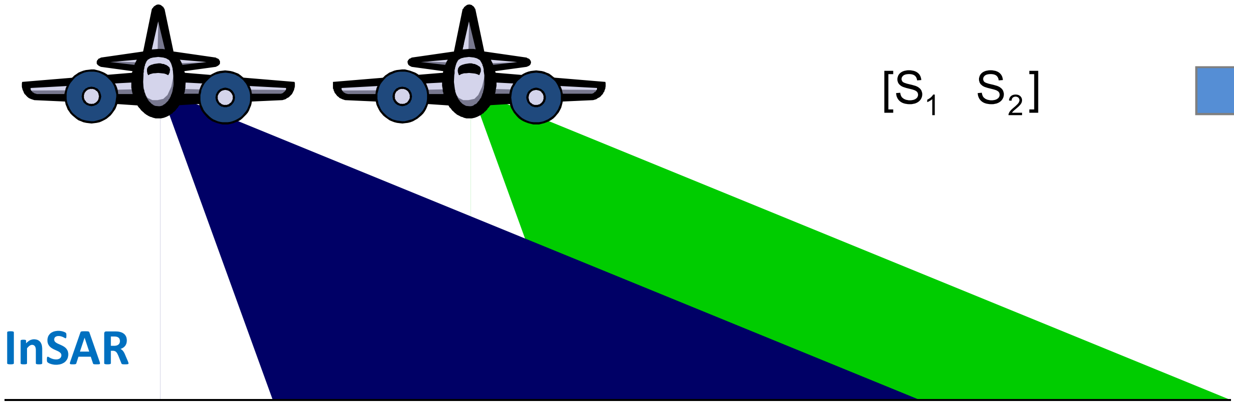

InSAR

$$[S_1 \quad S_2]$$

Interferometric Coherences

$$\tilde{\gamma}(S_1\ S_2) = \frac{< S_1\ S_2^{*} >}{\sqrt{< S_1\ S_1^{*} > < S_2\ S_2^{*} >}}$$

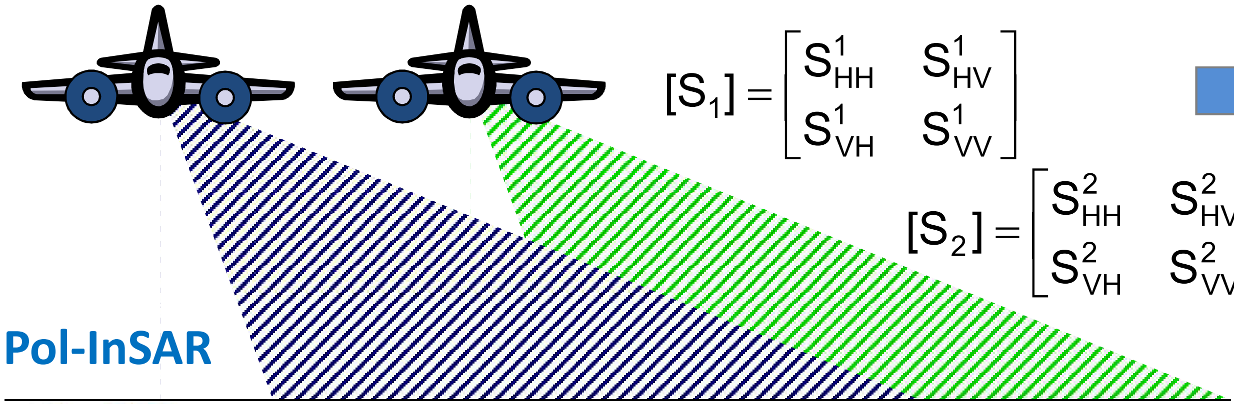

Pol-InSAR

$$[S_1] = \begin{bmatrix} S_{HH}^1 & S_{HV}^1 \\ S_{VH}^1 & S_{VV}^1 \end{bmatrix}$$

$$[S_2] = \begin{bmatrix} S_{HH}^2 & S_{HV}^2 \\ S_{VH}^2 & S_{VV}^2 \end{bmatrix}$$

Polarimetric / Interferometric Coherences

$$\tilde{\gamma}(S_{ij}^1\ S_{mn}^2) = \frac{< S_{ij}^1\ S_{mn}^{2\ *} >}{\sqrt{< S_{ij}^1\ S_{ij}^{1*} > < S_{mn}^2\ S_{mn}^{2\ *} >}}$$

Complex Coherences on the Unit Circle

$$\tilde{\gamma} := \frac{\sum_{k=1}^{N} S_1(k) S_2^*(k)}{\sqrt{\sum_{k=1}^{N} S_1(k) S_1^*(k) \sum_{k=1}^{N} S_2(k) S_2^*(k) >}} = \exp(i \ \mathrm{Arg}(\tilde{\gamma}) \ ) \cdot |\tilde{\gamma}|$$

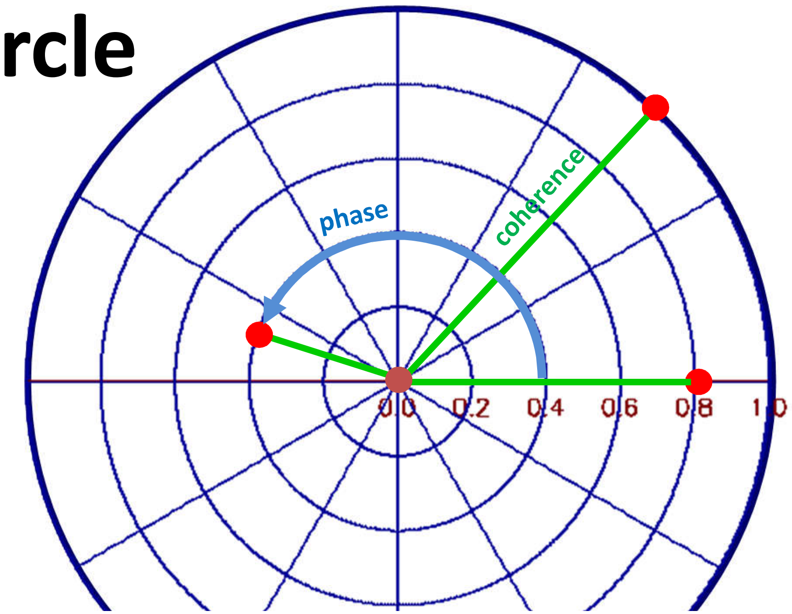

Correlation Coefficient	$0 \leq |\tilde{\gamma}| = \gamma \leq 1$
Interferometric Phase	$0 \leq \mathrm{Arg}(\tilde{\gamma}) = \varphi \leq 2\pi$

Cramer Rao Bounds:

(expresses the lower bound on the variance of the estimator):

Correlation Coefficient $\quad \mathrm{VAR}(|\tilde{\gamma}|)_{CR} = \frac{(1-|\gamma|^2)^2}{2N}$

Interferometric Phase $\quad \mathrm{VAR}(\varphi)_{CR} = \frac{1-|\gamma|^2}{2N|\gamma|^2}$

$\varphi = \arg(\tilde{\gamma})$ **and N is the number of Looks**

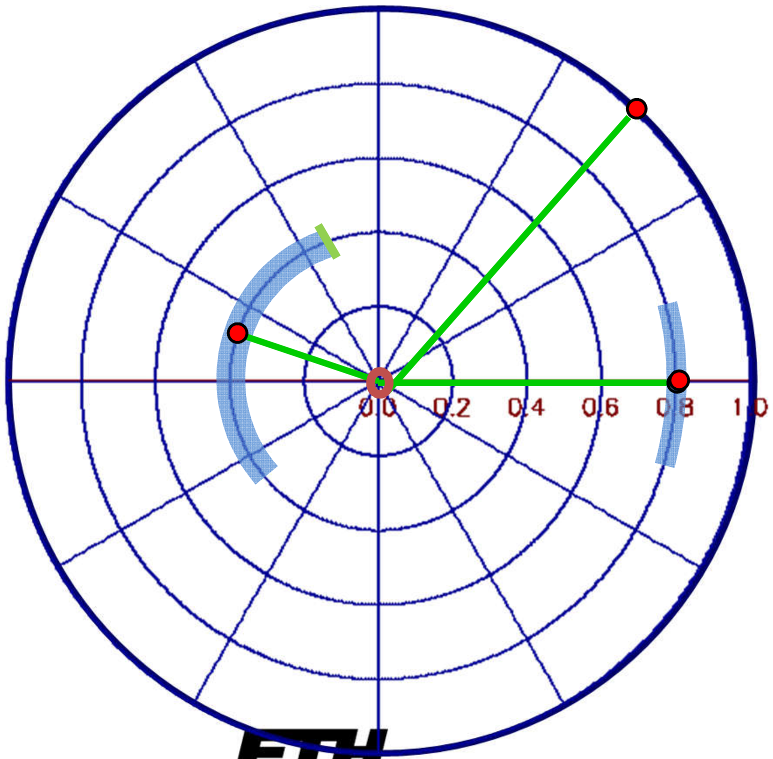

hajnsek@ifu.baug.ethz.ch
irena.hajnsek@dlr.de

Why is Interferometry important for Volume Scatterers?

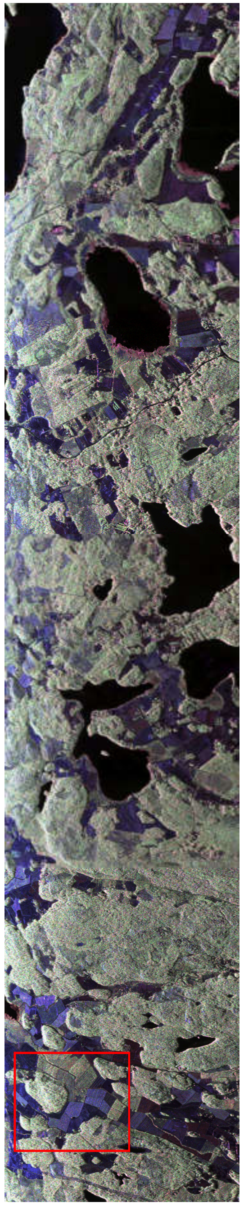

E-SAR / Test Site: Helsinki, Finland

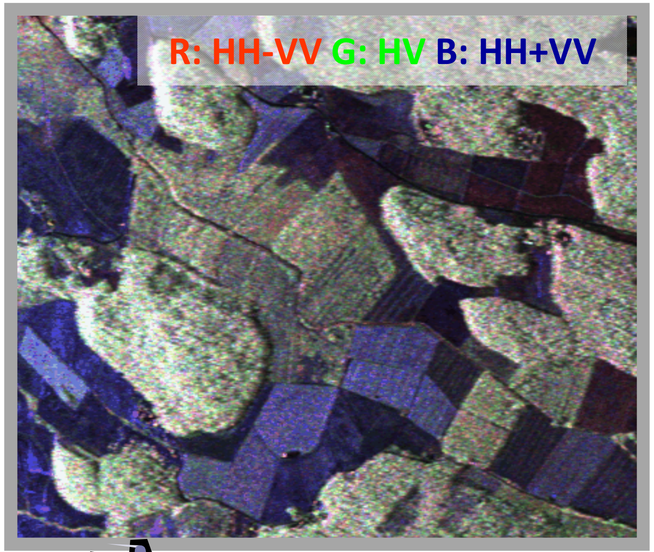

HH-VV Coherence

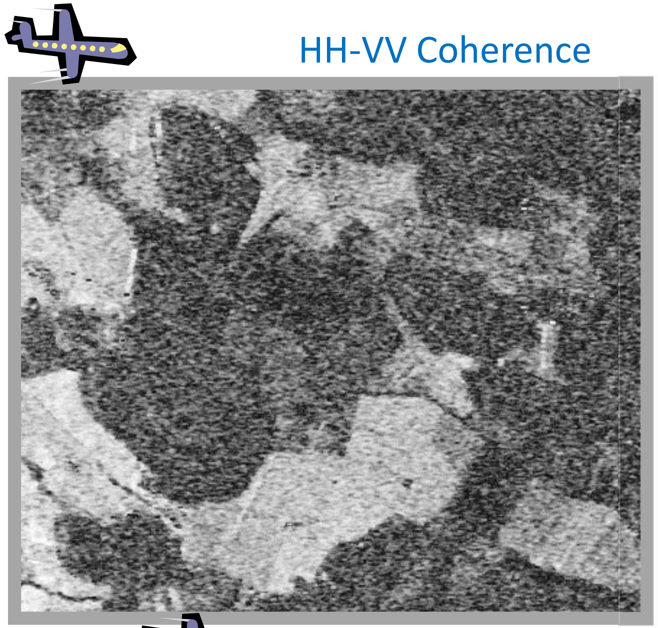

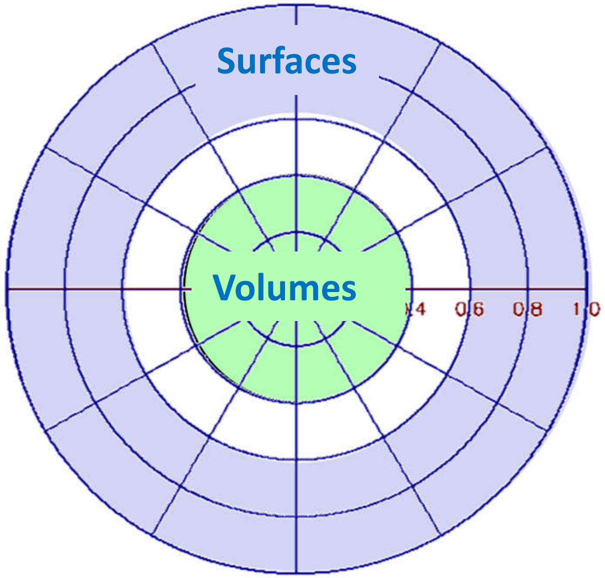

HH-HH Coherence

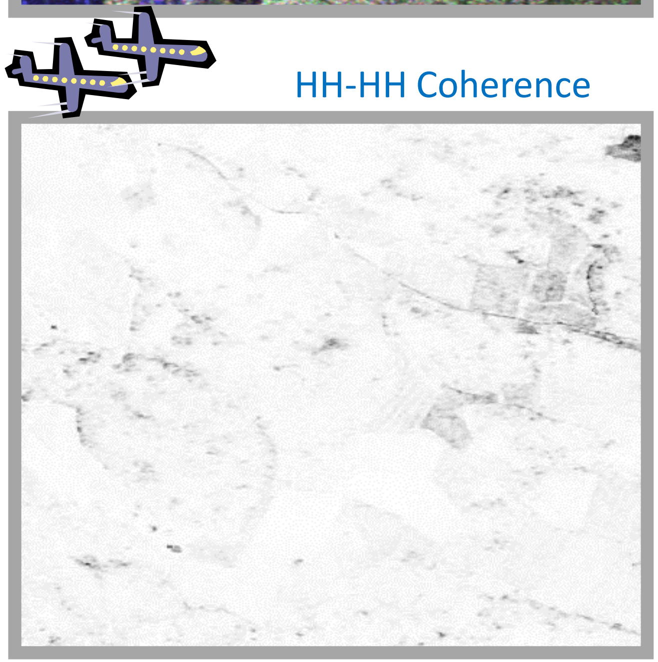

HH-HH Coherence

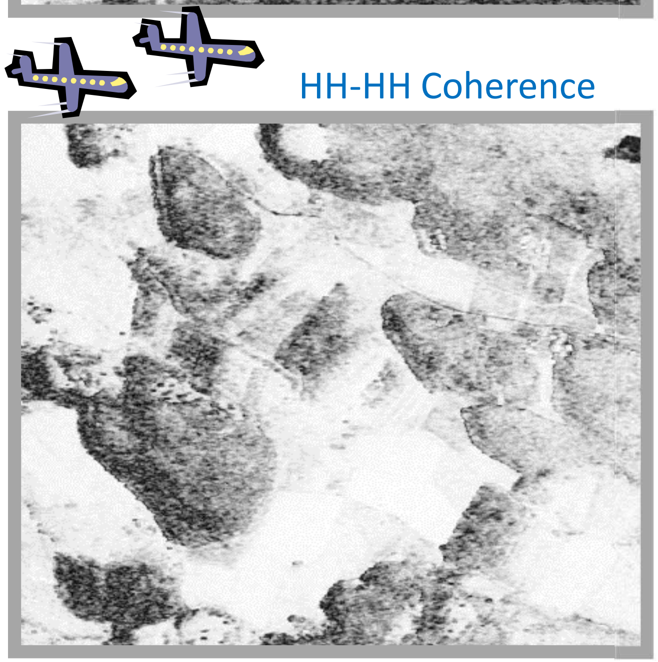

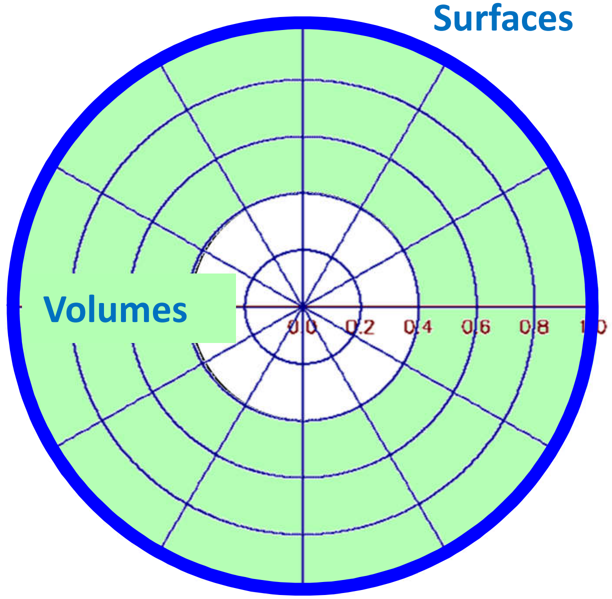

hajnsek@ifu.baug.ethz.ch
irena.hajnsek@dlr.de

ETH
Eidgenössische Technische Hochschule Zürich
Swiss Federal Institute of Technology Zurich

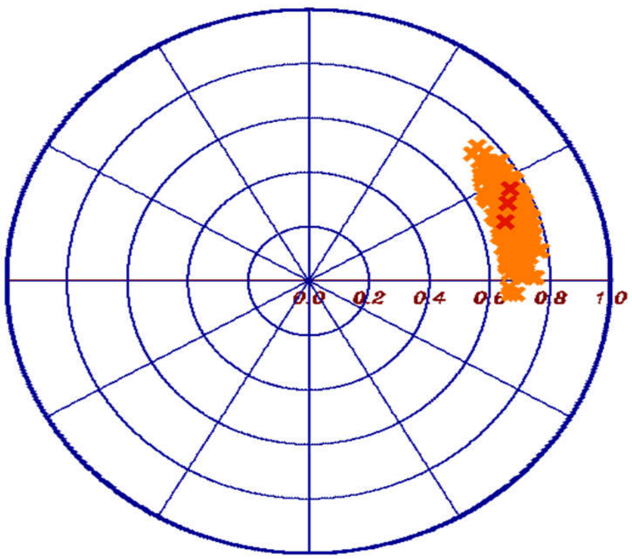

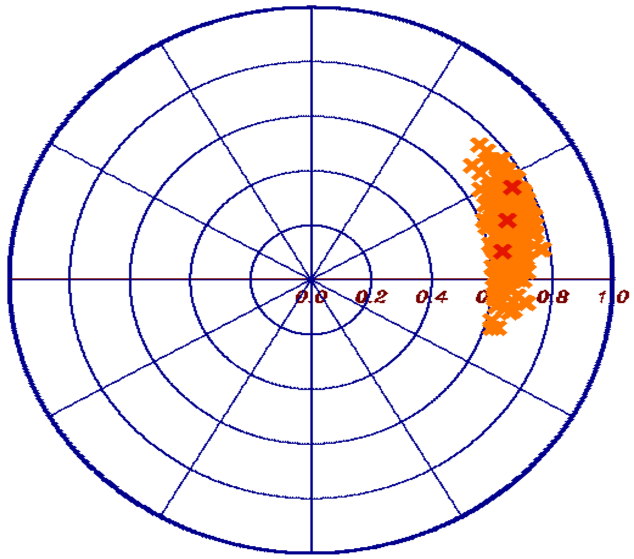

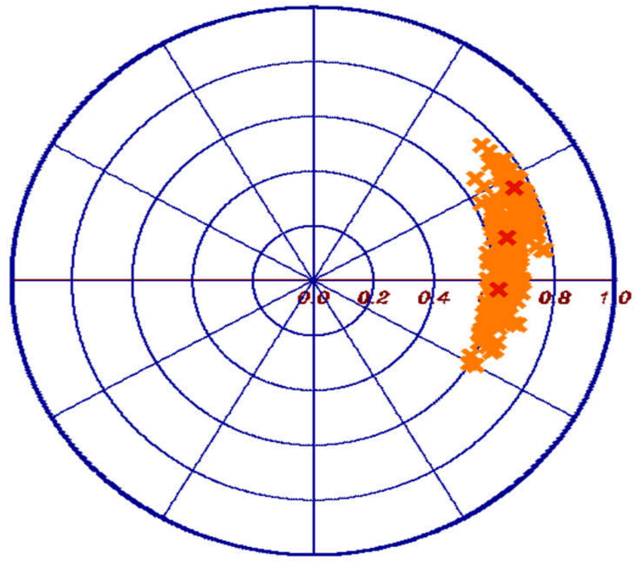

Pol-InSAR: Basic Principles & Ideas

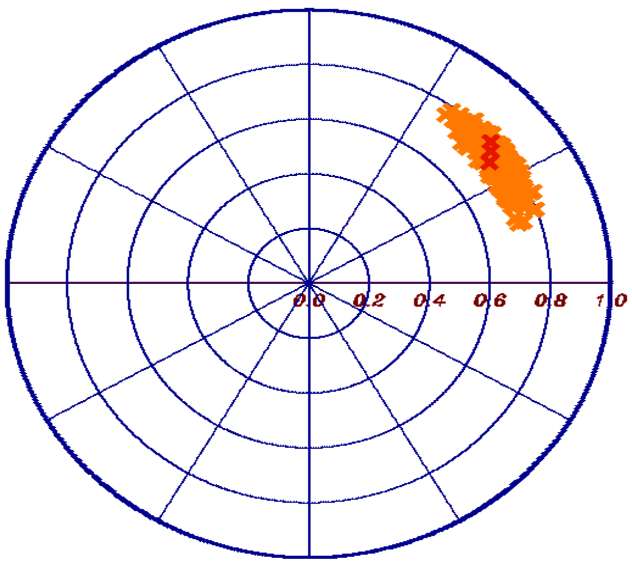

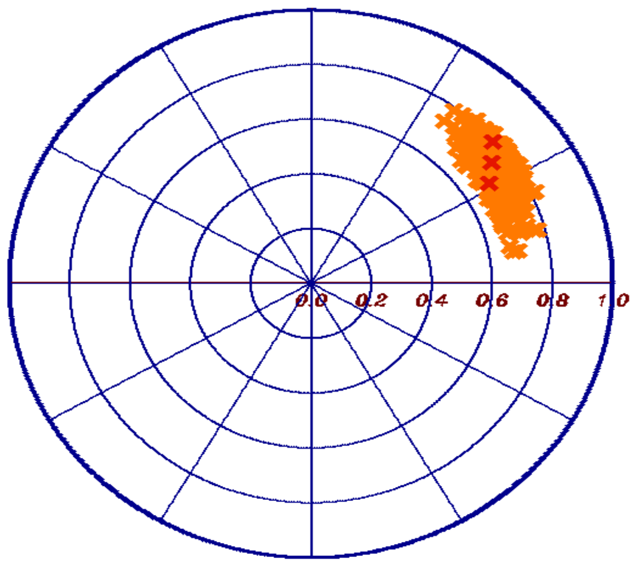

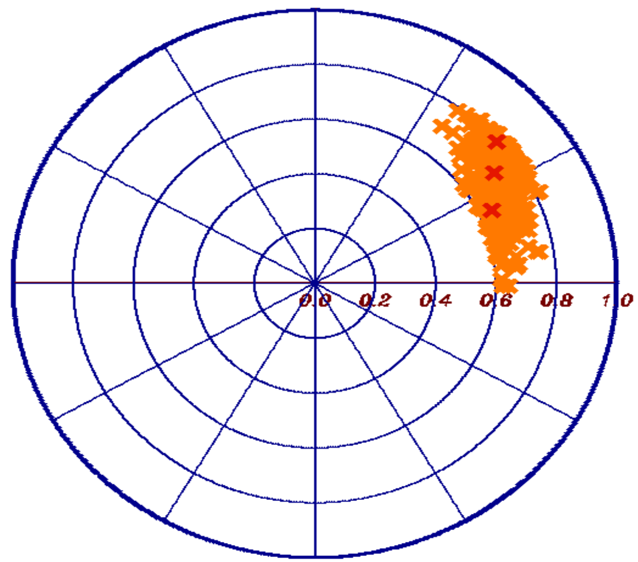

hajnsek@ifu.baug.ethz.ch
irena.hajnsek@dlr.de

SAR Interferometry for Volume Structure

S_1 S_2

Interferometric Coherence

$$\tilde{\gamma}(S_1\, S_2) = \frac{< S_1\, S_2^* >}{\sqrt{< S_1\, S_1^* > < S_2\, S_2^* >}}$$

Volume Coherence

$$\tilde{\gamma}_{Vol}(f(z),k_z) = e^{ik_z z_o} \frac{\int_o^{h_V} f(z)\, e^{ik_z z} dz}{\int_o^{h_V} f(z)\, dz}$$

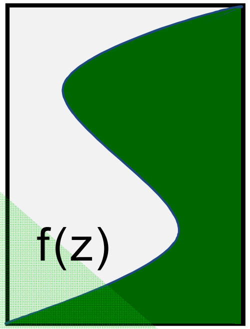

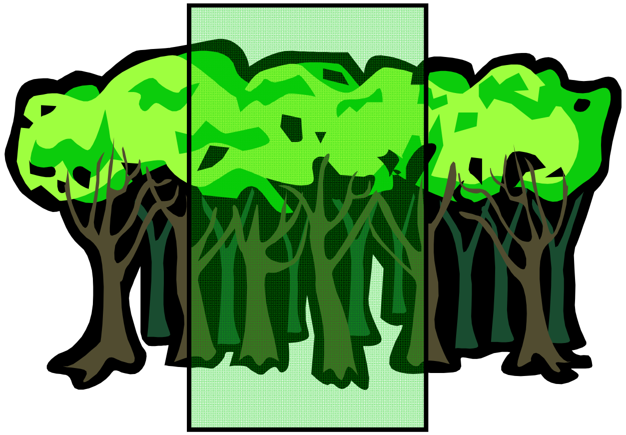

$f(z)$ ... vertical reflectivity function

Vertical Wavenumber: $\kappa_z = \frac{\kappa \Delta\theta}{\sin(\theta_0)}$

$$\tilde{\gamma} = \tilde{\gamma}_{Temporal}\ \gamma_{SNR}\ \tilde{\gamma}_{Vol}$$

- $\tilde{\gamma}_{Temporal}$ ... temporal decorrelation
- γ_{SNR} ... additive noise decorrelation
- $\tilde{\gamma}_{Volume}$ ... geometric decorrelation

S_1 S_2

Interferometric Coherence

$$\tilde{\gamma}(S_1\ S_2) = \frac{\langle S_1\ S_2^* \rangle}{\sqrt{\langle S_1\ S_1^* \rangle \langle S_2\ S_2^* \rangle}}$$

SAR Interferometry for Volume Structure

Volume Coherence

$$\tilde{\gamma}_{Vol}(f(z),k_z) = e^{ik_z z_o} \frac{\int_o^{h_v} f(z)\ e^{ik_z z} dz}{\int_o^{h_v} f(z)\ dz}$$

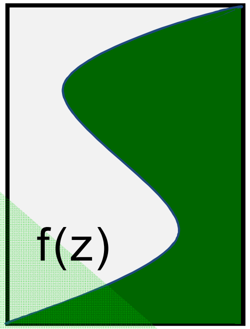

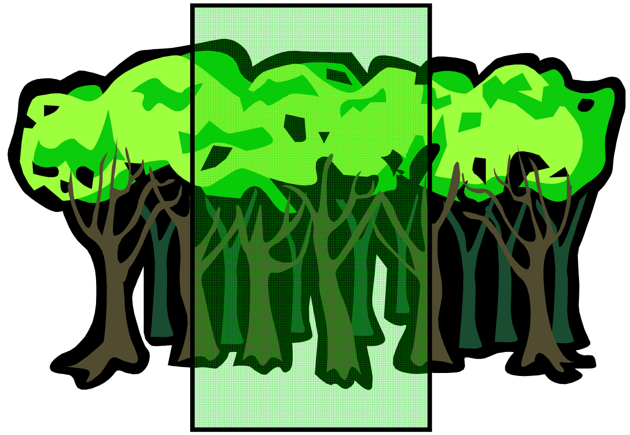

$f(z)$ ... vertical reflectivity function

Vertical Wavenumber: $\kappa_z = \dfrac{\kappa\Delta\theta}{\sin(\theta_0)}$

$$\tilde{\gamma} = \tilde{\gamma}_{Temporal}\ \gamma_{SNR}\ \tilde{\gamma}_{Vol}$$

- $\tilde{\gamma}_{Temporal}$ ... temporal decorrelation
- γ_{SNR} ... additive noise decorrelation
- $\tilde{\gamma}_{Volume}$ ... geometric decorrelation

SAR interferometry allows to reconstruct the vertical reflectivity function f(z) of a volume scatterer by means of interferometric (volume) coherence measurements at different vertical wavenumbers κ_z, i.e. at different spatial baselines.

Normalised Fourier Transform of
the vertical reflectivity function f(z)

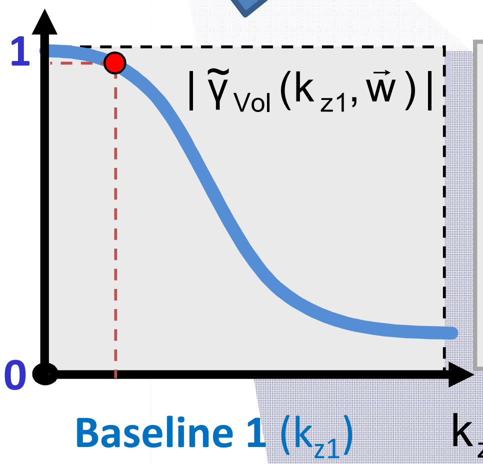

$$\tilde{\gamma}_{Vol}(k_{z1}) = e^{ik_{z1}z_o} \frac{\int_o^{h_v} f(z)\, e^{ik_{z1}z} dz}{\int_o^{h_v} f(z)\, dz}$$

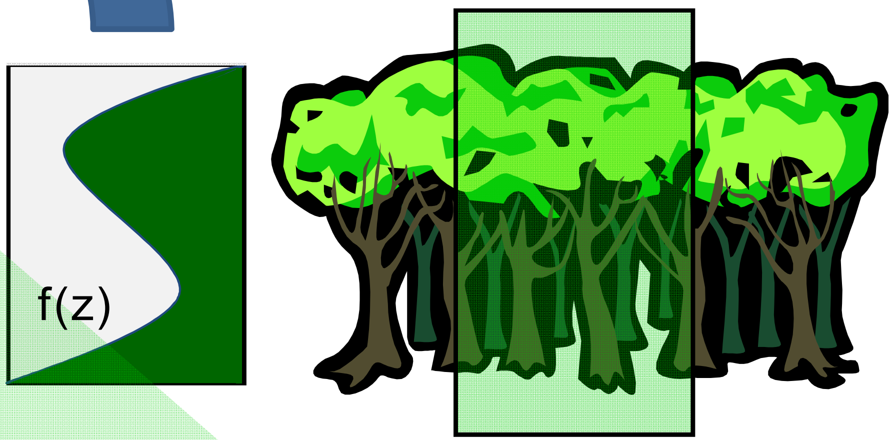

f(z) … vertical reflectivity function

Vertical Wavenumber: $\kappa_z = \dfrac{\kappa\Delta\theta}{\sin(\theta_0)}$

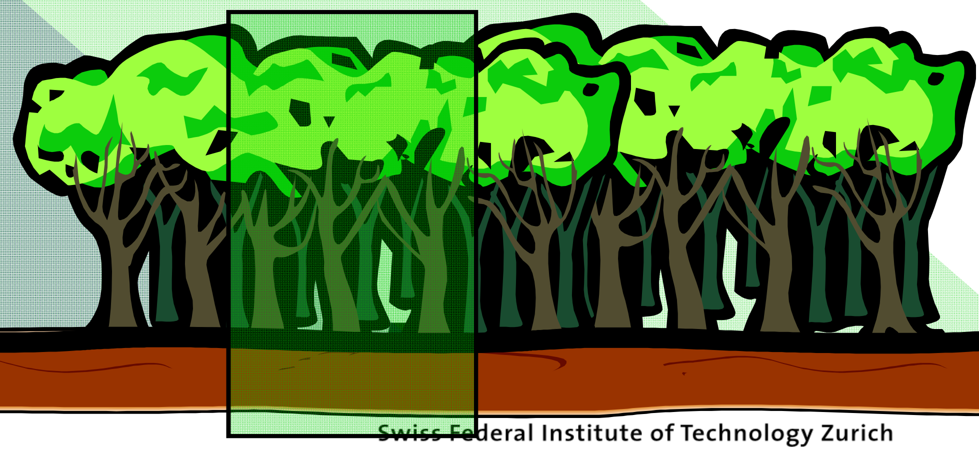

Mult ine SAR Inte etry

Multibaseline SAR Interferometry

Baseline 3 (k_{z3})

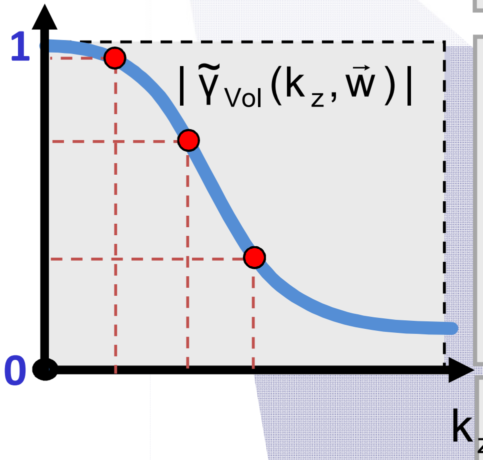

Baseline 2 (k_{z2})

$$\tilde{\gamma}_{Vol}(k_{z3}) = e^{ik_z z_o} \frac{\int_o^{h_v} f(z)\, e^{ik_{z3} z} dz}{\int_o^{h_v} f(z)\, dz}$$

$$\tilde{\gamma}_{Vol}(k_{z1}) = e^{ik_{z1} z_o} \frac{\int_o^{h_v} f(z)\, e^{ik_{z1} z} dz}{\int_o^{h_v} f(z)\, dz}$$

$$\tilde{\gamma}_{Vol}(k_{z2}) = e^{ik_z z_o} \frac{\int_o^{h_v} f(z)\, e^{ik_{z2} z} dz}{\int_o^{h_v} f(z)\, dz}$$

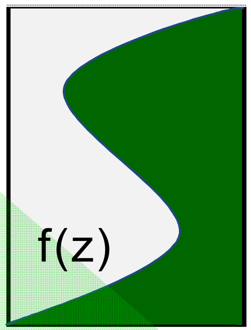

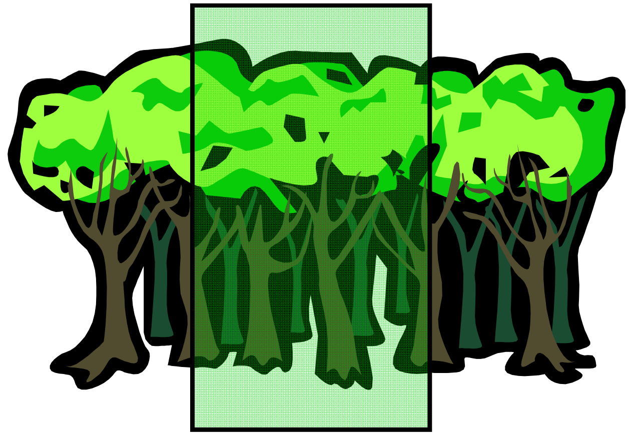

f(z) … vertical reflectivity function

Vertical Wavenumber: $\kappa_z = \frac{\kappa \Delta\theta}{\sin(\theta_0)}$

Multi-baseline measurements allow to sample **the spectrum of the vertical reflectivity** FT{f(z)} @ **different spatial baselines** (i.e. spatial frequencies) k_z**.**

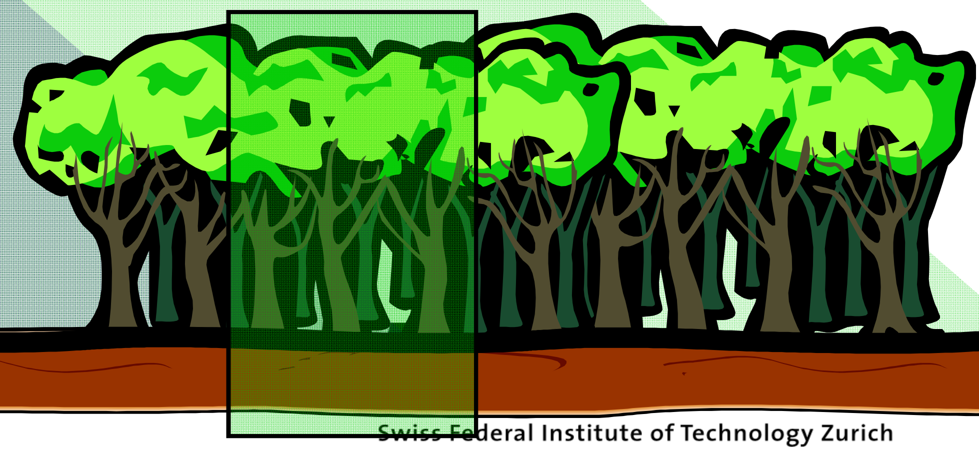

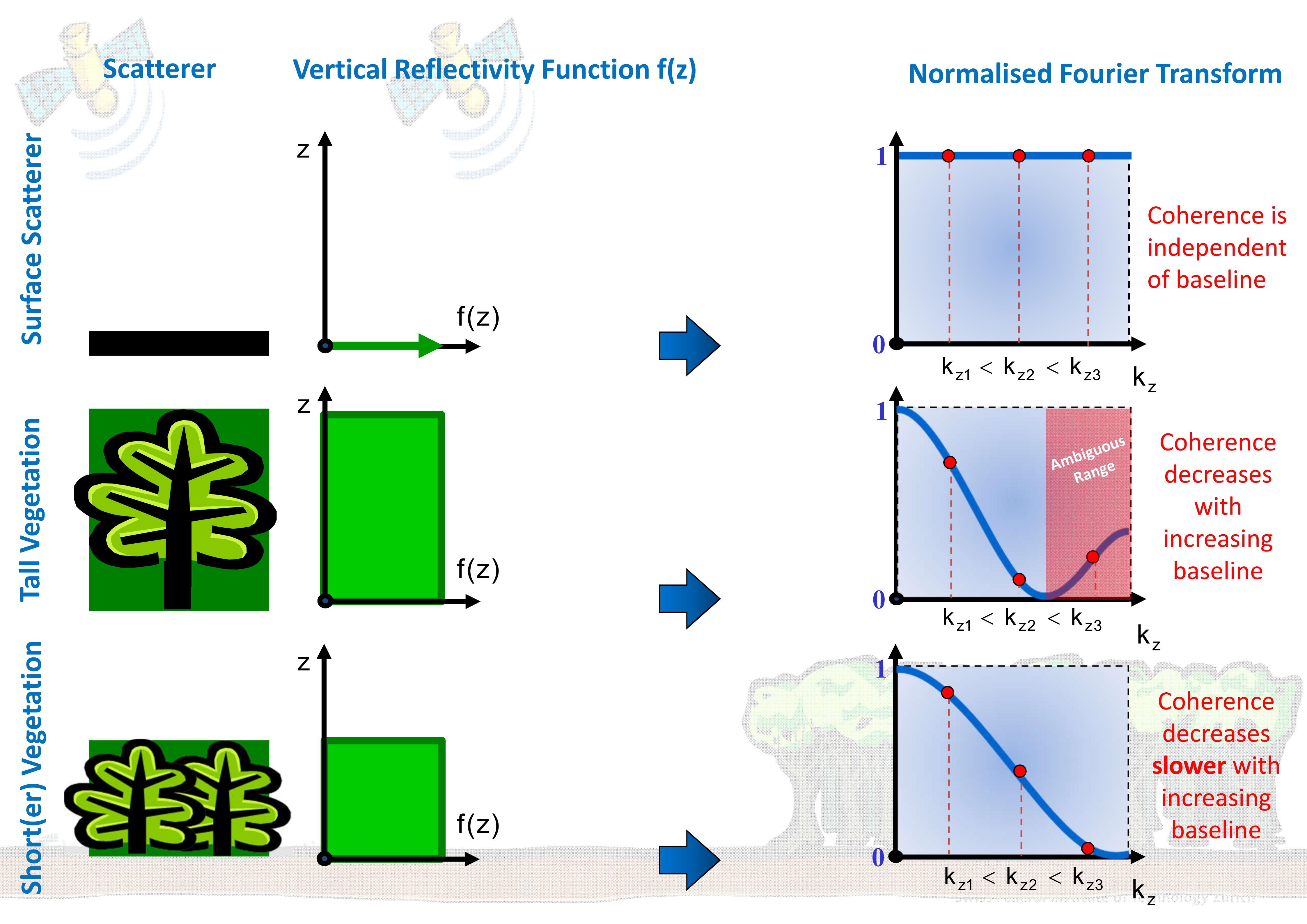

Scatterer
Vertical Reflectivity Function f(z)
Normalised Fourier Transform
Surface Scatterer
Tall Vegetation
Short(er) Vegetation
z
f(z)
1
0
$k_{z1} < k_{z2} < k_{z3}$
k_z
Coherence is independent of baseline
Ambiguous Range
Coherence decreases with increasing baseline
Coherence decreases **slower** with increasing baseline

Amplitude Image

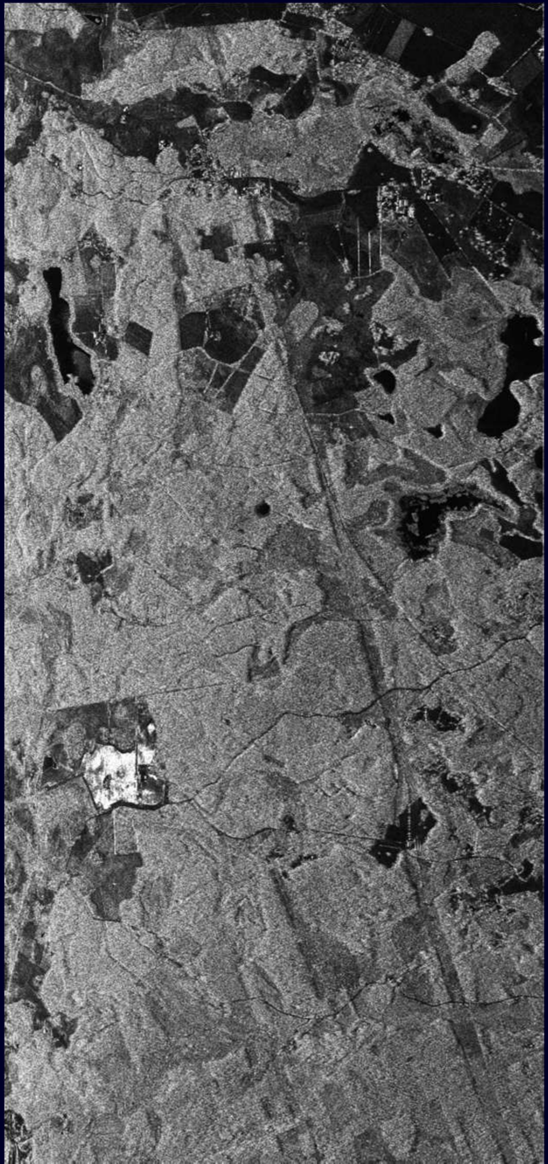

Interferometric Coherence: Volume Decorrelation

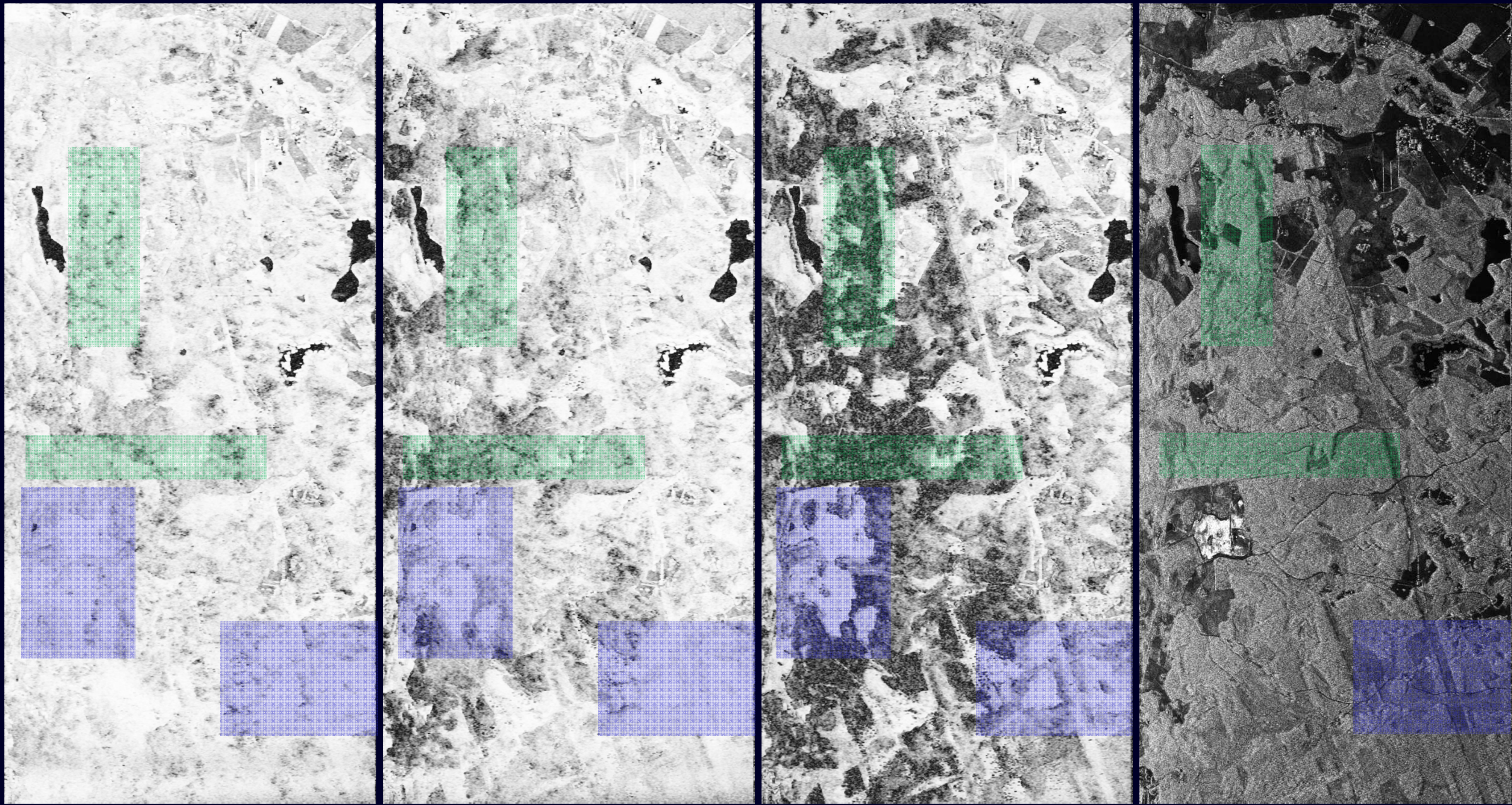

Spatial Baseline 3m **8m** **16m** **24m**

Polarimetric SAR Interferometry

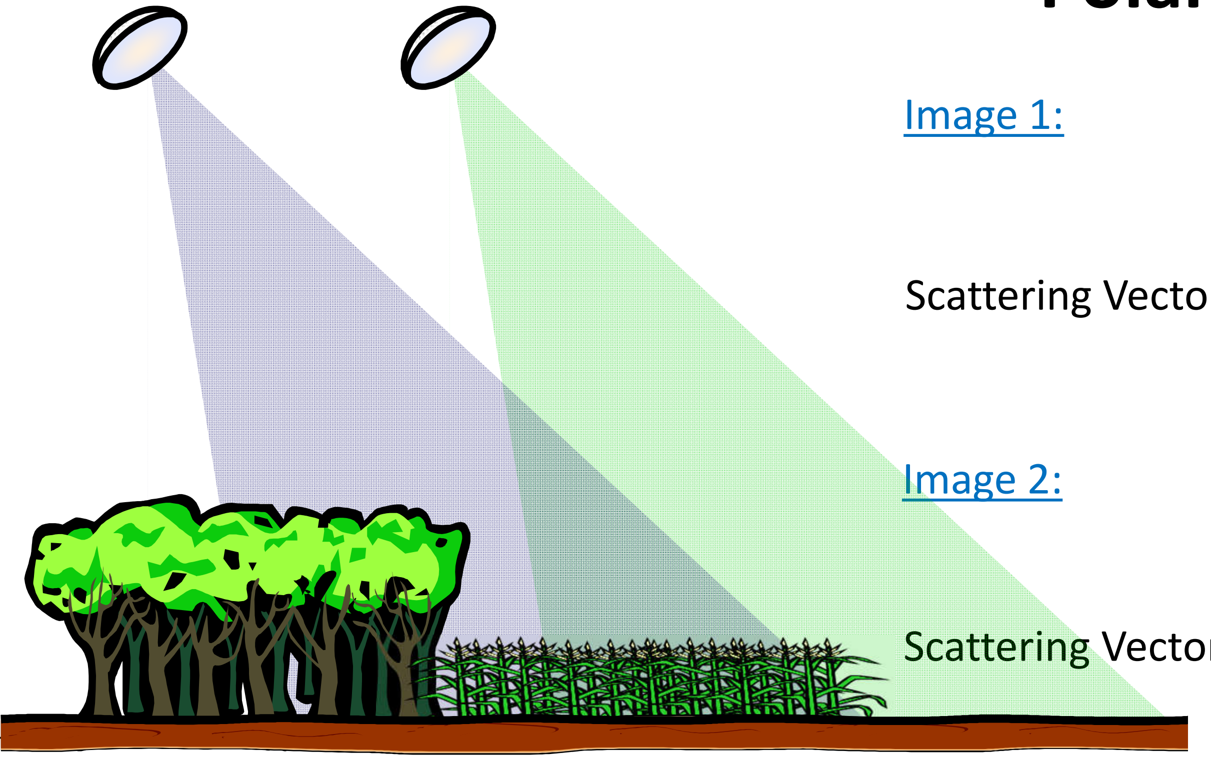

Image 1: Scattering Matrix: $[S_1] = \begin{bmatrix} S^1_{HH} & S^1_{HV} \\ S^1_{VH} & S^1_{VV} \end{bmatrix}$

Scattering Vector 1: $\vec{k}_1 = \frac{1}{\sqrt{2}}[S^1_{HH} + S^1_{VV} \quad S^1_{HH} - S^1_{VV} \quad 2S^1_{HV}]^T$

Image 2: Scattering Matrix: $[S_2] = \begin{bmatrix} S^2_{HH} & S^2_{HV} \\ S^2_{VH} & S^2_{VV} \end{bmatrix}$

Scattering Vector 2: $\vec{k}_2 = \frac{1}{\sqrt{2}}[S^2_{HH} + S^2_{VV} \quad S^2_{HH} - S^2_{VV} \quad 2S^2_{HV}]^T$

Image formation: $i_1 = \vec{w}_1^+ \cdot \vec{k}_1$ and $i_2 = \vec{w}_2^+ \cdot \vec{k}_2$ … projection of the scattering vector on a (complex) unitary vector $\vec{w}_i$

$\vec{w}_i$ used to select a given polarisation out of all possible polarisations provided by the scattering matrix [S]

Example: $S_{HH} + S_{VV}$ image: $\vec{w} = [1 \quad 0 \quad 0]^T \rightarrow i = \vec{w}^+ \cdot \vec{k}_j = \frac{1}{\sqrt{2}}(S^j_{HH} + S^j_{VV})$

S_{HH} image: $\vec{w}_1 = [1/\sqrt{2} \quad 1/\sqrt{2} \quad 0]^T \rightarrow i_j = \vec{w}^+ \cdot \vec{k}_j = S^j_{HH}$

Polarimetric SAR Interferometry

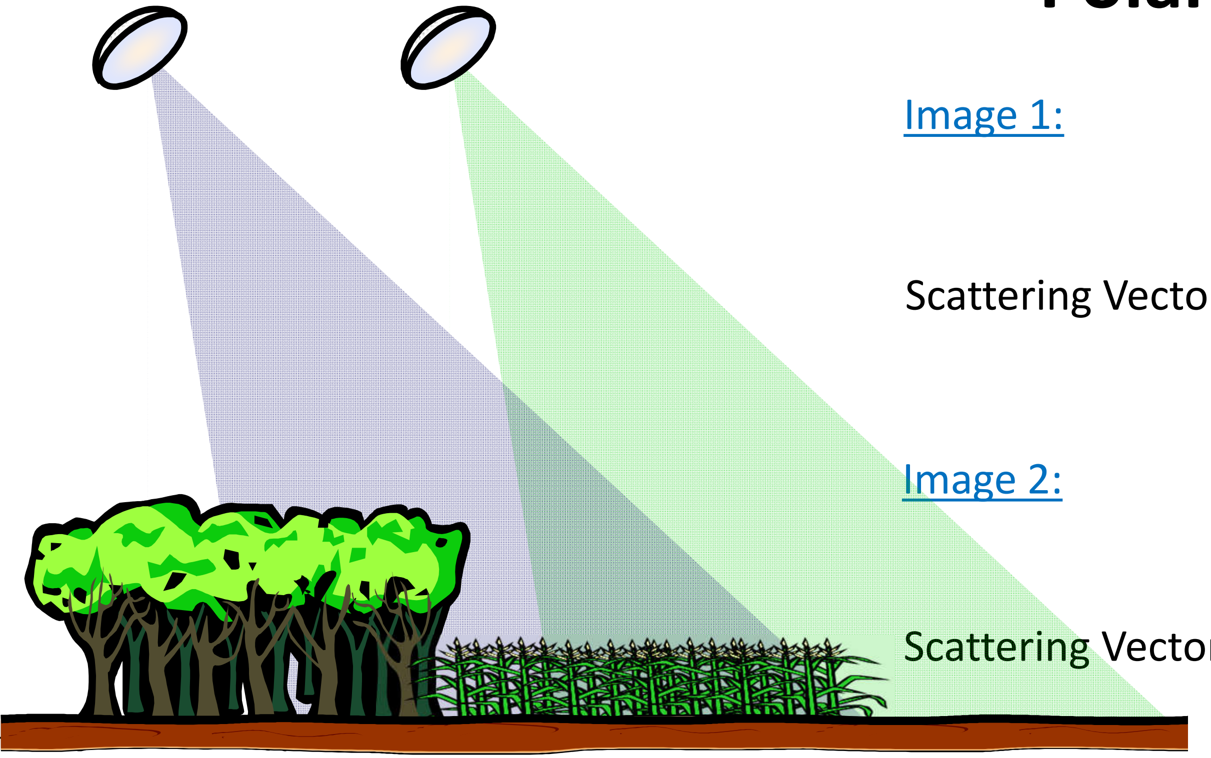

Image 1: Scattering Matrix: $[S_1]=\begin{bmatrix} S^1_{HH} & S^1_{HV} \\ S^1_{VH} & S^1_{VV}\end{bmatrix}$

Scattering Vector 1: $\vec{k}_1=\frac{1}{\sqrt{2}}[S^1_{HH}+S^1_{VV} \quad S^1_{HH}-S^1_{VV} \quad 2S^1_{HV}]^T$

Image 2: Scattering Matrix: $[S_2]=\begin{bmatrix} S^2_{HH} & S^2_{HV} \\ S^2_{VH} & S^2_{VV}\end{bmatrix}$

Scattering Vector 2: $\vec{k}_2=\frac{1}{\sqrt{2}}[S^2_{HH}+S^2_{VV} \quad S^2_{HH}-S^2_{VV} \quad 2S^2_{HV}]^T$

Image formation: $i_1=\vec{w}_1^+\cdot\vec{k}_1$ and $i_2=\vec{w}_2^+\cdot\vec{k}_2$ where $\vec{w}_i$ are complex unitary vectors*

Interferogram formation: $i_1\ i_2^*=(\vec{w}_1^+\cdot\vec{k}_1)(\vec{w}_2^+\cdot\vec{k}_2)^+=\vec{w}_1^+(\vec{k}_1\cdot\vec{k}_2^+)\vec{w}_2=\vec{w}_1^+[\Omega]\vec{w}_2$

Interferometric Coherence: $\tilde{\gamma}(\vec{w}_1,\vec{w}_2)=\frac{<i_1\ i_2^*>}{\sqrt{<i_1\ i_1^*><i_2\ i_2^*>}}=\frac{<\vec{w}_1^+[\Omega]\vec{w}_2>}{\sqrt{<(\vec{w}_1^+[T_{11}]\vec{w}_1)><(\vec{w}_2^+[T_{22}]\vec{w}_2)>}}$

where $[T_{11}]=<\vec{\kappa}_1\cdot\vec{\kappa}_1^+>$ $[T_{22}]=<\vec{\kappa}_2\cdot\vec{\kappa}_2^+>$ and $[\Omega]=<\vec{\kappa}_1\cdot\vec{\kappa}_2^+>$

---

* $\vec{w}_i$ used to select a polarisation state out of all possible polarisations provided by the scattering matrix [S]

Polarisation 3

$$\tilde{\gamma}_{Vol}(f(z)) = e^{ik_z z_o}\frac{\int_o^{h_v} f(z)\, e^{ik_z z} dz}{\int_o^{h_v} f(z)\, dz}$$

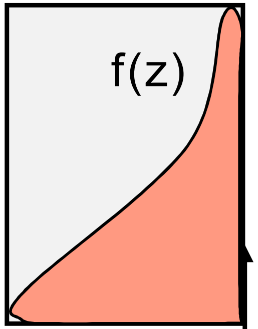

Polarisation 1

$$\tilde{\gamma}_{Vol}(f(z)) = e^{ik_z z_o}\frac{\int_o^{h_v} f(z)\, e^{ik_z z} dz}{\int_o^{h_v} f(z)\, dz}$$

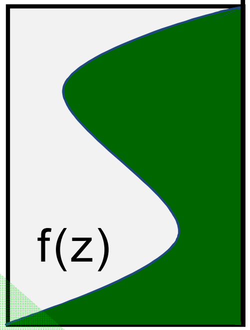

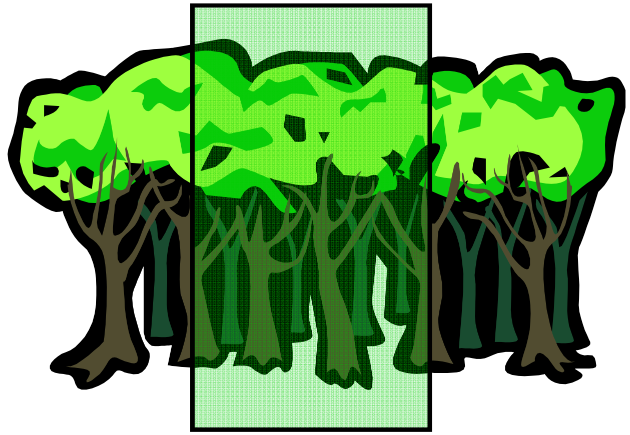

Polarisation 2

$$\tilde{\gamma}_{Vol}(f(z)) = e^{ik_z z_o}\frac{\int_o^{h_v} f(z)\, e^{ik_z z} dz}{\int_o^{h_v} f(z)\, dz}$$

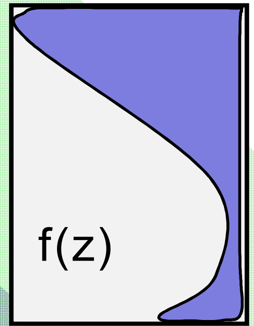

f(z) … vertical reflectivity function

Polarimetric SAR Interferometry

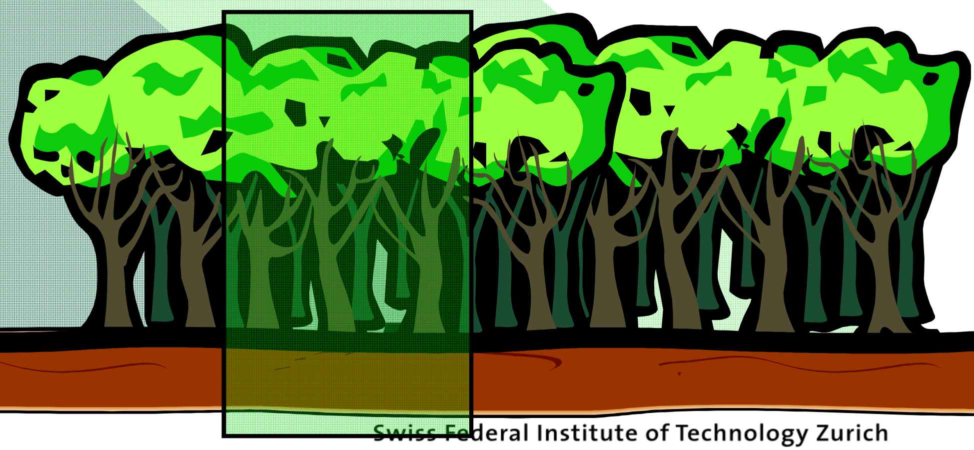

Interferometric Coherence: Volume Decorrelation

Amplitude Image HH **Sp. Baseline 16m** **Pol 1** **Pol2** **Pol 3**

Earth Observation and Remote Sensing

hajnsek@ifu.baug.ethz.ch
irena.hajnsek@dlr.de

ETH
Eidgenössische Technische Hochschule Zürich
Swiss Federal Institute of Technology Zurich

Geometrical Representation

Interferometric Coherence: $\tilde{\gamma}(\vec{w}_i, \vec{w}_i) = |\tilde{\gamma}(\vec{w}_i, \vec{w}_i)| \cdot \exp(i \operatorname{Arg}\{\tilde{\gamma}(\vec{w}_i, \vec{w}_i)\})$

Radius

Angle

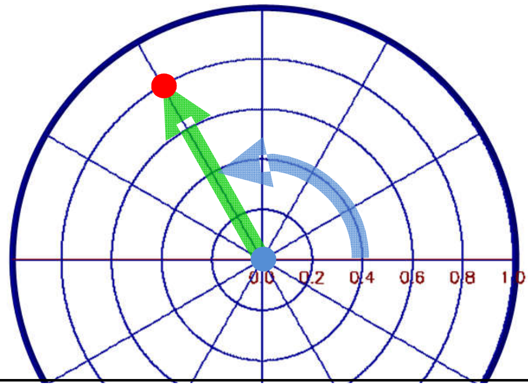

► can be represented by a single point on the unit circle

Coherence Region:

$$\tilde{\gamma}(\vec{w}_i, \vec{w}_i) \quad \forall \quad \vec{w}_i = \begin{bmatrix} \cos\alpha \exp(i\varphi_1) \\ \sin\alpha\cos\beta\exp(i\varphi_2) \\ \sin\alpha\sin\beta\exp(i\varphi_3) \end{bmatrix} \quad 0 \le \alpha \le \frac{\pi}{2} \quad -\pi \le \beta \le \pi \quad \in C$$

Shape and size depend on acquisition parameters and the structure of the underlying scatterer.

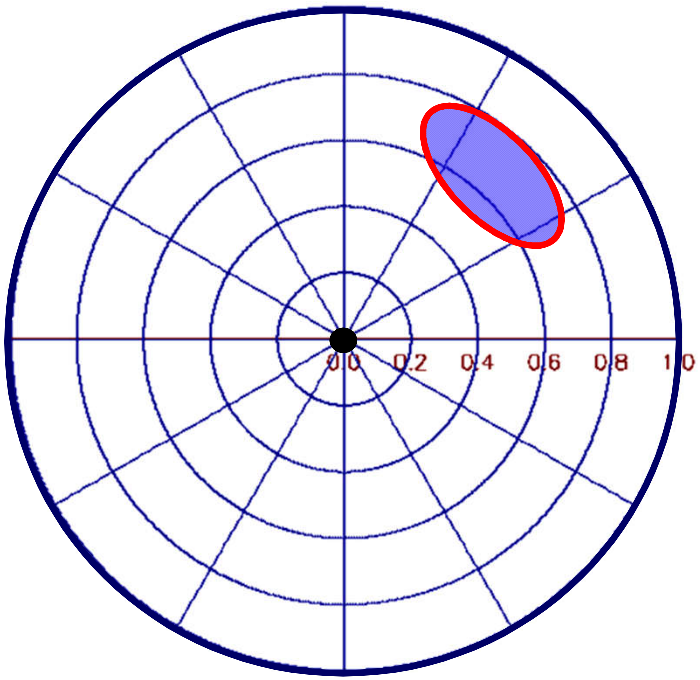

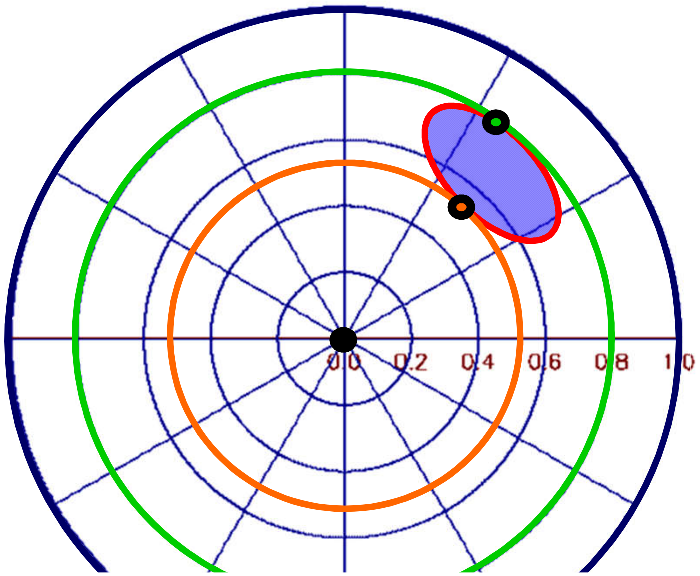

Max./ Min. Interferometric Coherence as function of the polarisation used to form the interferogram

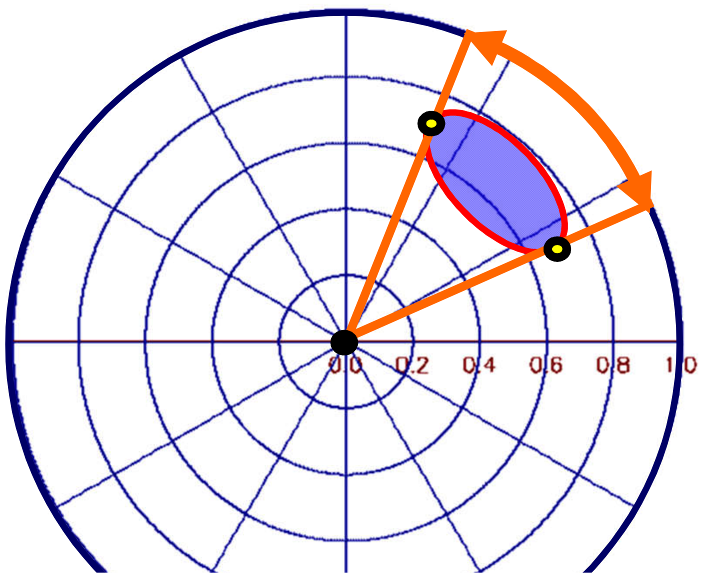

Max. Phase Difference between interferograms formed at different polarisations

Coherence Region Interpretation

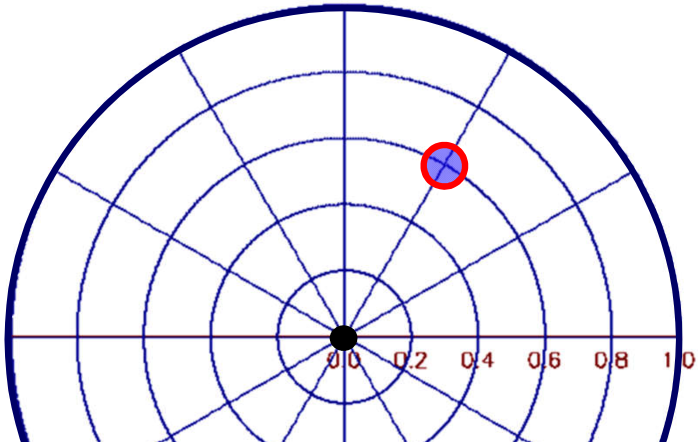

Point Like Coherence Region

i.e. InSAR Coherence and Phase are independent of polarisation.

Pol-InSAR does not provide any additional information compared to InSAR !!!

(Random) Volume scattering

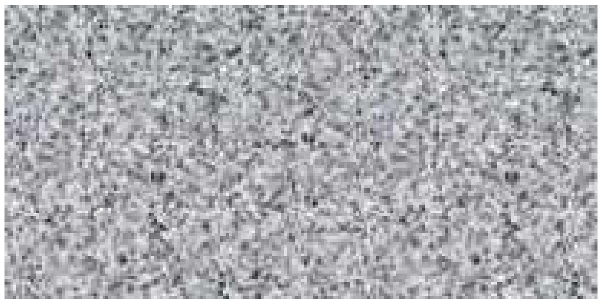

hajnsek@ifu.baug.ethz.ch
irena.hajnsek@dlr.de

Coherence Region Interpretation

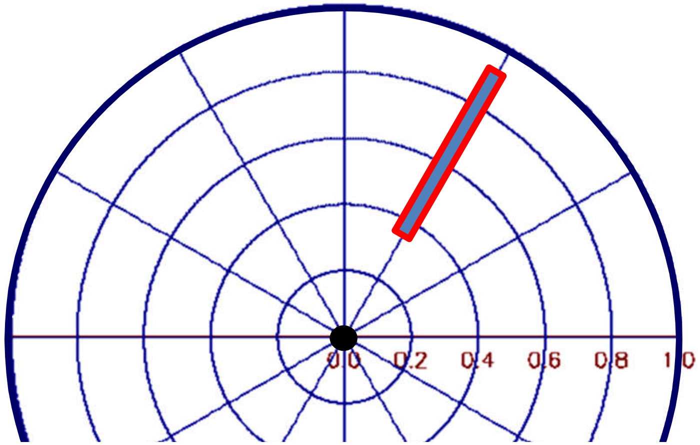

Radial Coherence Region

i.e. InSAR Coherence changes with polarisation but not the location of the phase center.

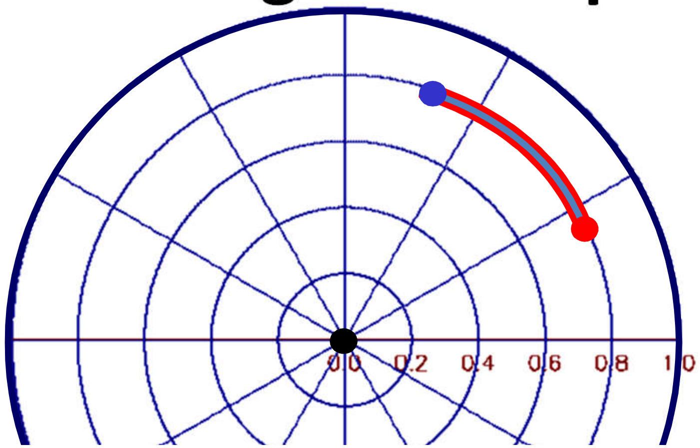

Radial Coherence Region

i.e. InSAR Phase changes, but not the InSAR coherence with polarisation

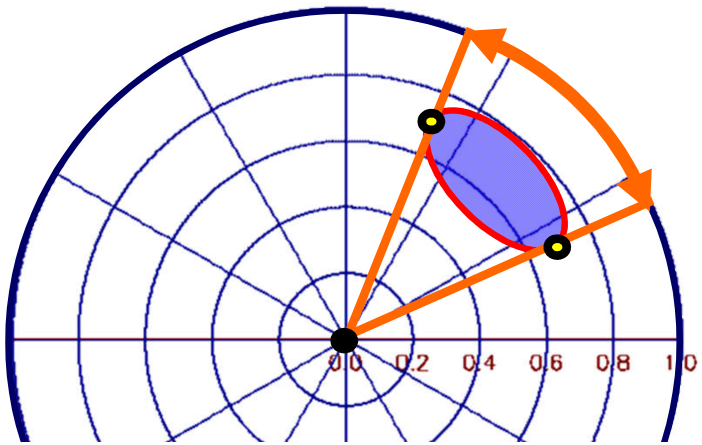

Elliptical Coherence Region

i.e. InSAR Coherence and Phase changes with polarisation.

Surface Scattering

$$\tilde{\gamma}(\vec{w}) = \gamma_{SNR}(\vec{w})\ \tilde{\gamma}_{Vol} \overset{\tilde{\gamma}_{Vol}:=1}{=} \gamma_{SNR}(\vec{w})$$

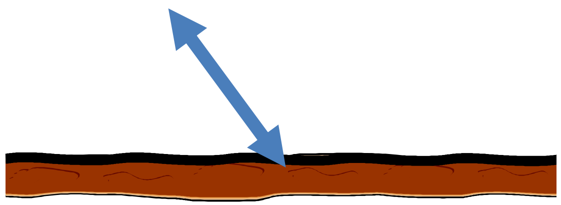

(Polarised) Coherent scaterrers at different heights

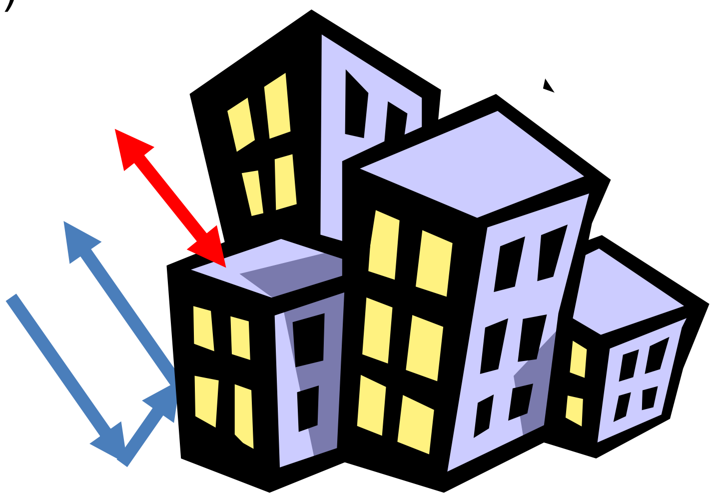

(Depolarising) Scaterrers at different heights

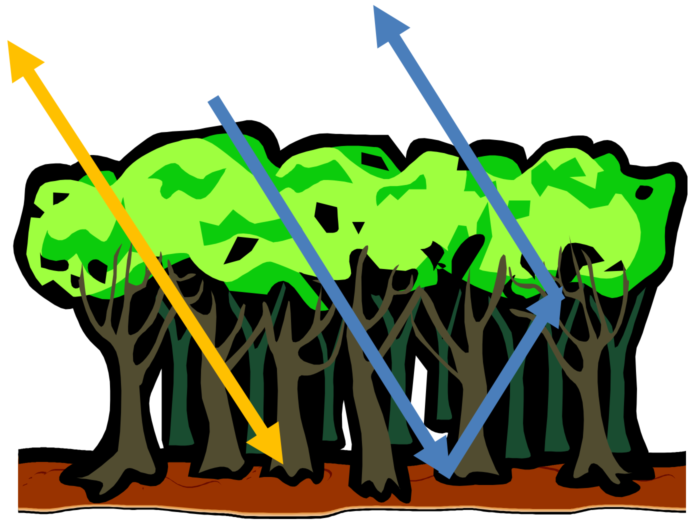

Coherence Region (CR)

Interferometric Coherence: $$\boxed{\tilde{\gamma}(\vec{w}_1,\vec{w}_2)=\frac{<\vec{w}_1[\Omega]\vec{w}_2^{\,+}>}{\sqrt{<\vec{w}_1[T_{11}]\vec{w}_1^{\,+}><\vec{w}_2[T_{22}]\vec{w}_2^{\,+}>}}}$$

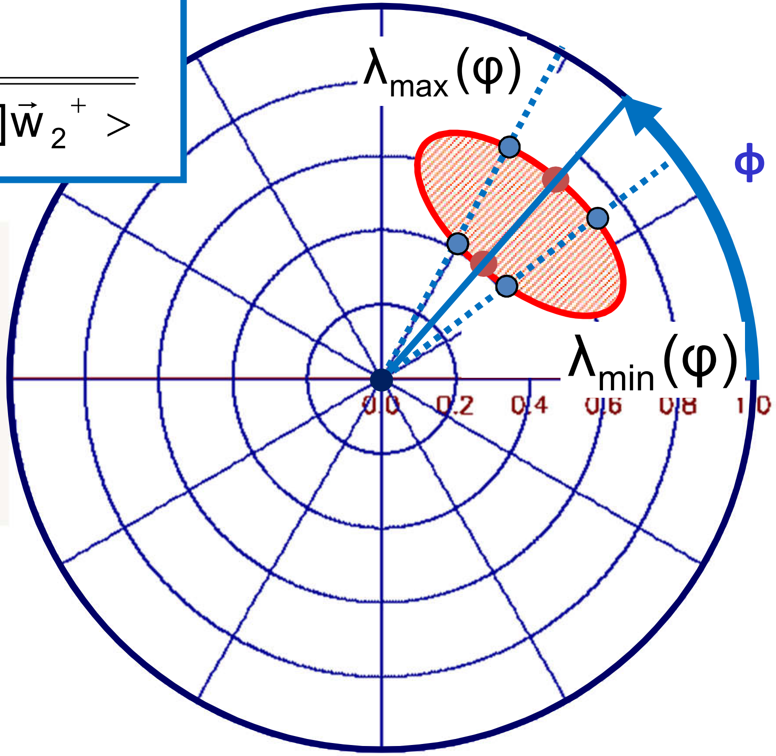

The boundary of the coherence region can be reconstructed by estimating for each angle ϕ the max (λ_1) and min (λ_2) coherences:

Optimisation Problem ($\vec{w}_1=\vec{w}_2$): $$\boxed{[T]^{-1}[\Omega_\varphi]\ \vec{w}=\lambda\ \vec{w}}$$

where $$[T]=\frac{1}{2}([T_{11}]+[T_{22}]),\quad \lambda=-(\lambda_1+\lambda_2^*)\qquad [\Omega_\varphi]=\frac{1}{2}(\exp(i\varphi)[\Omega]+\exp(-i\varphi)[\Omega]^+)$$

and $$[T_{11}]:=<\vec{k}_1\cdot\vec{k}_1^+>\qquad [T_{22}]:=<\vec{k}_2\cdot\vec{k}_2^+>\qquad [\Omega]:=<\vec{k}_1\cdot\vec{k}_2^+>$$

<u>Coherence Region:</u> $\forall\varphi\rightarrow\lambda_{max},\lambda_{min}$ that have to be connected to provide the boundary of the CR

Shape and size are characterised by the acquisition and scattering parameters

Structure Parameters & Applications

Forest

- Forest Height
- Forest (Vertical) Structure
- Forest Biomass
- Underlying Topography

→

- Forest Ecology
- Forest Management
- Ecosystem Modeling
- Climate Change

Agriculture

- Underlying Soil Moisture
- Moisture of Vegetation Layer
- Height of Vegetation Layer
- Soil Roughness

→

- Farming Management
- Ecosystem Modeling
- Water Cycle / CC
- Desertification

Snow & Ice

- Ice Layer Structure
- Penetration Depth (Ice)
- Snow Layer Thickness
- Snow Water Equivalent

→

- Ecosystem Change
- Water Cycle
- Water Management

hajnsek@ifu.baug.ethz.ch
irena.hajnsek@dlr.de

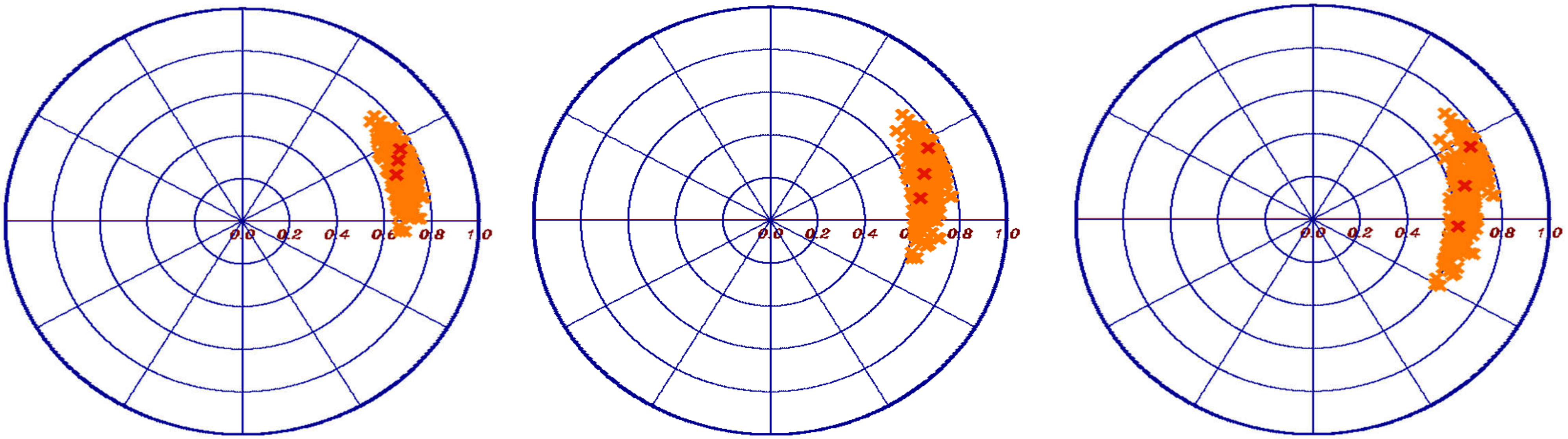

Model-Based Parameter Inversion

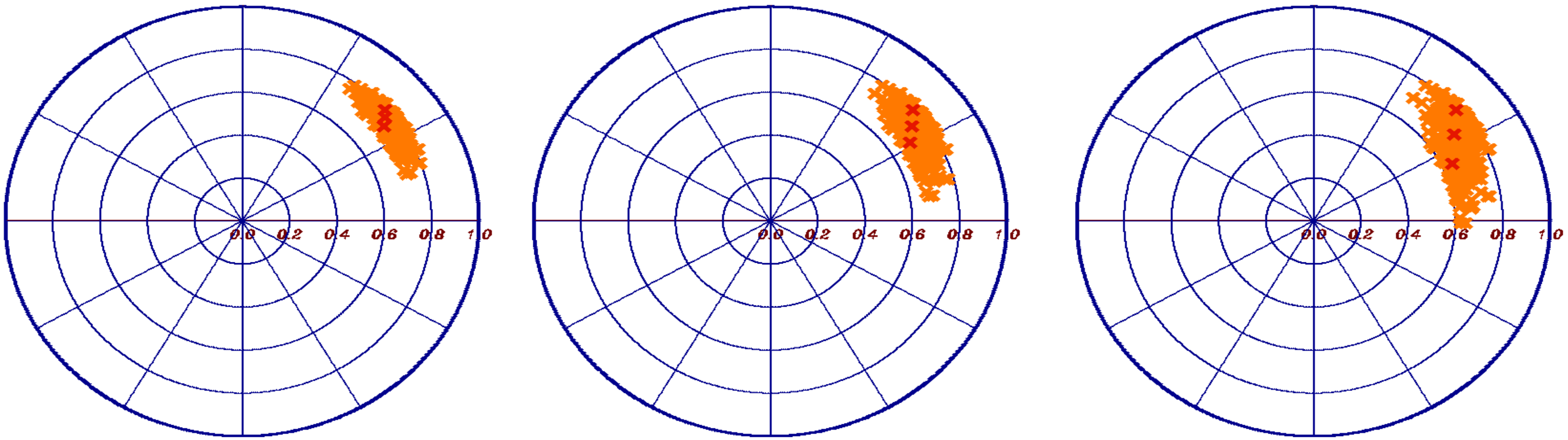

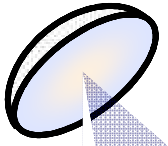

S_1 $\quad$ S_2

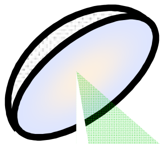

Interferometric Coherence

$$\tilde{\gamma}(S_1\ S_2) = \frac{< S_1\ S_2^* >}{\sqrt{< S_1\ S_1^* > < S_2\ S_2^* >}}$$

Volume Coherence

$$\tilde{\gamma}_{Vol}(f(z)) = e^{ik_z z_o} \frac{\int_o^{h_v} f(z) e^{ik_z z} dz}{\int_o^{h_v} f(z)\ dz}$$

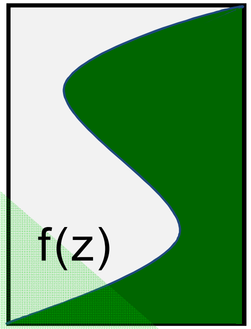

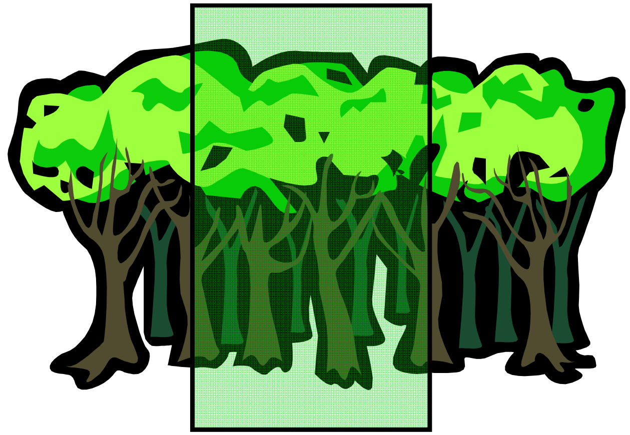

2 Layer Inversion Model

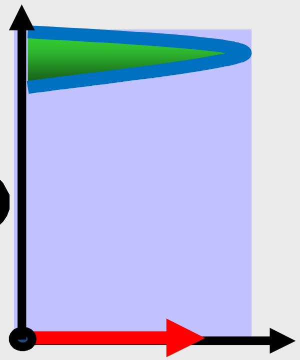

Volume Layer $\quad$ Ground Layer

$$f(z) = m_V f_V(z) + m_G \delta(z - z_0)$$

$$\tilde{\gamma}_{Vol}(\vec{w}) = \exp(i\varphi_0) \frac{\tilde{\gamma}_V + m(\vec{w})}{1 + m(\vec{w})}$$

$f_V(z)$ ... volume reflectivity function

Volume Coherence

$$\tilde{\gamma}_V = \frac{I}{I_0} \quad \begin{cases} I = \int_0^{h_V} \exp(i\kappa_z z') f_V(z') dz' \\ I_0 = \int_0^{h_V} f_V(z') dz' \end{cases}$$

$$m(\vec{w}) = \frac{m_G(\vec{w})}{m_V(\vec{w}) I_0}$$

$$\kappa_z = \frac{\kappa \Delta\theta}{\sin(\theta_0)}$$

$f_V(z)$ has to be parameterised (N param)

Volume Height	h_V
Topography	φ_0
G/V Ratio	$m(\vec{w})$

3+N Unknowns

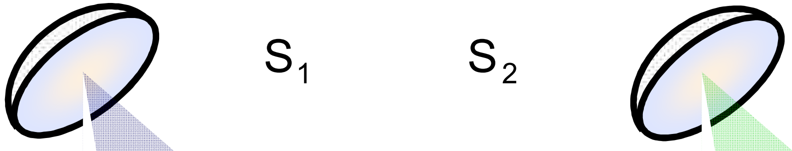

Interferometric Coherence

$$\tilde{\gamma}(S_1\, S_2) = \frac{< S_1\, S_2^* >}{\sqrt{< S_1\, S_1^* > < S_2\, S_2^* >}}$$

Volume Coherence

$$\tilde{\gamma}_{Vol}(f(z)) = e^{ik_z z_o} \frac{\int_o^{h_v} f(z)\, e^{ik_z z} dz}{\int_o^{h_v} f(z)\; dz}$$

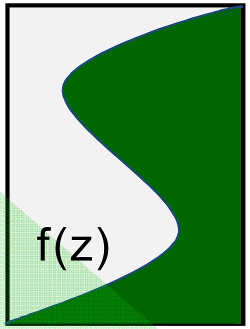

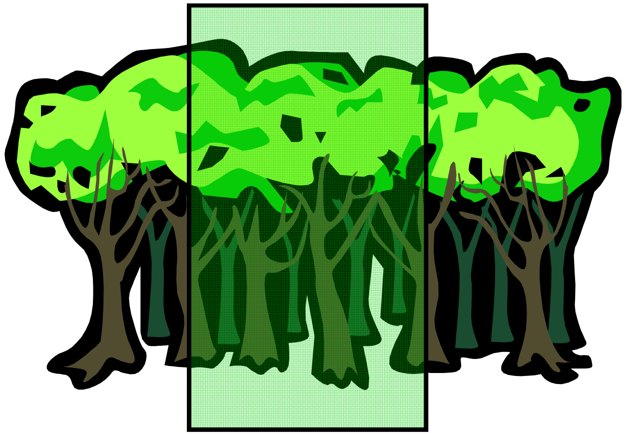

2 Layer Inversion Model

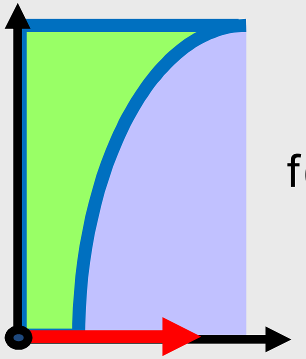

Volume Layer Ground Layer

$$f(z) = m'_V e^{\left(\frac{2\ \sigma\ z}{\cos\theta_0}\right)} + m'_G \delta(z - z_0)$$

$$\tilde{\gamma}_{Vol}(\vec{w}) = \exp(i\varphi_0) \frac{\tilde{\gamma}_V + m(\vec{w})}{1 + m(\vec{w})}$$

$$f_V(z) = e^{\left(\frac{2\ \sigma\ z}{\cos\theta_0}\right)}$$ ... volume reflectivity function = exponential function

Volume Coherence

$$\tilde{\gamma}_V = \frac{I}{I_0} \quad \begin{cases} I = \int_0^{h_V} \exp(i\kappa_z z')\ m_V \exp\left(\frac{2\ \sigma\ z'}{\cos\theta_0}\right) dz' \\ I_0 = \int_0^{h_V} m_V \exp\left(\frac{2\ \sigma\ z'}{\cos\theta_0}\right) dz' \end{cases}$$

$$m(\vec{w}) = \frac{m_G(\vec{w})}{m_V(\vec{w}) I_0} \qquad \kappa_z = \frac{\kappa\Delta\theta}{\sin(\theta_0)}$$

σ	"Volume Extinction"
Volume Height	h_V
Topography	φ_0
G/V Ratio	$m(\vec{w})$

4 Unknowns

Modeling approaches for $f_V(z)$

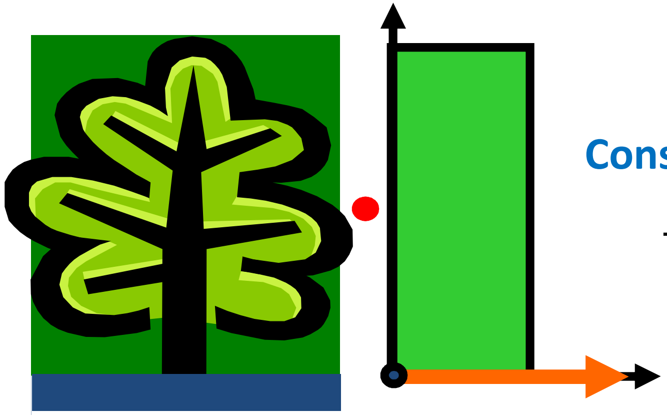

Constant Profile

$$f_V(z) = ct.$$

Linear Profile f(h_V,σ)

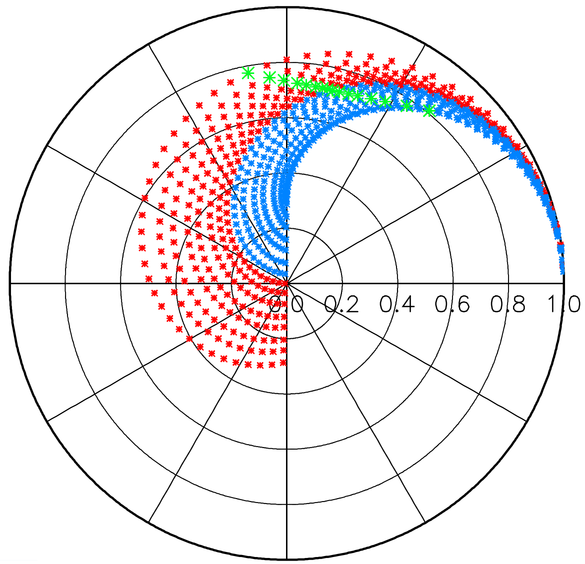

Exp. Profile f(h_V, σ)

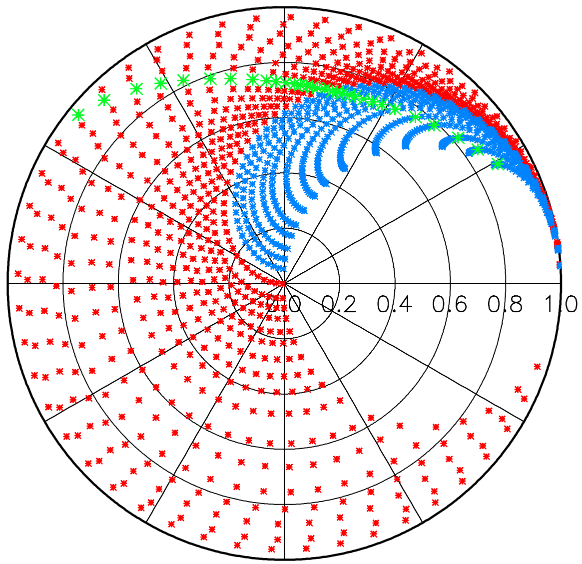

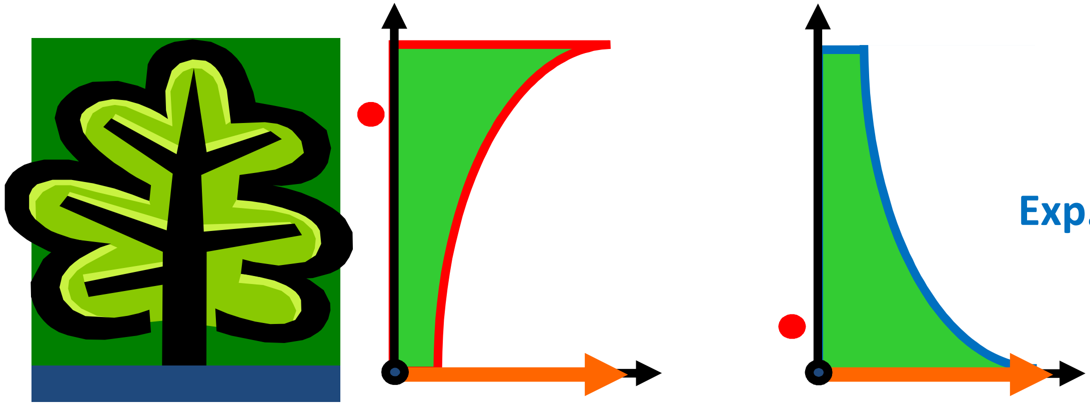

Exp. Profile

$$f_V(z) = \exp\left(\pm \frac{2\ \sigma\ z}{\cos\ \theta_0}\right)$$

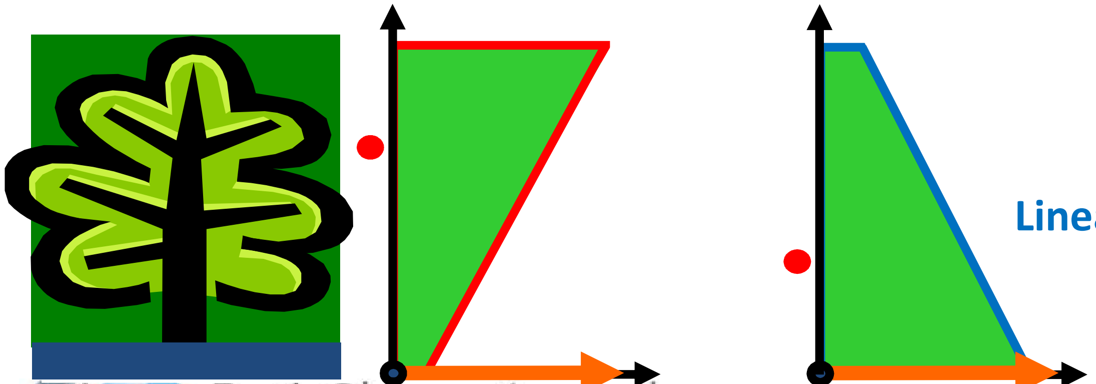

Linear Profile

$$f_V(z) = (\pm \frac{2\ \sigma\ z}{\cos\ \theta_0} + 1)$$

Polarimetric Behaviour: Random vs. Oriented Volume

Random Volume: The vertical reflectivity function is independent of polarisation (or each polarisation sees the same volume vertical reflectivity $f_v(z)$)

$$f_v := f_v(z) \mapsto \tilde{\gamma}_V(\kappa_z)$$

Oriented Volume: The vertical reflectivity function changes with polarisation (or each polarisation sees a different volume vertical reflectivity $f_v(z)$)

$$f_v := f_v(z,\vec{w}) \mapsto \tilde{\gamma}_V(\kappa_z,\vec{w})$$

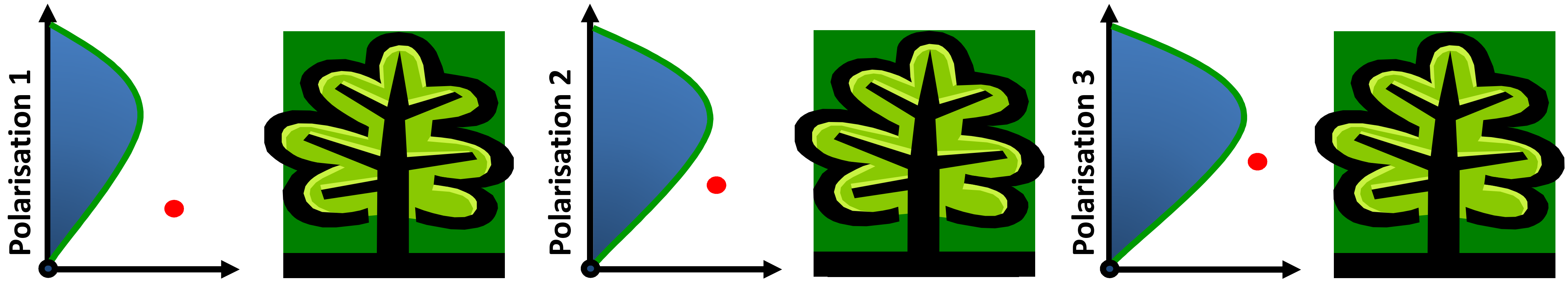

Earth Observation and Remote Sensing

hajnsek@ifu.baug.ethz.ch
irena.hajnsek@dlr.de

ETH
Eidgenössische Technische Hochschule Zürich
Swiss Federal Institute of Technology Zurich

Polarimetric Behaviour: 3-dim vs 2-dim Ground Scatterer

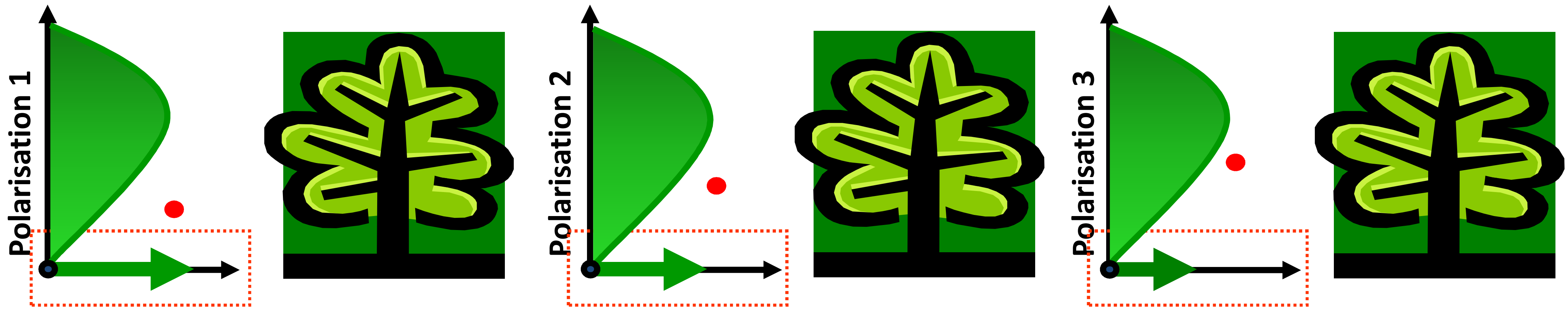

3-dim ground scatterer: A ground scattering component is visible in all polarisations (or there is no polarisation that "switches-off" the ground)

$$\forall\ \vec{w}\quad m(\vec{w}) \neq 0$$

2-dim ground scatterer: There is (at least) one polarisation in which the ground disappears

$$\exists\ \vec{w} \mapsto m(\vec{w}) = 0$$

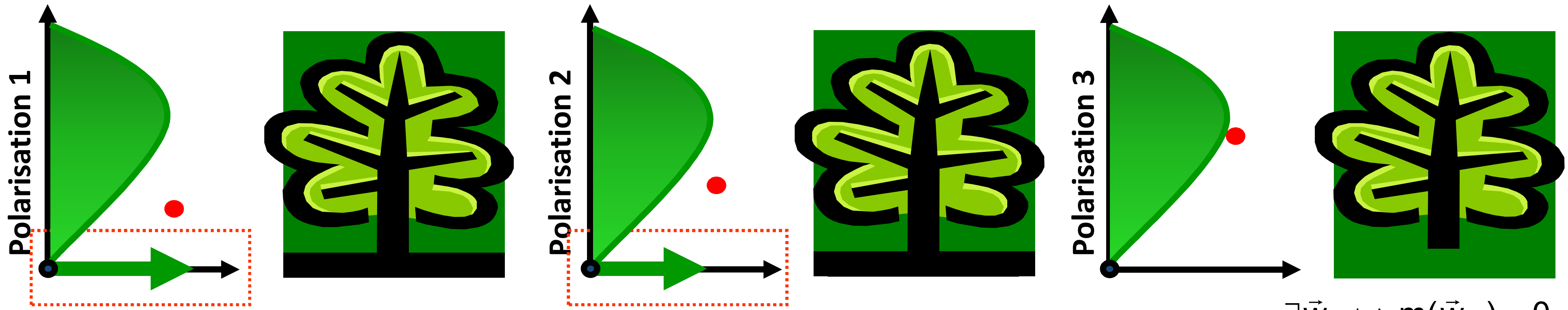

$$\exists \vec{w}_x \mapsto m(\vec{w}_x) = 0$$

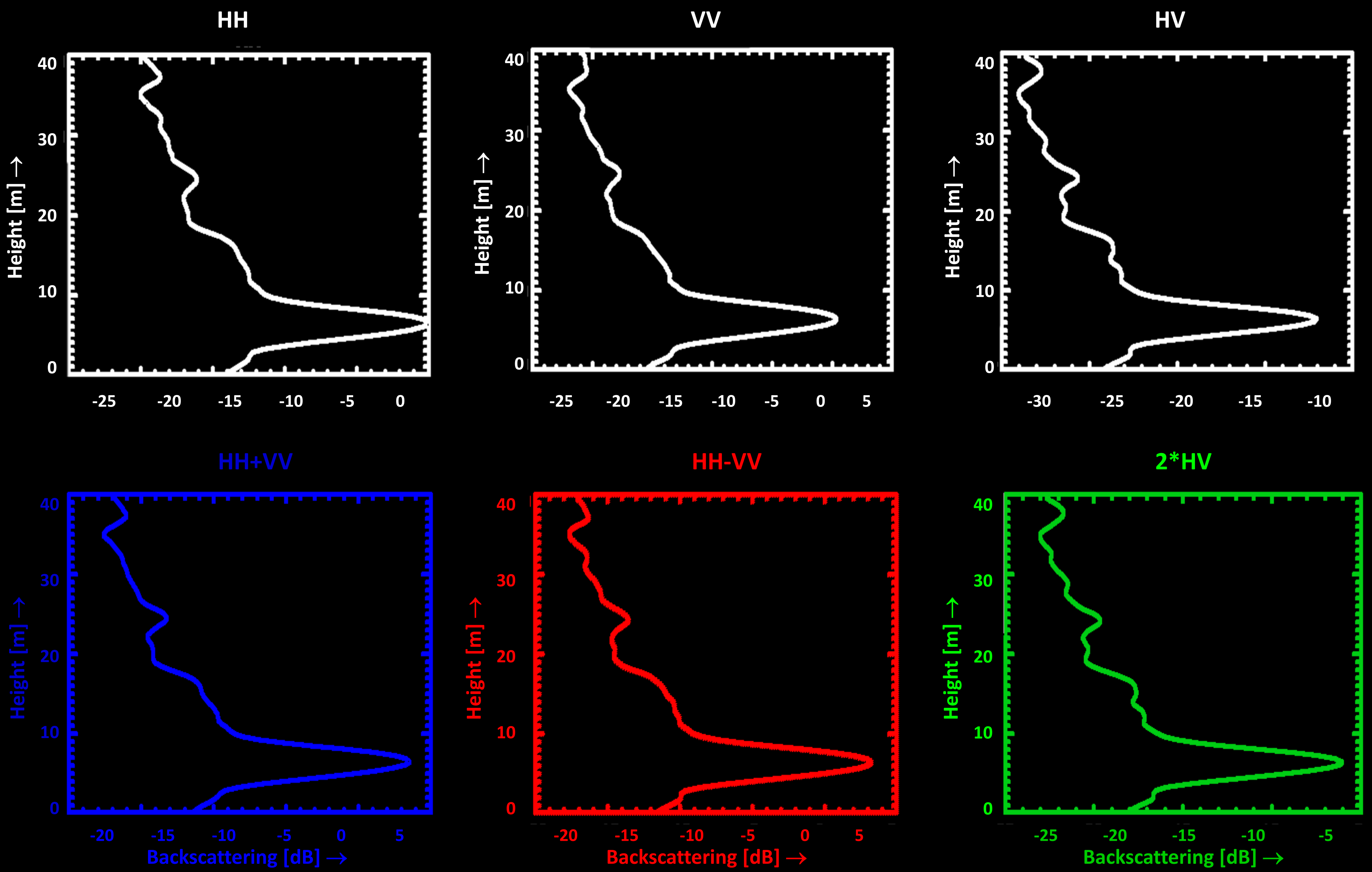

Bare Surface Backscattering Profiles

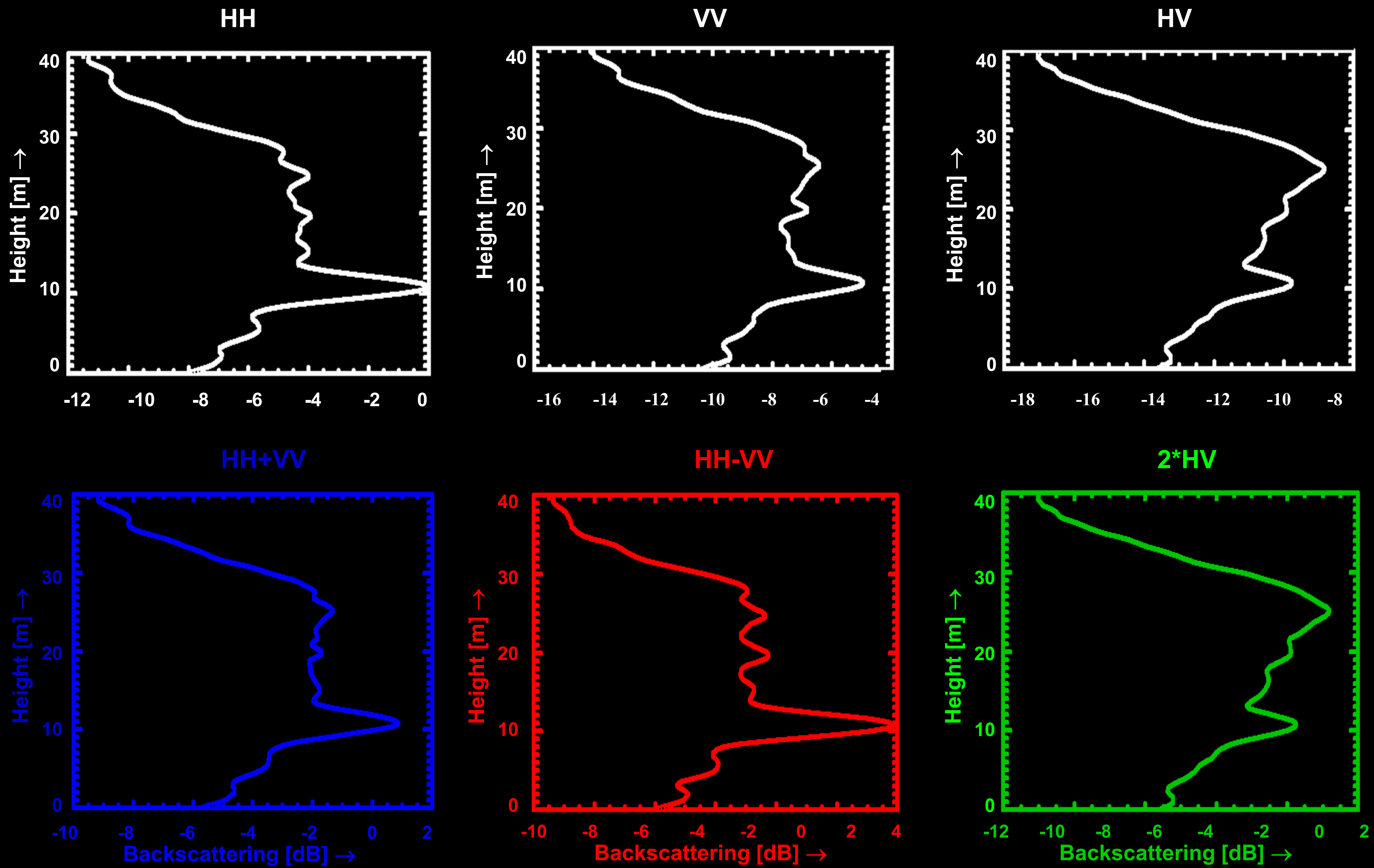

Mixed Forest Backscattering Profiles (12-20 m height)

RVoG Scattering Model: Geometrical Interpretation

Interferometric Coherence:
(2 Layer Random Volume)

$$\tilde{\gamma}(\vec{w}) = \exp(i\varphi_0)\frac{\tilde{\gamma}_V + m(\vec{w})}{1+m(\vec{w})}$$

$$\boxed{\tilde{\gamma}(\vec{w}) = \exp(i\varphi_0)\left[\tilde{\gamma}_V + \frac{m(\vec{w})}{1+m(\vec{w})}(1-\tilde{\gamma}_V)\right]}$$

$$\tilde{\gamma}(\vec{w}) = \exp(i\varphi_0)[\;B \;+\; X(\vec{w})\;\; A\;]$$

Equation of a straight line in the complex plane ▶

<u>The coherence region of the RVoG model is a line segment !!!</u>

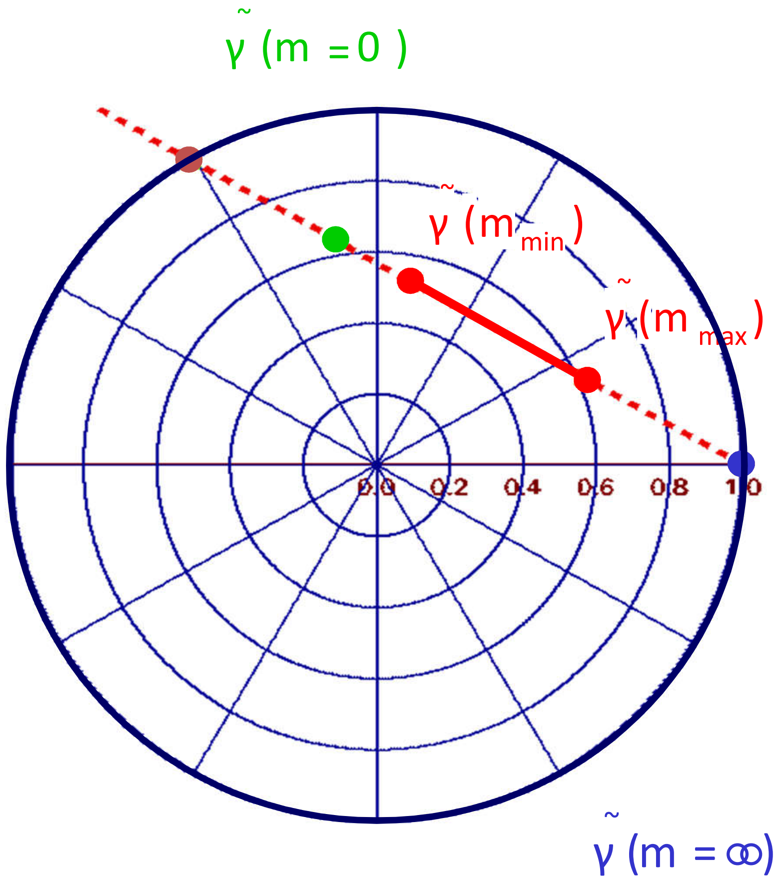

- The ends of the segment correspond to the coherences given by the max / min G-V Ratio: $\tilde{\gamma}(m_{max})$ and $\tilde{\gamma}(m_{min})$
- One of the line-unit circle intersection points correspond to the “Ground only” point, i.e. $\tilde{\gamma}(m=\infty) = \exp(i\varphi_0)$
- The second line-unit circle intersection points is non-physical
- The “Volume only” point (i.e. $\tilde{\gamma}(m(\vec{w})=0) = \exp(i\varphi_0)\tilde{\gamma}_V$) lies on the line but (in general) not on the coherence region segment

RVoG Solution on the Unit Circle

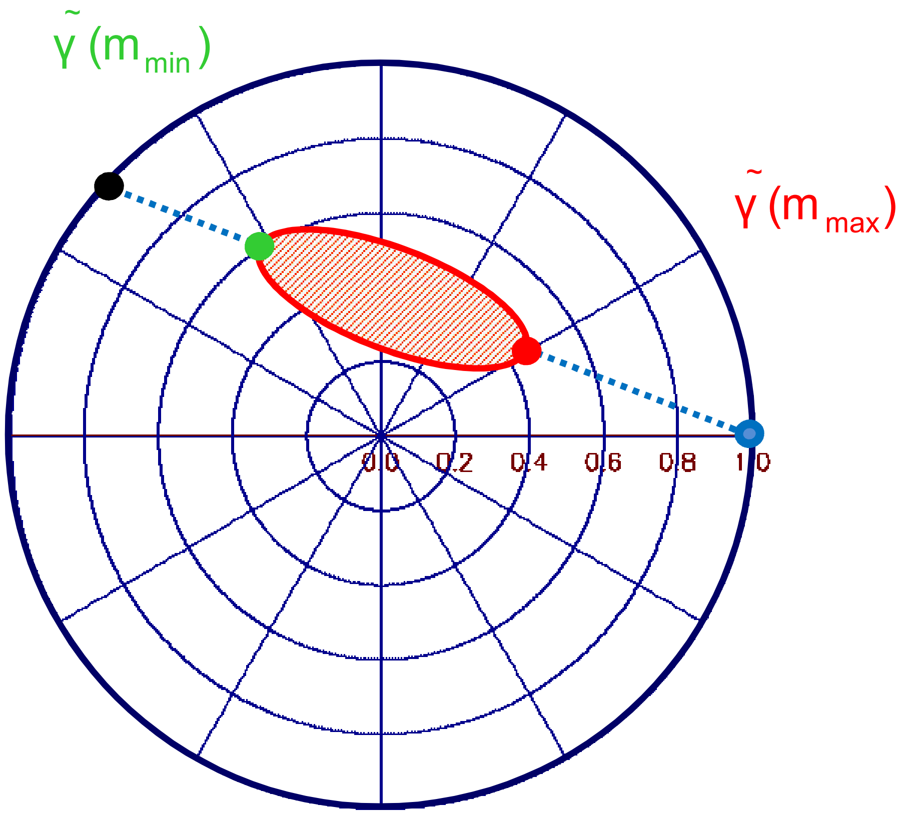

1. Estimation of the Coherence Region (CR);
2. Line fit through the extreme points of the CR

   $\tilde{\gamma}(m_{min})$ and $\tilde{\gamma}(m_{max})$

3. Estimation of the line-circle intersection point that corresponds to the underlying ground, i.e.:

   $\tilde{\gamma}(m = \infty) = \exp(i\varphi_0)$

RVoG Solution on the Unit Circle

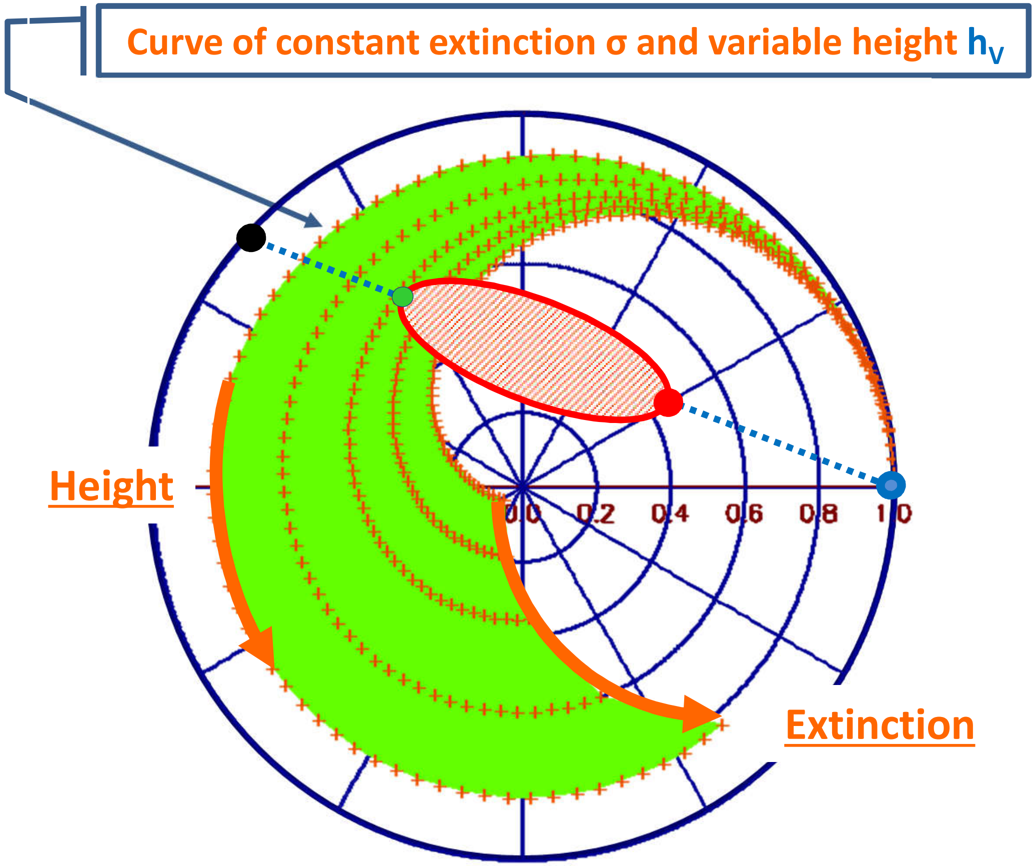

$$\tilde{\gamma}(m=0)=\exp(i\phi_0)\frac{\int_0^{h_V}\exp(i\kappa_z z')\exp\left(\frac{2\sigma z'}{\cos\theta_0}\right)dz'}{\int_0^{h_V}\exp\left(\frac{2\sigma z'}{\cos\theta_0}\right)dz'}$$

4. From the underlying ground point $\tilde{\gamma}=\exp(i\varphi_0)$ a Volume Height–Extinction Look-Up Table (LUT) is initialised that provides at every intersection with the line a solution couple (h_V,σ)

There is no unique solution of the RVoG model in the context of a single baseline !!!

5. <u>Regularisation:</u> Assuming a 2-dim ground, i.e. $\tilde{\gamma}(m_{min})=\tilde{\gamma}(m=0)$ leads to a unique (h_V,σ) solution through the intersection of $\tilde{\gamma}(m_{min})$ with the LUT

hajnsek@ifu.baug.ethz.ch
irena.hajnsek@dlr.de

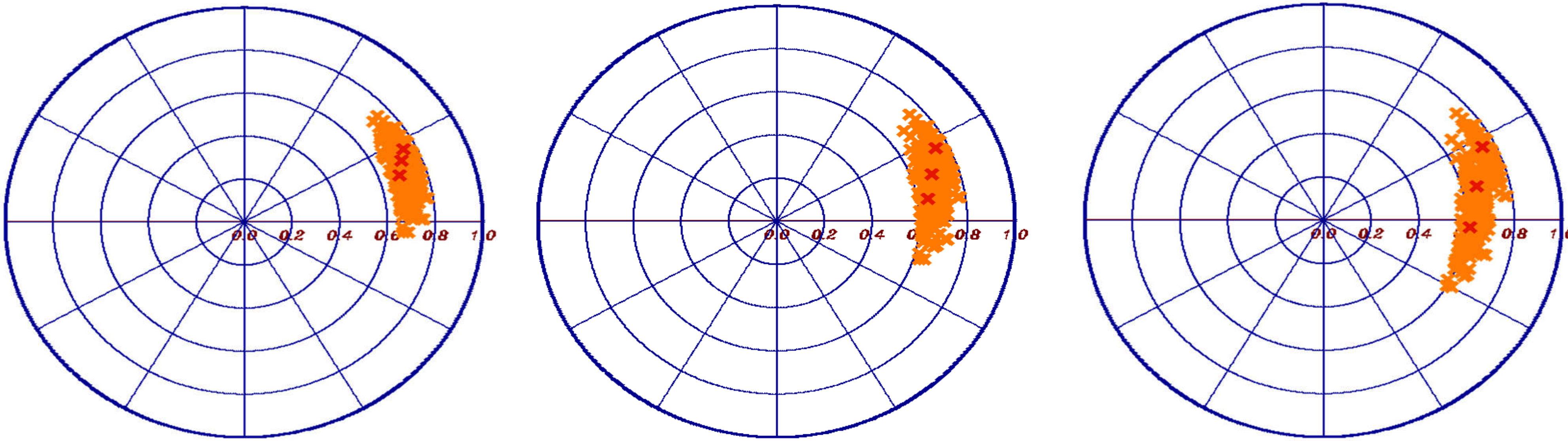

RVoG Inversion: Validation

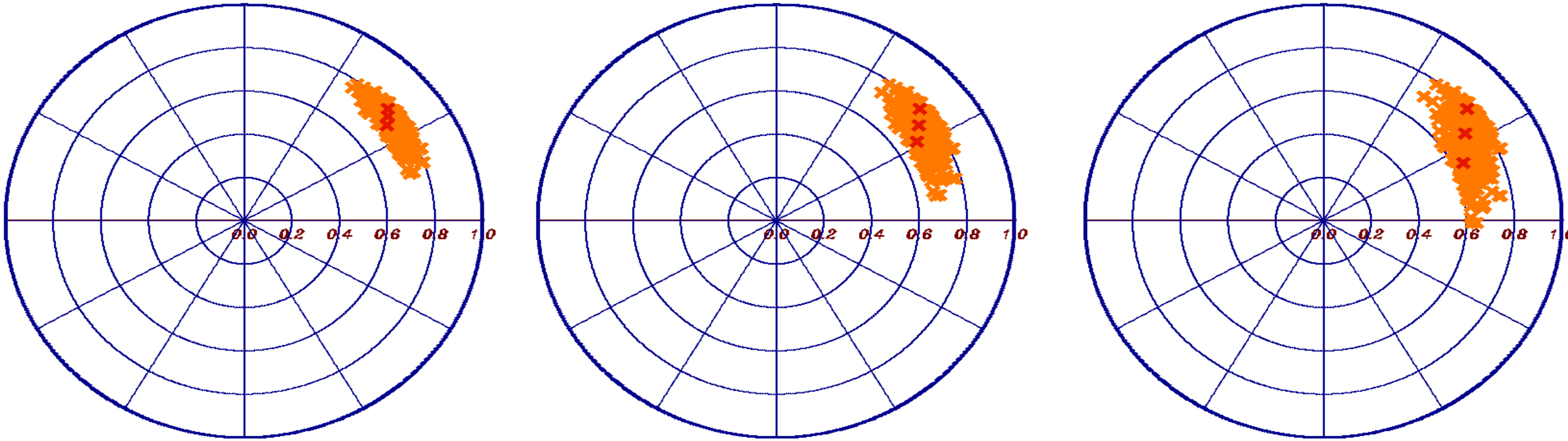

Structure Parameters & Applications

Forest

- Forest Height
- Forest (Vertical) Structure
- Forest Biomass
- Underlying Topography

→

- Forest Ecology
- Forest Management
- Ecosystem Modeling
- Climate Change

Agriculture

- Underlying Soil Moisture
- Moisture of Vegetation Layer
- Height of Vegetation Layer
- Soil Roughness

→

- Farming Management
- Ecosystem Modeling
- Water Cycle / CC
- Desertification

Snow & Ice

- Ice Layer Structure
- Penetration Depth (Ice)
- Snow Layer Thickness
- Snow Water Equivalent

→

- Ecosystem Change
- Water Cycle
- Water Management

hajnsek@ifu.baug.ethz.ch
irena.hajnsek@dlr.de

Forest: The beginning of Pol-InSAR

SIR-C/X-SAR / Test Site: Kudara, Russia

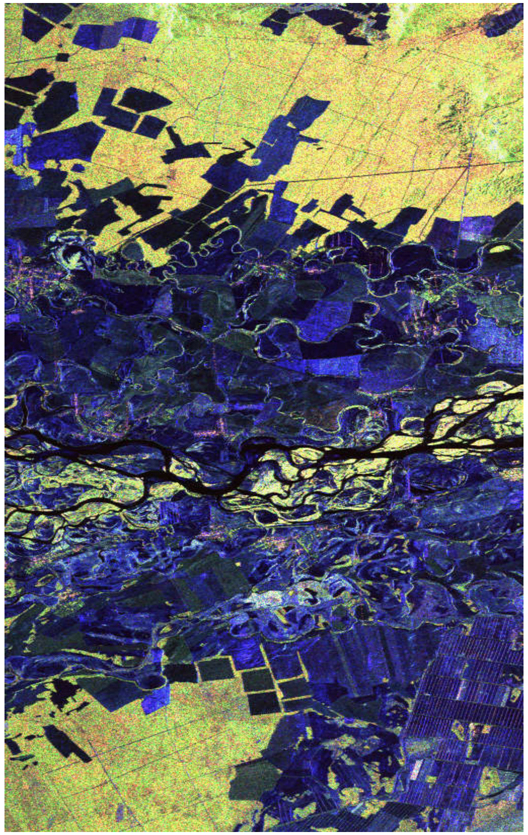

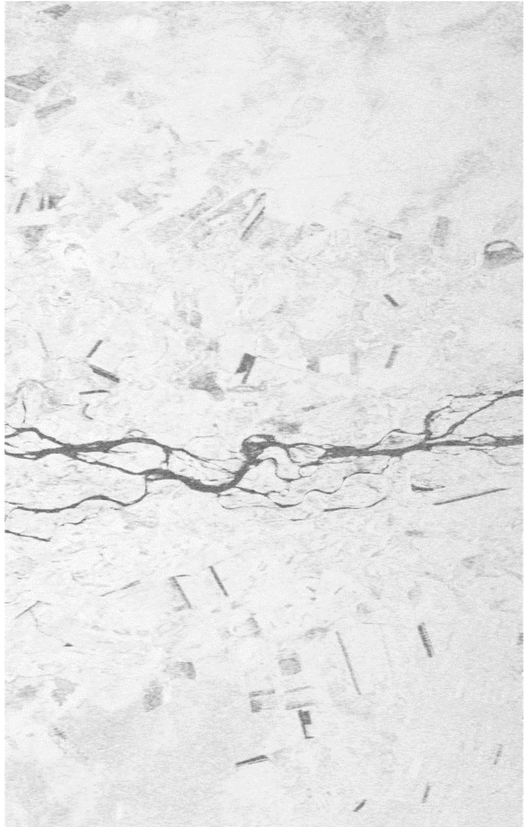

L-band / Pauli RGB

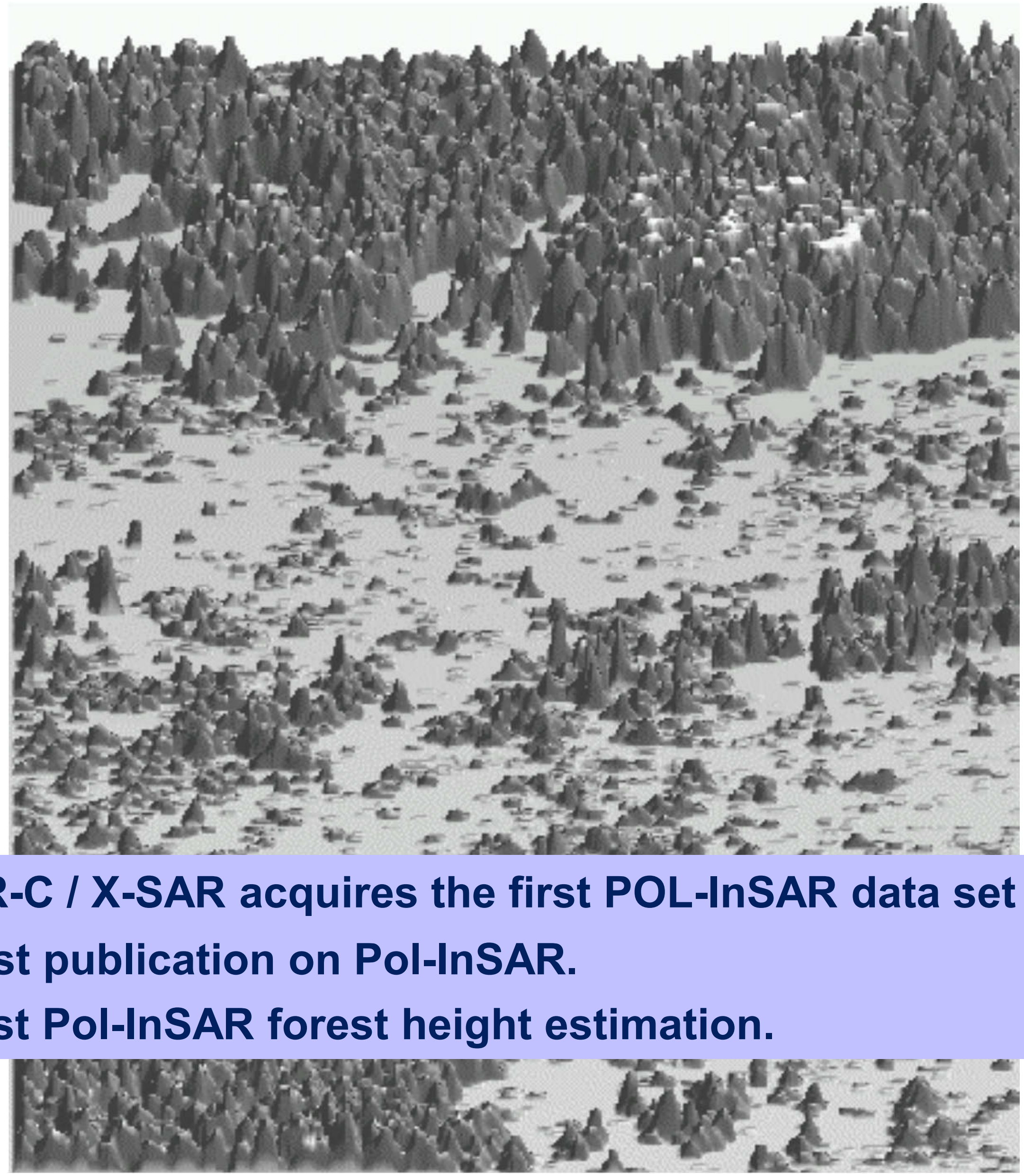

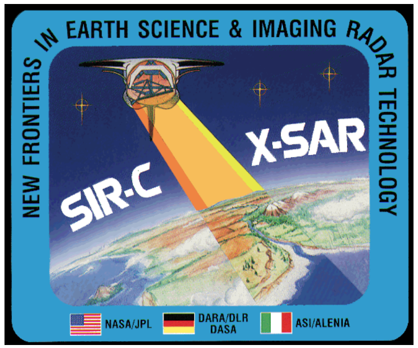

1994: SIR-C / X-SAR acquires the first POL-InSAR data set

1996: First publication on Pol-InSAR.

1998: First Pol-InSAR forest height estimation.

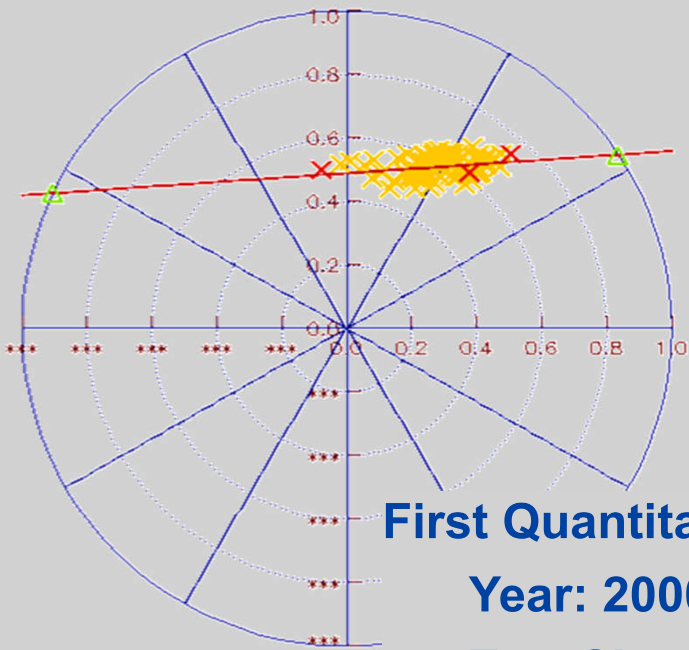

First Quantitative Pol-InSAR Demonstration:

Year: 2000 Sensor: E-SAR (DLR)

Test Site: Oberpfaffenhofen / Germany

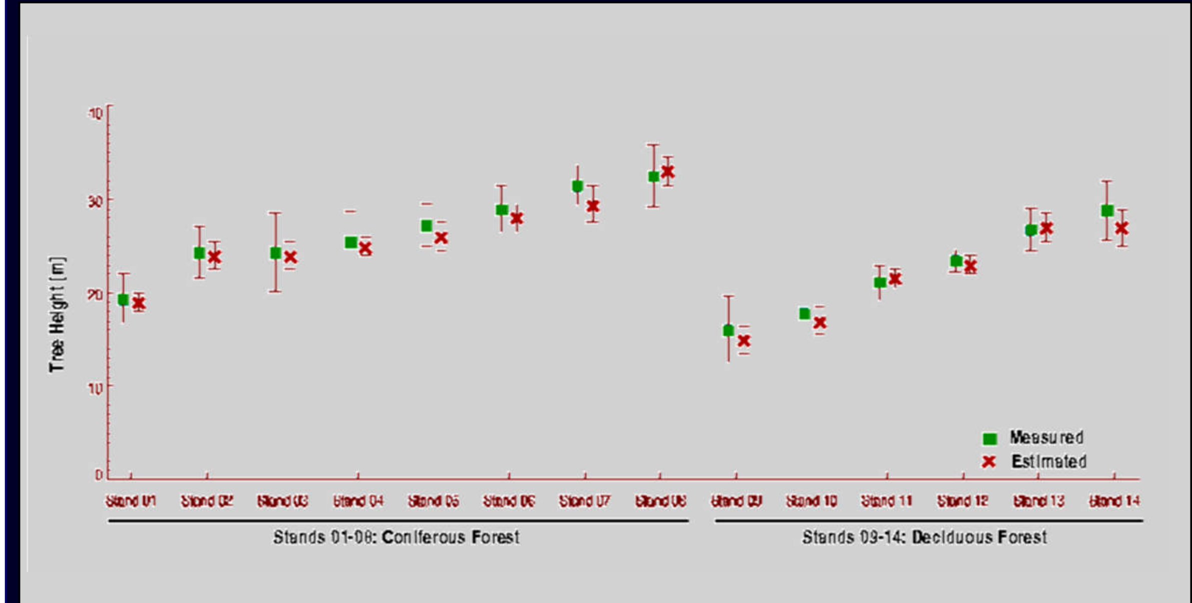

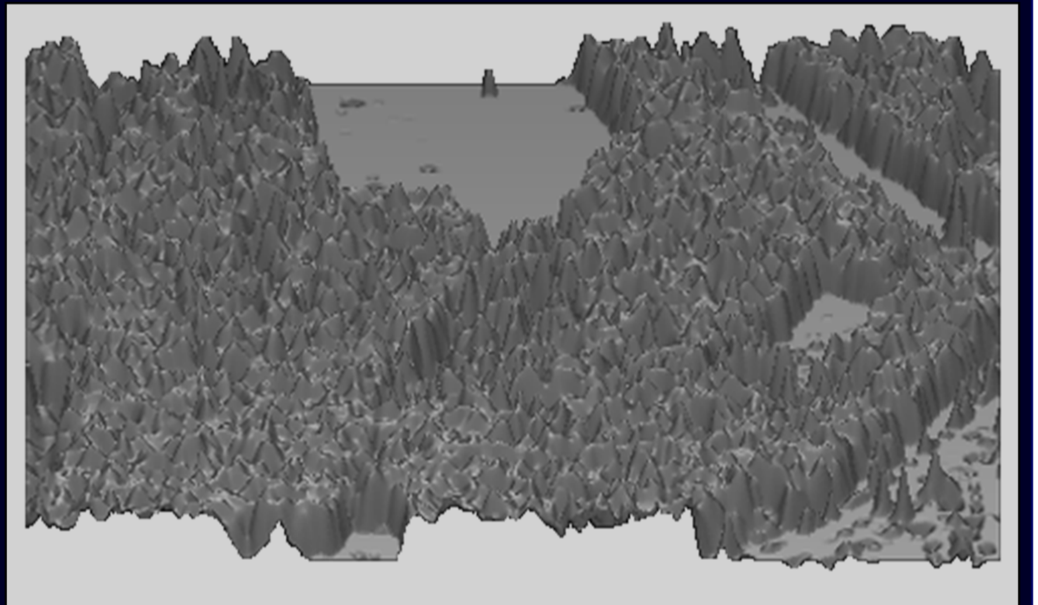

Traunstein Test Site

Forest type	Temperate
Topography	Moderate slopes
Height	25 ~ 35m
Species	N. Spruce, E. Beech, White Fir
Biomass	40 ~ 450 t/ha

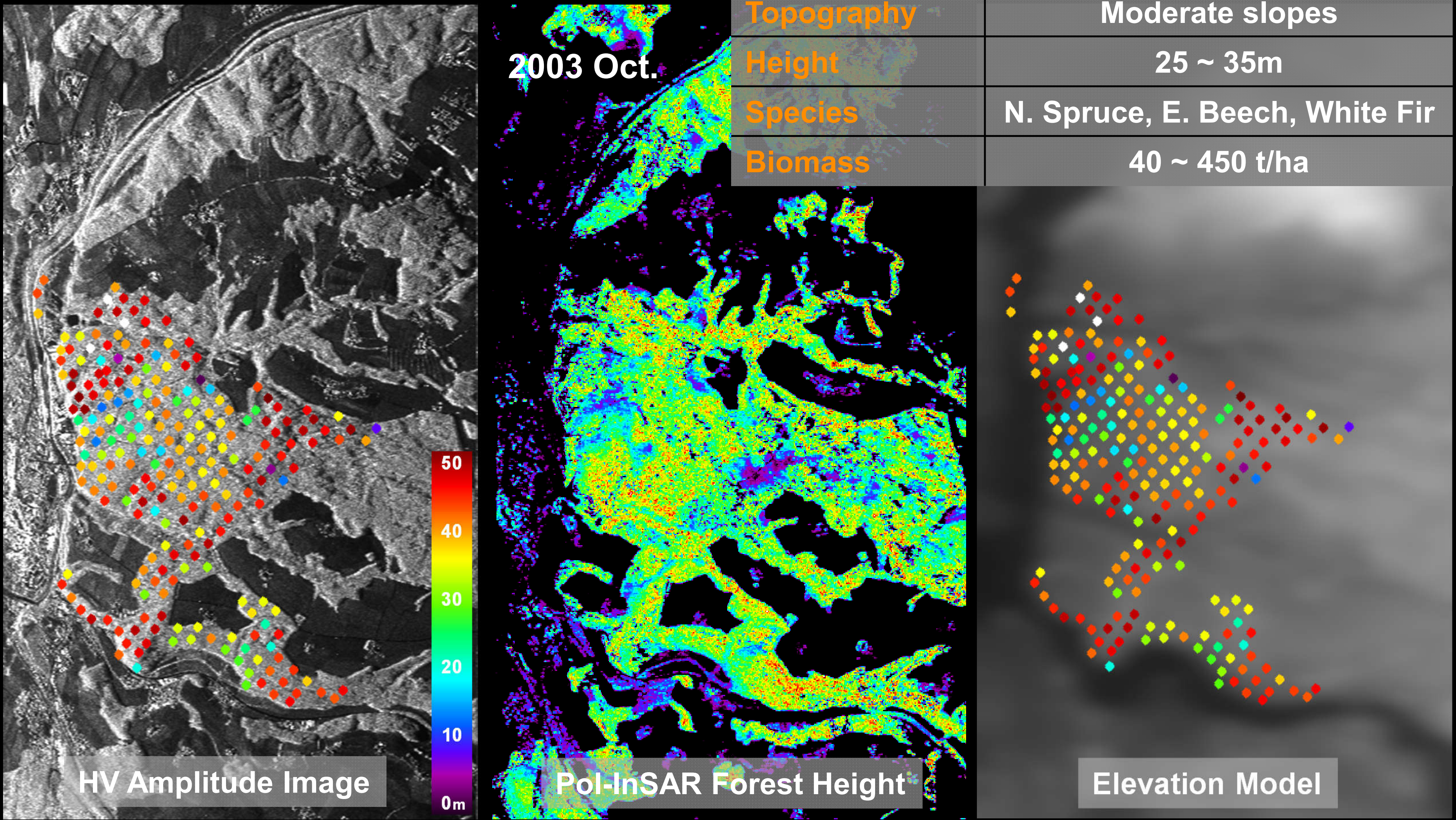

Traunstein Test Site

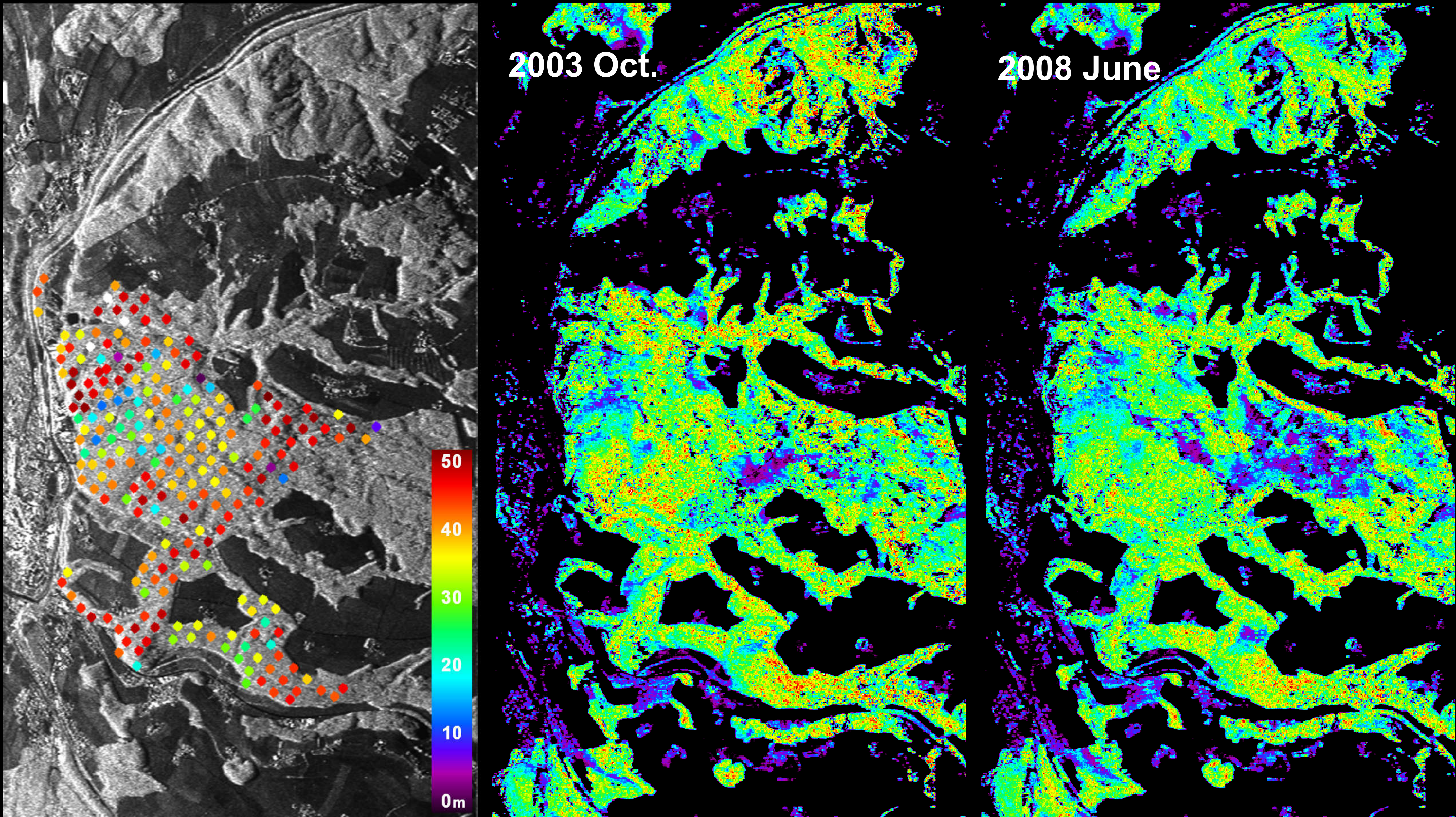

Traunstein Test Site

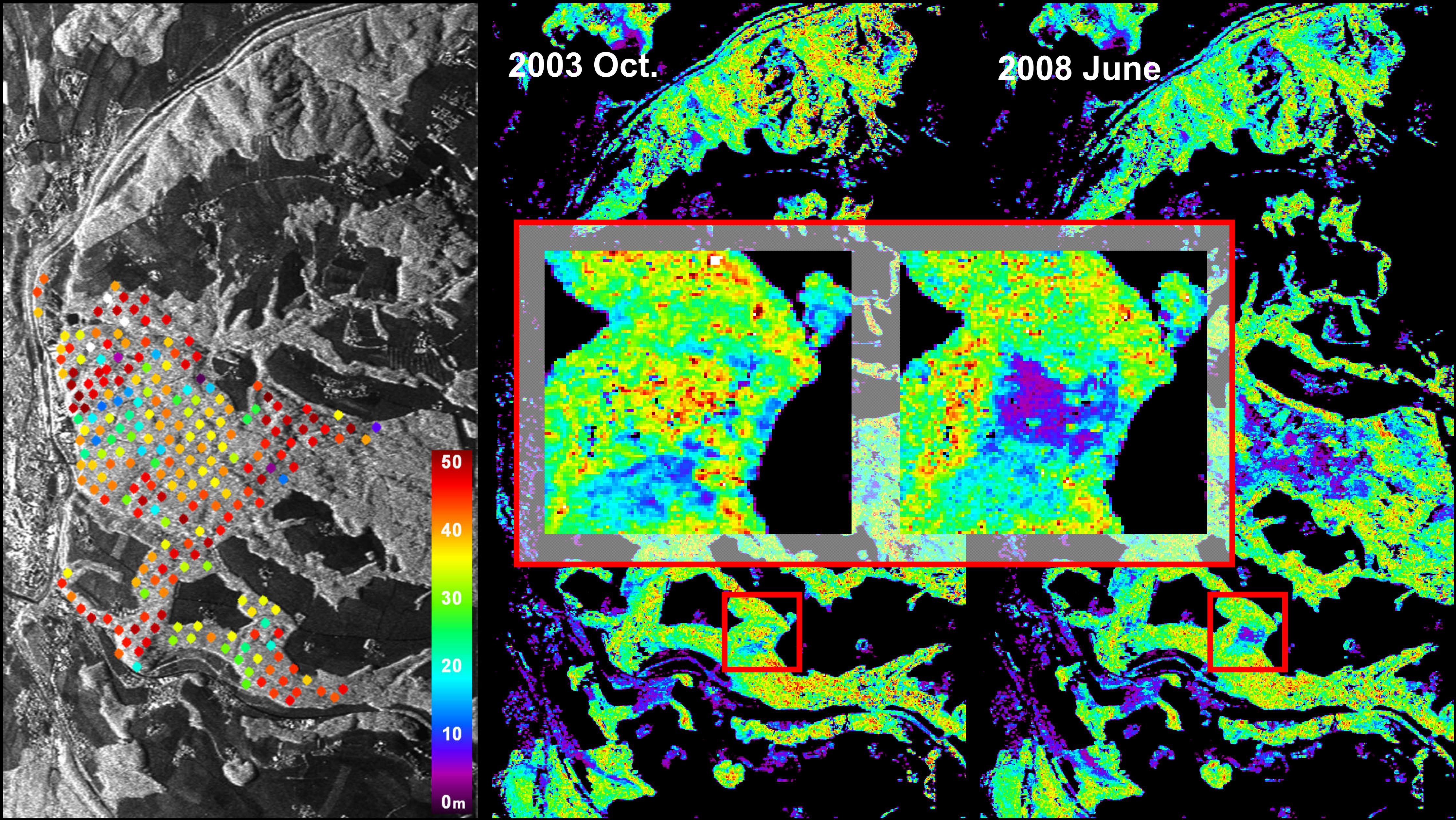

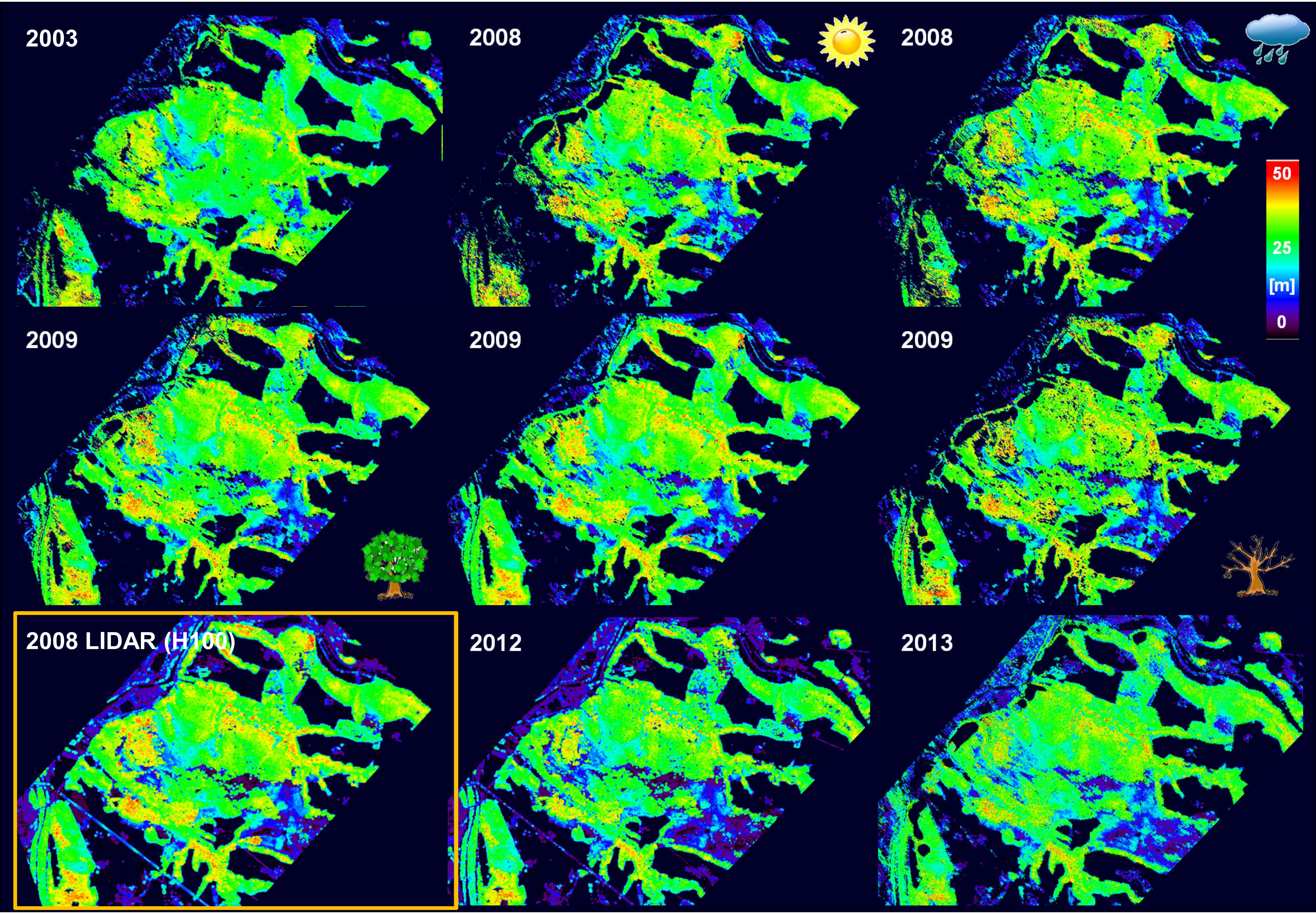

2003
2008
2008
50
25
[m]
0
2009
2009
2009
2008 LIDAR (H100)
2012
2013

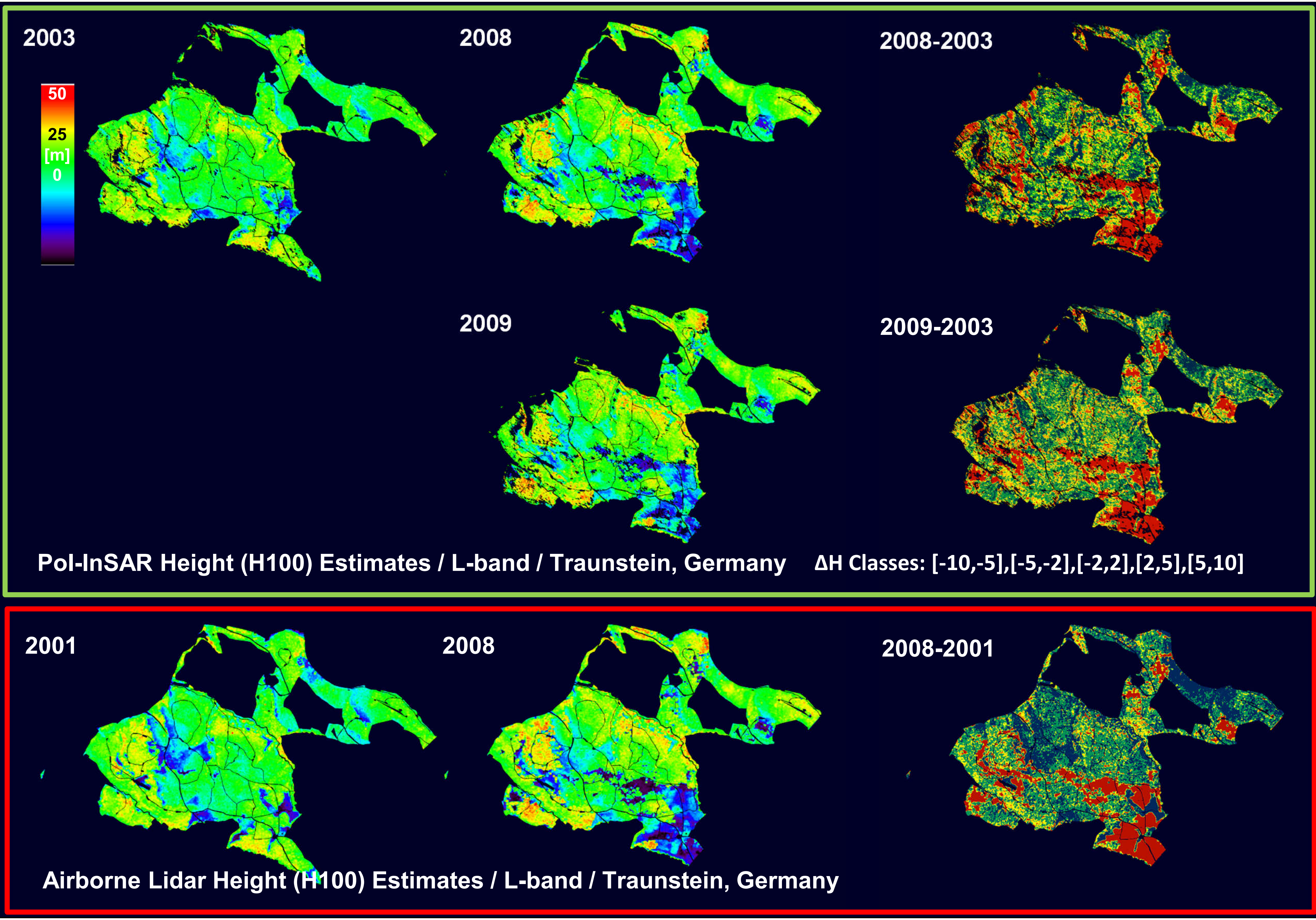
2003
2008
2008-2003
50
25
[m]
0
2009
2009-2003
Pol-InSAR Height (H100) Estimates / L-band / Traunstein, Germany
ΔH Classes: [-10,-5],[-5,-2],[-2,2],[2,5],[5,10]
2001
2008
2008-2001
Airborne Lidar Height (H100) Estimates / L-band / Traunstein, Germany

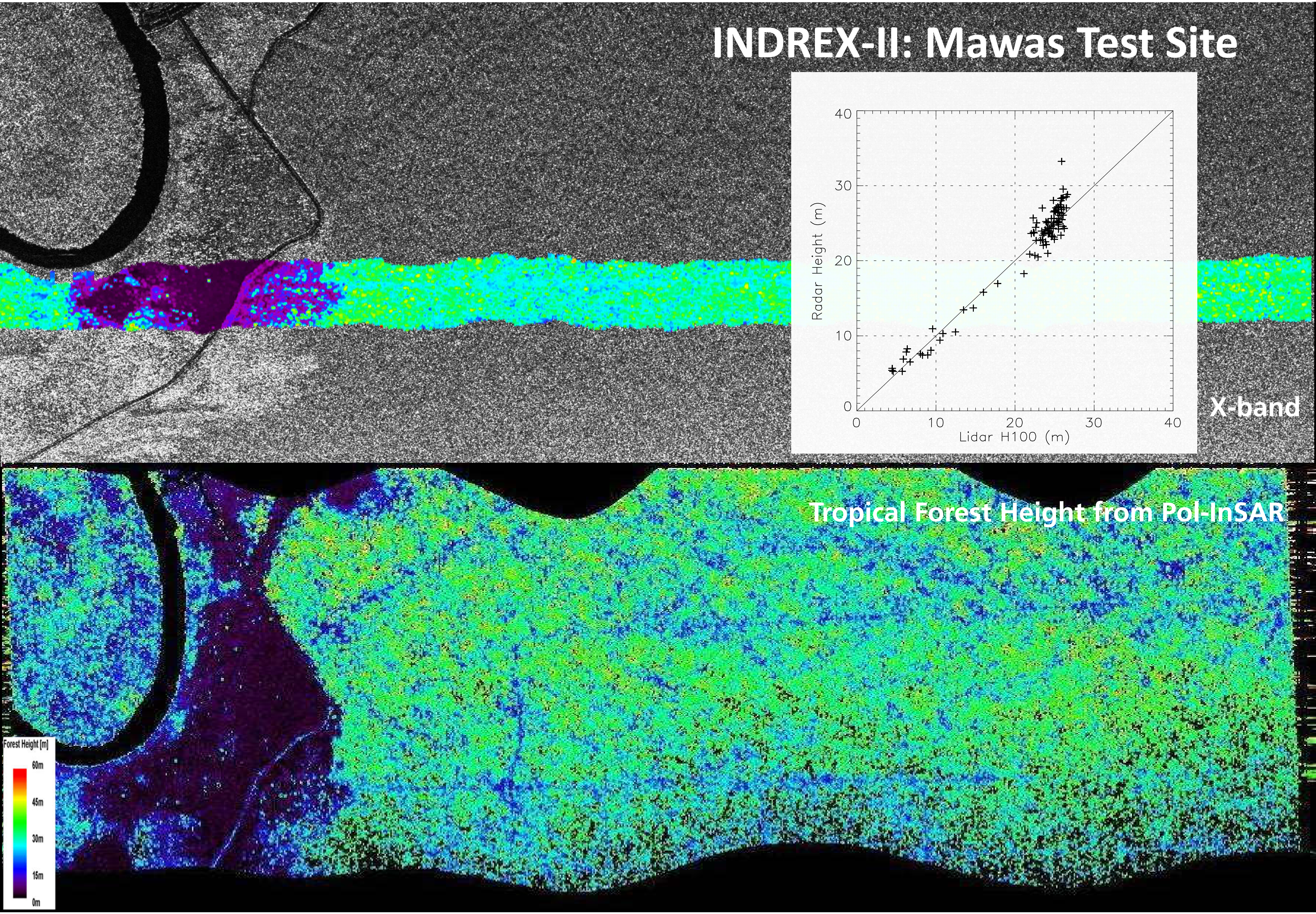

INDREX-II: Mawas Test Site
Radar Height (m)
Lidar H100 (m)
0
10
20
30
40
X-band
Tropical Forest Height from Pol-InSAR
Forest Height [m]
60m
45m
30m
15m
0m

Bangladesh Mangrove Height

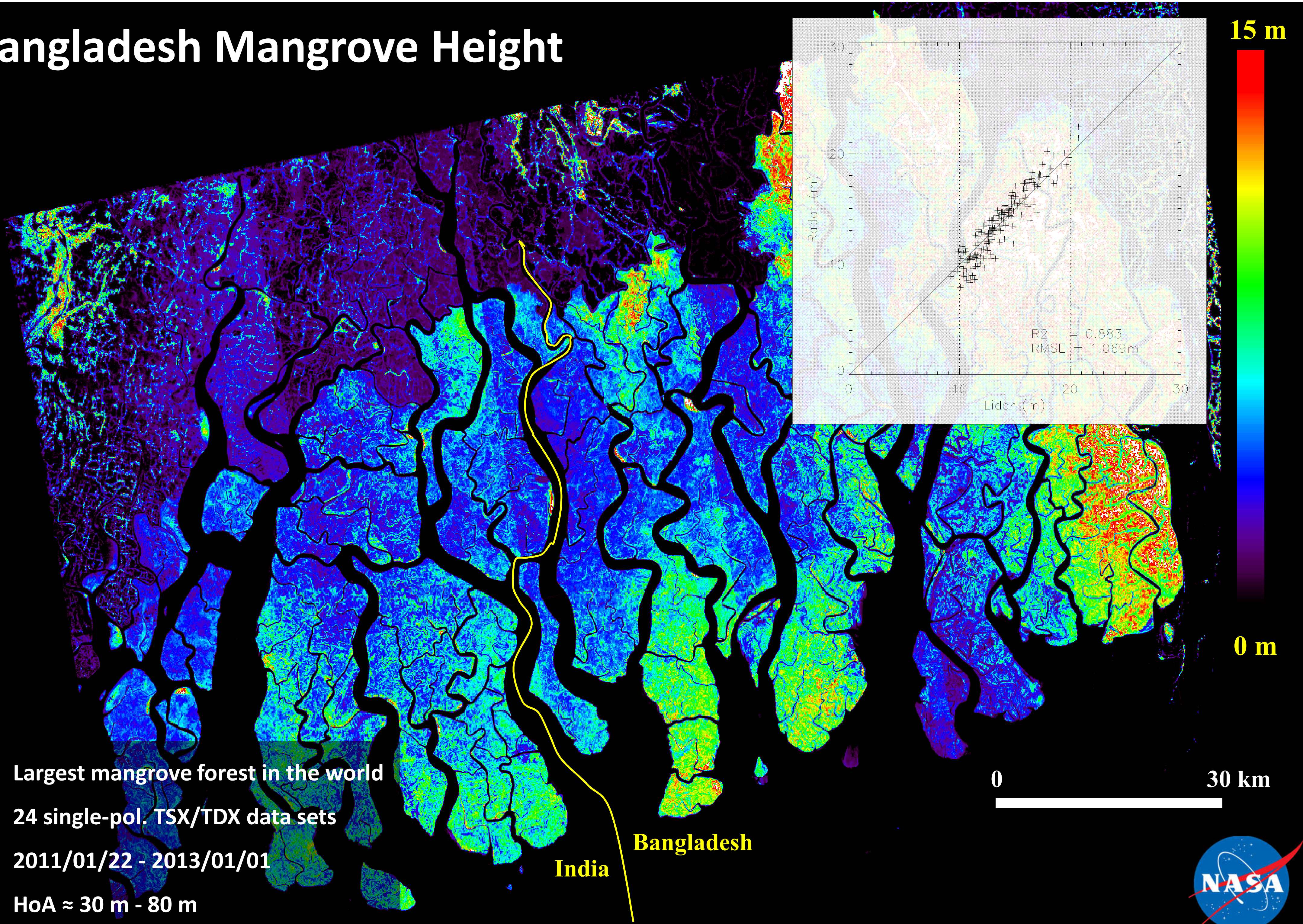

- Largest mangrove forest in the world
- 24 single-pol. TSX/TDX data sets
- 2011/01/22 - 2013/01/01
- HoA ≈ 30 m - 80 m

Polarimetric Coherence Tomography (PCT)

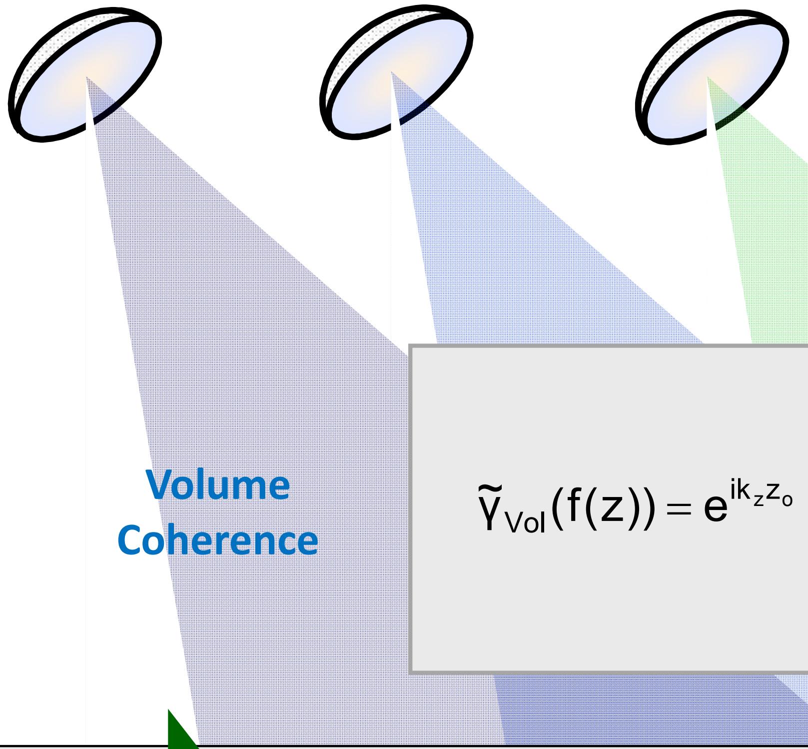

f(z) ... vertical reflectivity function

$$\tilde{\gamma}_{Vol}(f(z)) = e^{ik_z z_o}\frac{\int_o^{h_v} f(z)\, e^{ik_z z} dz}{\int_o^{h_v} f(z)\, dz}$$

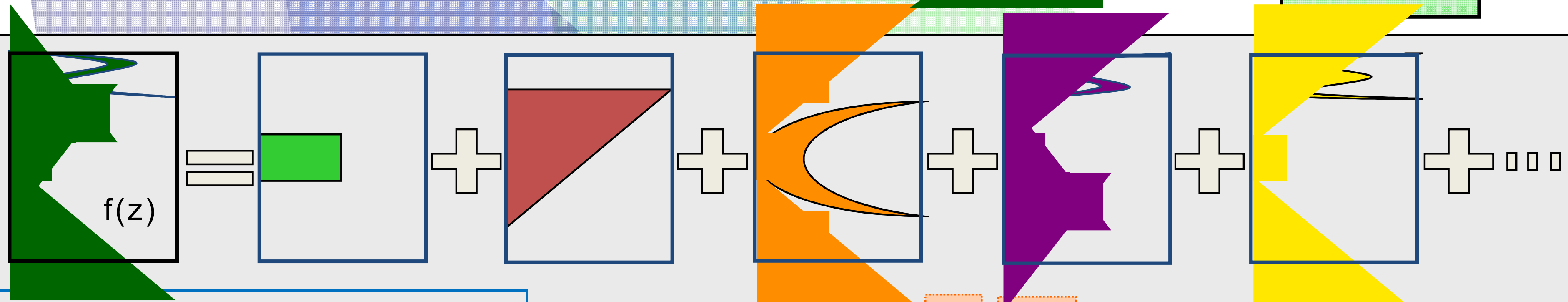

$$\tilde{\gamma}_{Vol}(f(z)) = e^{ik_z z_o}\frac{\int_o^{h_v} f(z)\, e^{ik_z z} dz}{\int_o^{h_v} f(z)\, dz}$$

$$\int_0^{h_v} f(z)\, e^{ik_z z} dz = \frac{h_v}{2}\, e^{i\frac{k_z h_v}{2}} \int_{-1}^{1} (1 + f(z'))\, e^{i\frac{k_z h_v}{2} z'} dz'$$

$$\int_0^{h_v} f(z)\, dz = \frac{h_v}{2} \int_{-1}^{1} (1 + f(z'))\, dz'$$

Fourier Legendre Series: $f(z') = \sum_n a_n P_n(z')$ **where** $a_n = \frac{2n+1}{2}\int_{-1}^{1} f(z')P_n(z')dz'$

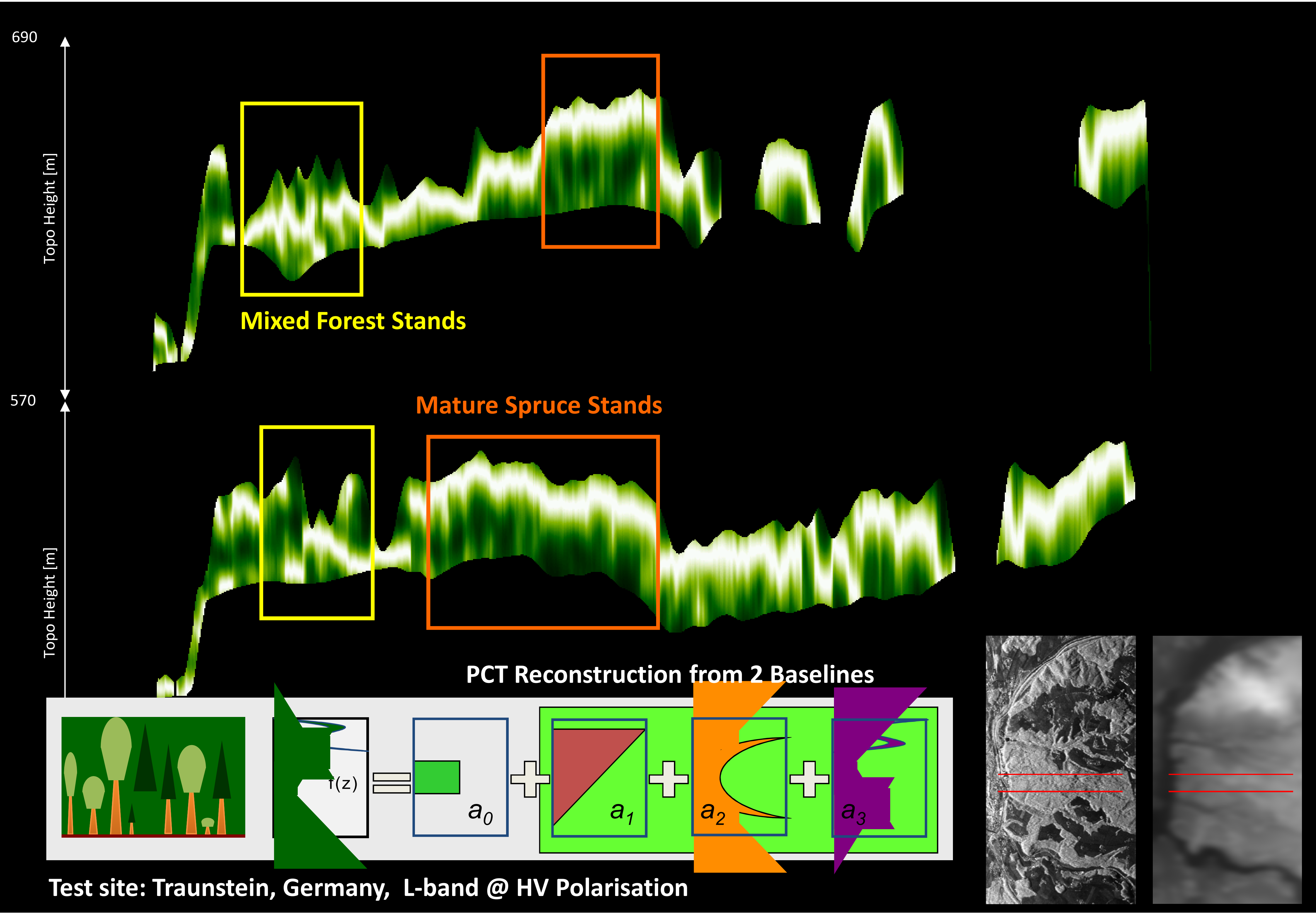

690
570
Topo Height [m]
Topo Height [m]
Mixed Forest Stands
Mature Spruce Stands
PCT Reconstruction from 2 Baselines
f(z)
a_0
a_1
a_2
a_3
Test site: Traunstein, Germany, L-band @ HV Polarisation

Agriculture Pol-InSAR Applications

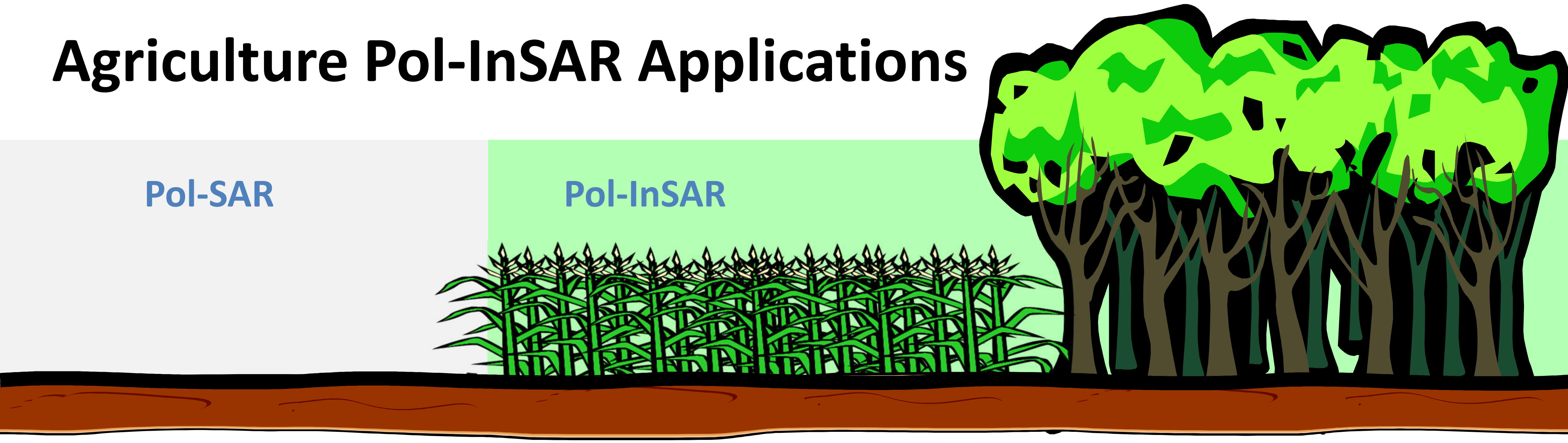

Bare Surfaces: Isolated Scattering Center
- Low Entropy scatterers -> High polarimetric coherence
- The interferometric coherence is baseline independent

Vegetated Surfaces: Volume Scatterers
- High Entropy scatterers -> Low polarimetric coherence
- The interferometric coherence depends on the baseline

Forest vs Agricultural Vegetation	Impact
Orientation effects in the vegetation layer	Anisotropic Propagation
Thinner / shorter vegetation layer	Increased importance of ground scattering
Short crop / plant phenological cycle	Short spatial / large temporal baseline
Variety of crop / plant structure	Abstract modelling

Agriculture Vegetation @ Alling/Germany 2000

Test Site: Kuettighoffen, Switzerland

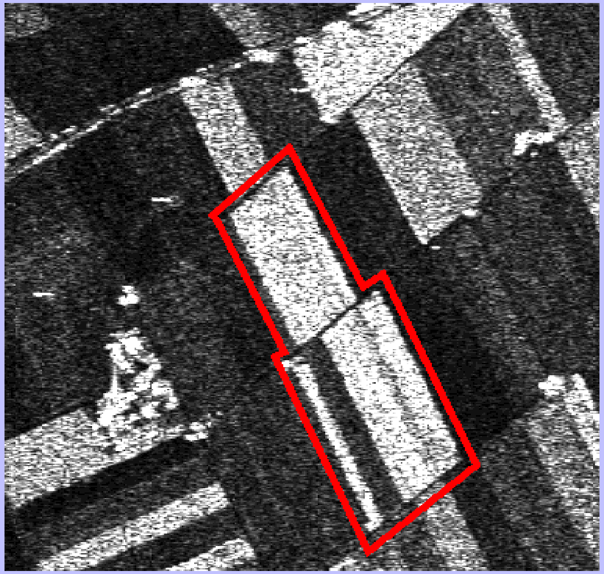

SAR Image @ L-band

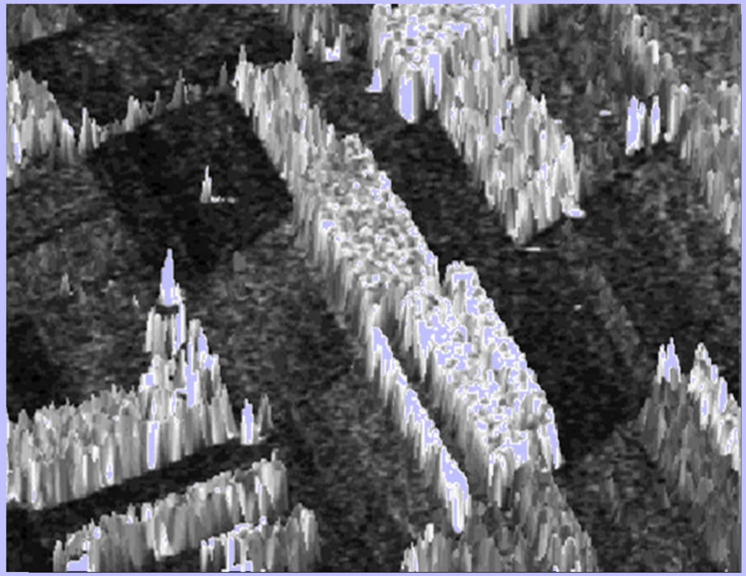

3-D Height Map

E-SAR / Test Site: Alling, Germany

Interferometric Coherence:

$$\tilde{\gamma}(\vec{w}) = \exp(i\varphi_0)\frac{\tilde{\gamma}_V(\vec{w}) + m(\vec{w})}{1 + m(\vec{w})}$$

$$\tilde{\gamma}_V(\vec{w}) = \frac{I}{I_0}$$

$$I = \int_0^{h_V} \exp(i\kappa_z z')\exp\left(\frac{2\,\sigma(\vec{w})\,z'}{\cos\theta_0}\right)dz'$$

$$I_0 = \int_0^{h_V} \exp\left(\frac{2\,\sigma(\vec{w})\,z'}{\cos\theta_0}\right)dz'$$

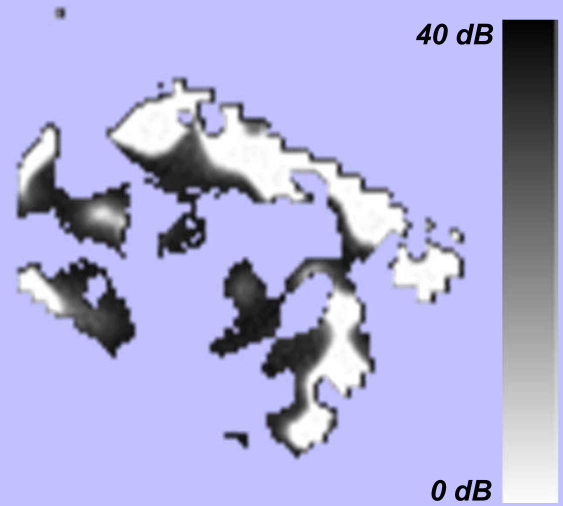

Differential Extinction

AGRISAR @ L-band in April 2006

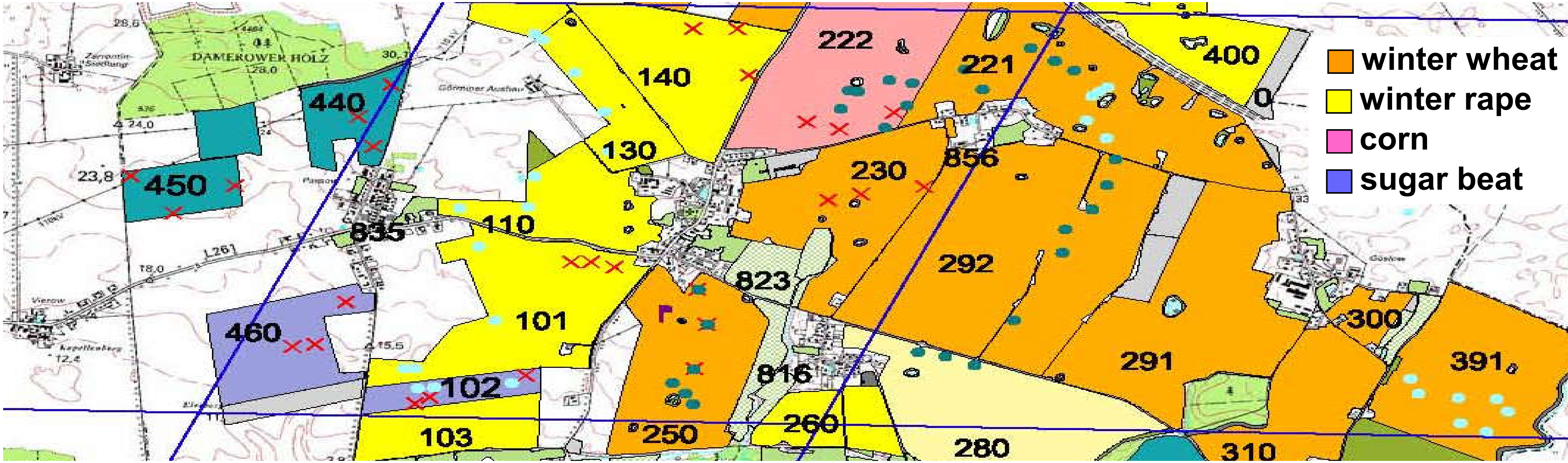

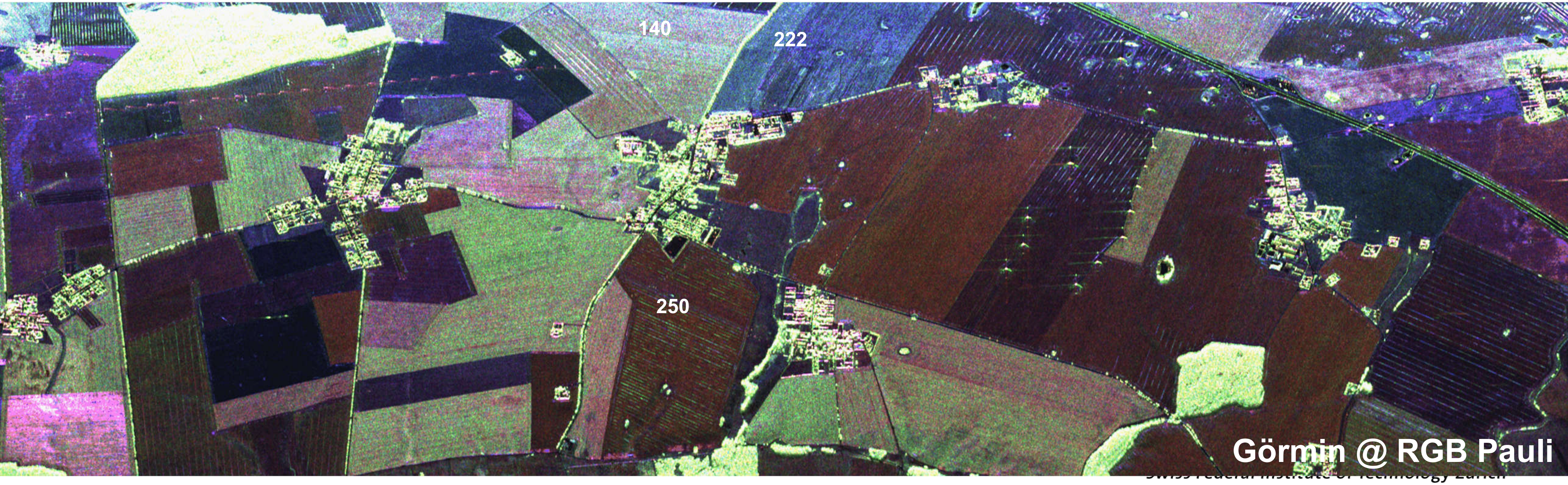

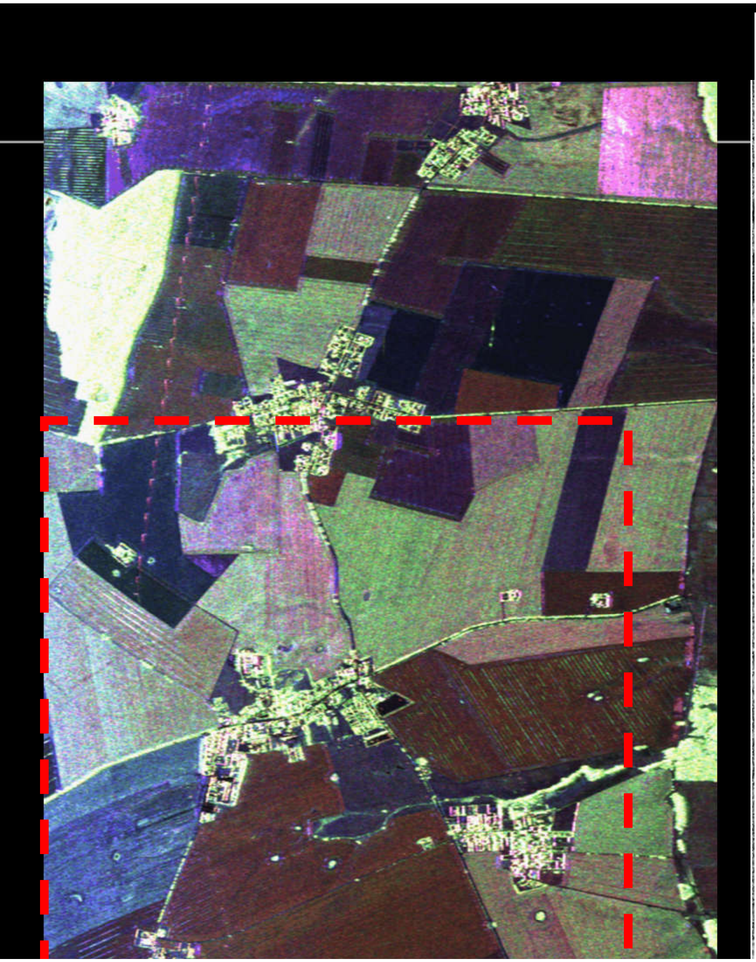

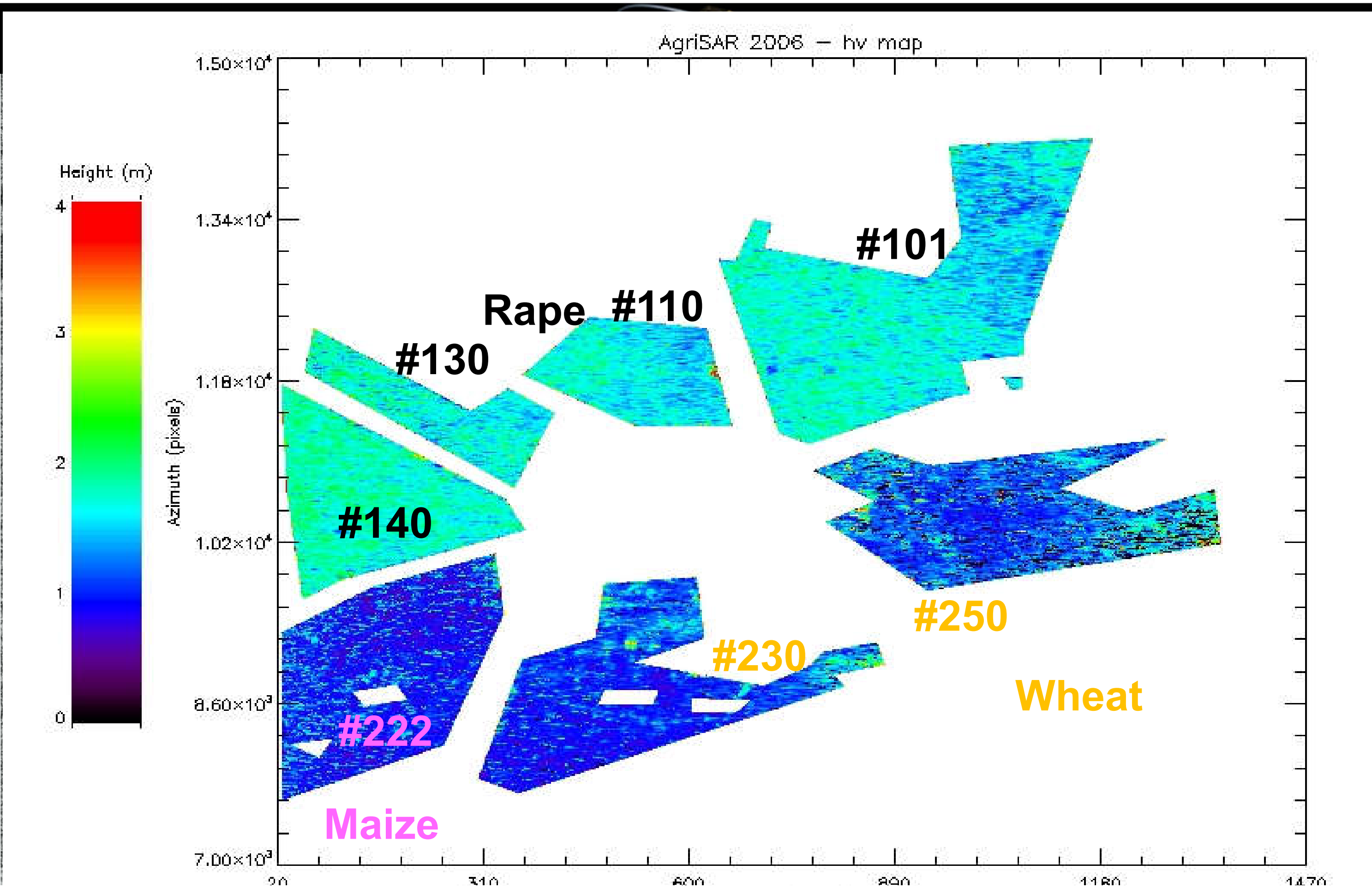

AgriSAR 2006 – hv map
Height (m)
Azimuth (pixels)
Rape
#101
#110
#130
#140
#222
Maize
#230
#250
Wheat

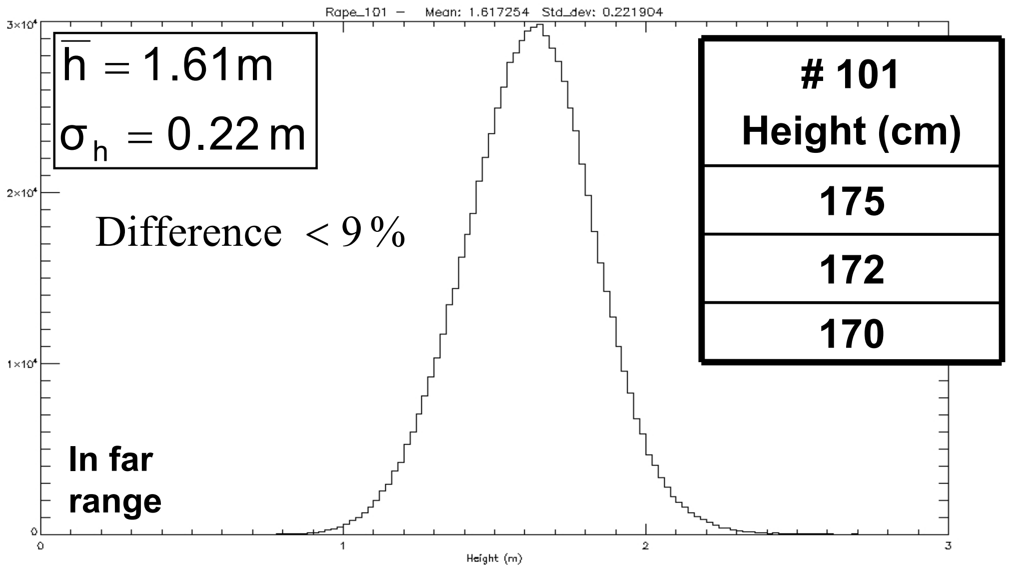

Rape_101 – Mean: 1.617254 Std_dev: 0.221904
$\bar{h} = 1.61\,m$
$\sigma_h = 0.22\,m$
Difference $< 9\,\%$
101
Height (cm)
175
172
170
In far range
Height (m)

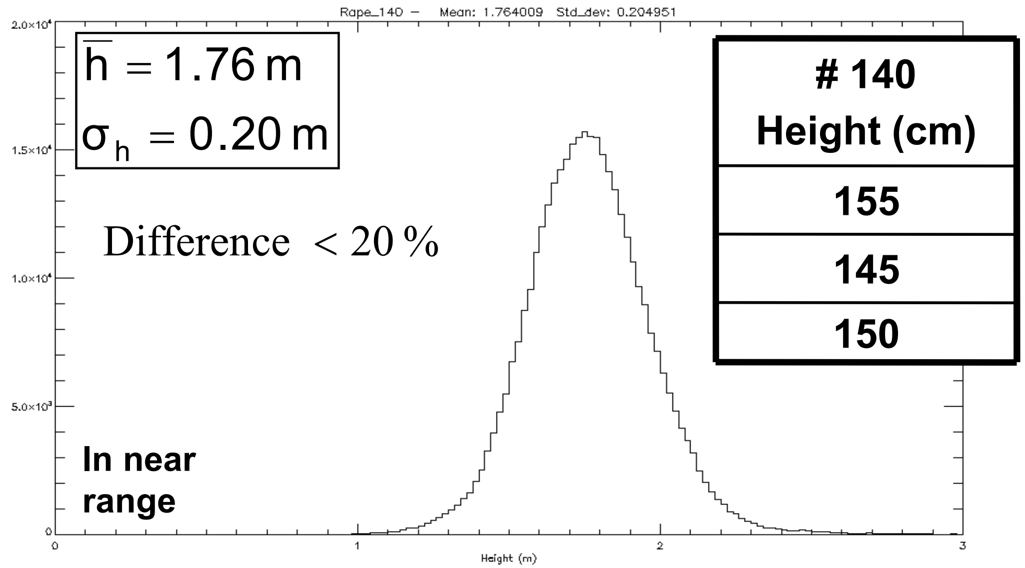

Rape_140 – Mean: 1.764009 Std_dev: 0.204951
$\bar{h} = 1.76\,m$
$\sigma_h = 0.20\,m$
Difference $< 20\,\%$
140
Height (cm)
155
145
150
In near range
Height (m)

CROP-EX 2014: Crop height estimation from Pol-InSAR data

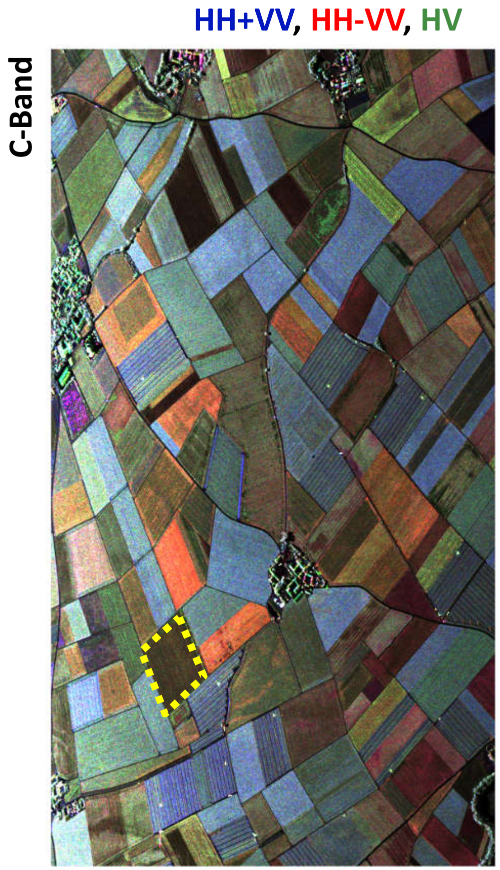

Wheat

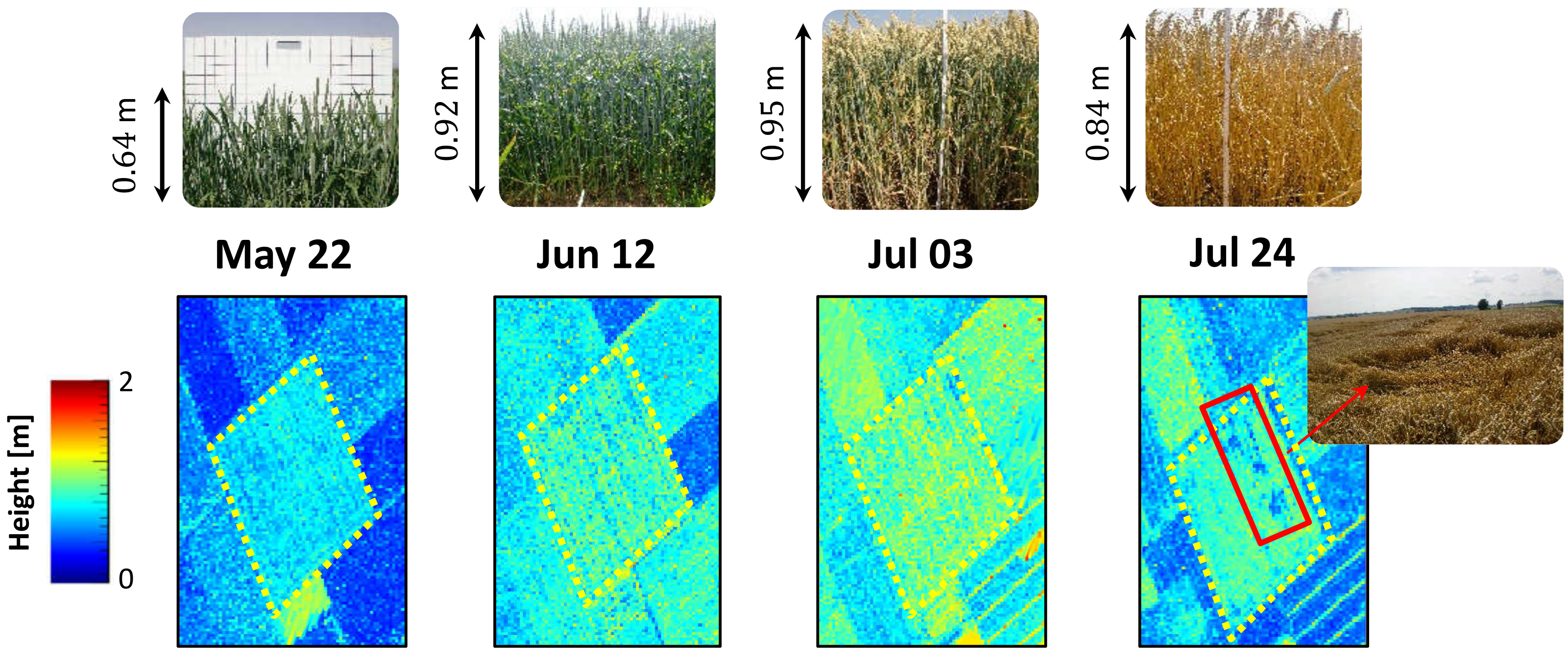

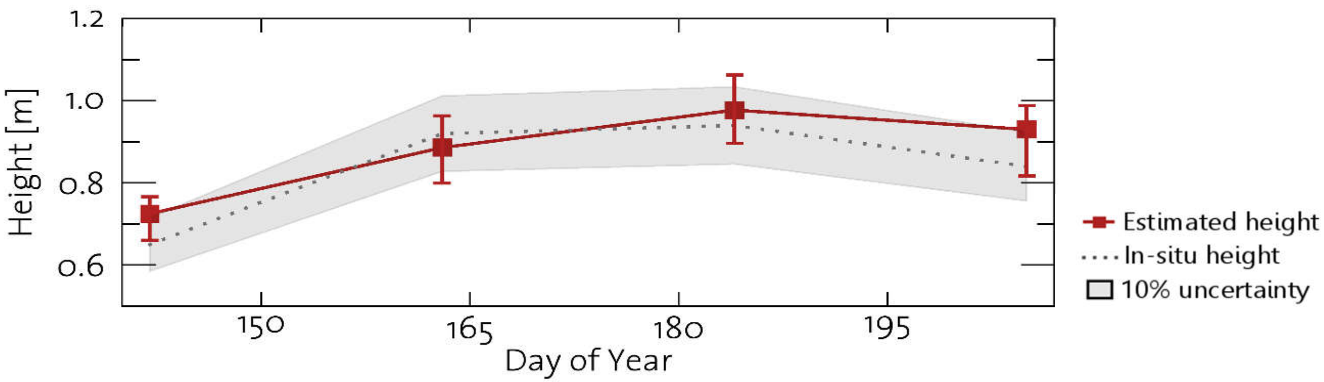

Sensor: DLR's F-SAR (airborne)
Frequency: C-Band (≈5 GHz)
Number of spatial baselines: 2 (k_V between 2 rad and 4 rad)
Max. temporal baseline: 90 minutes
Equivalent Number of Looks: 100

CROP-EX 2014: Crop height estimation from Pol-InSAR data

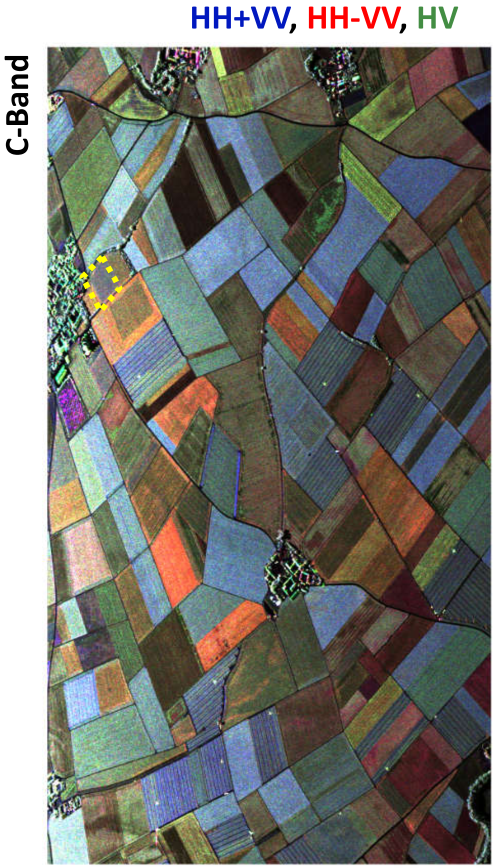

Maize

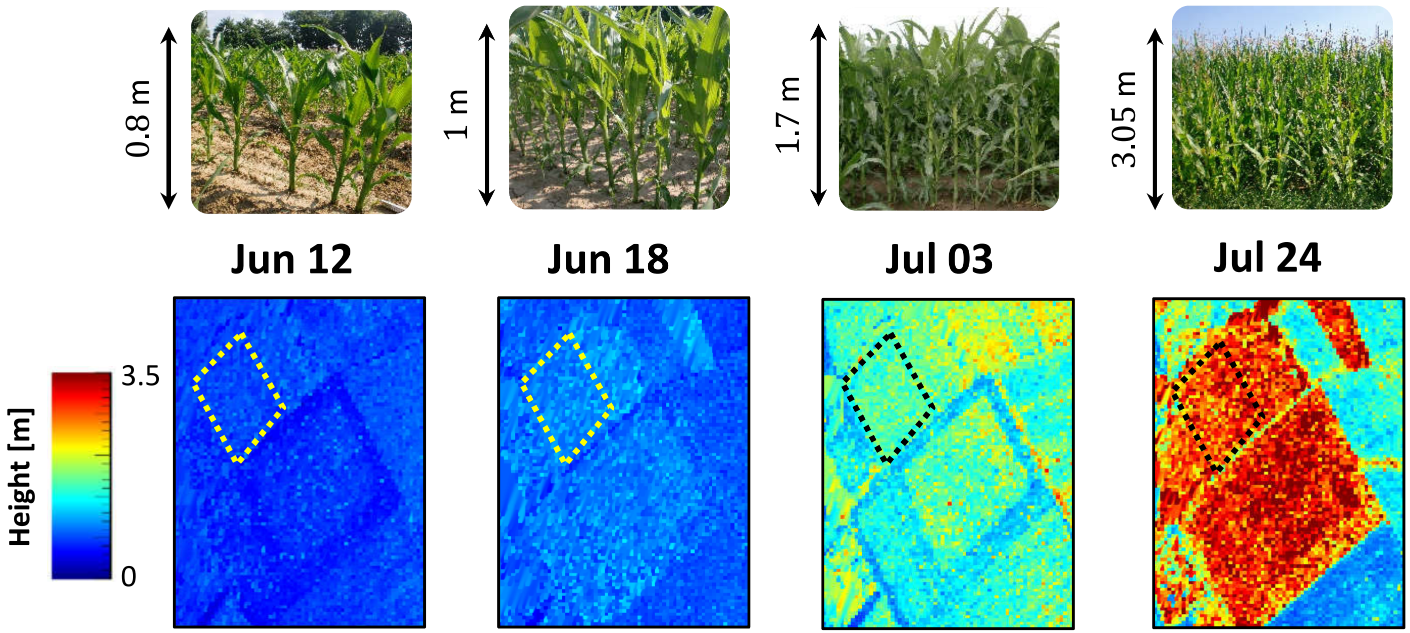

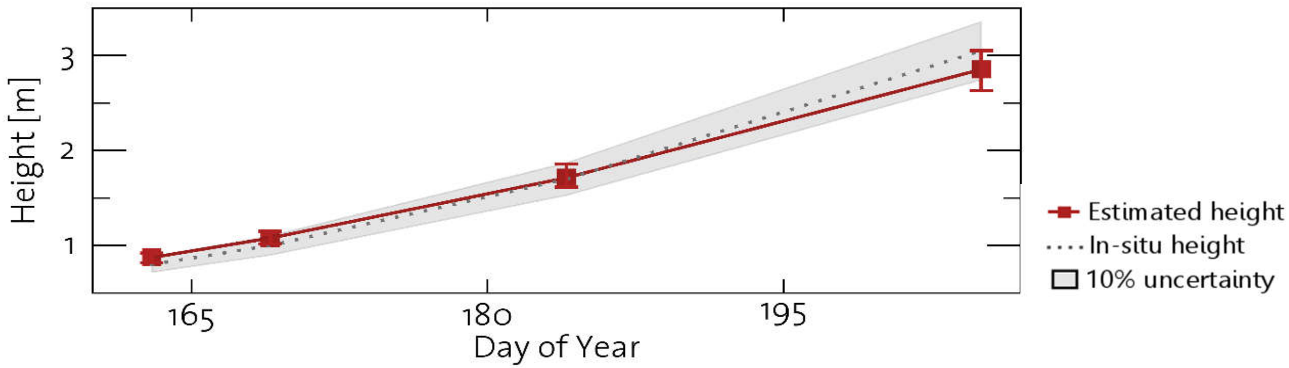

Sensor: DLR's F-SAR (airborne)
Frequency: C-Band (≈5 GHz)
Number of spatial baselines: 2 (k_V between 2 rad and 4 rad)
Max. temporal baseline: 90 minutes
Equivalent Number of Looks: 100

Earth Observation and Remote Sensing

ETH
Eidgenössische Technische Hochschule Zürich
Swiss Federal Institute of Technology Zurich

D-InSAR Soil Mapping @ different Polarisation and L-band

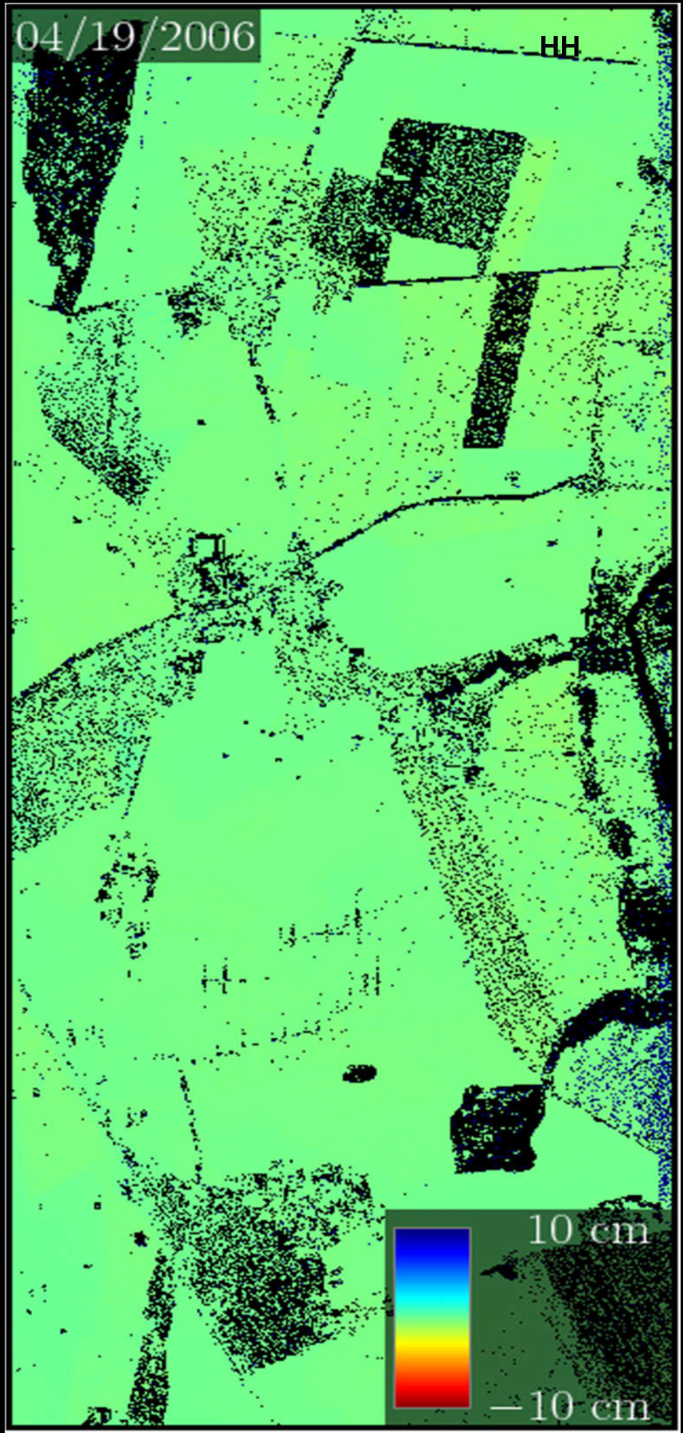

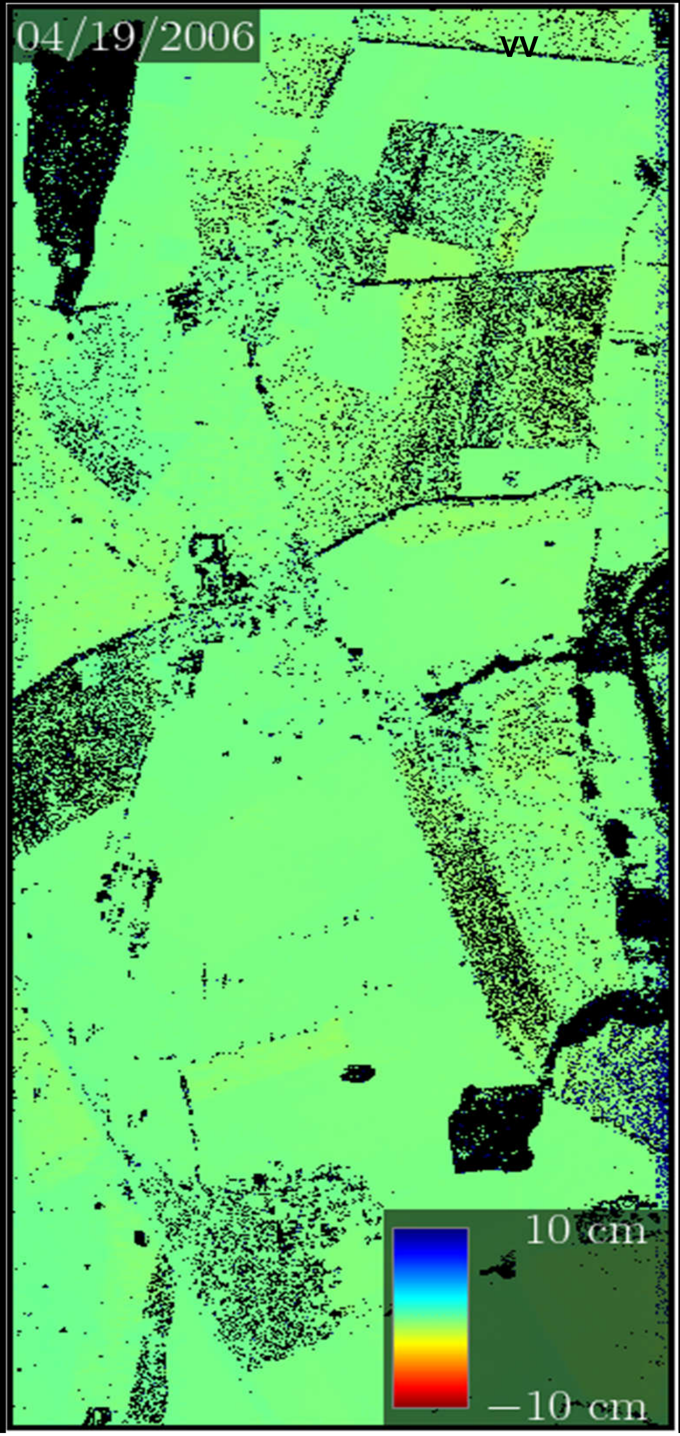

Deformation Change in Time @ Winter Rape (101-1)

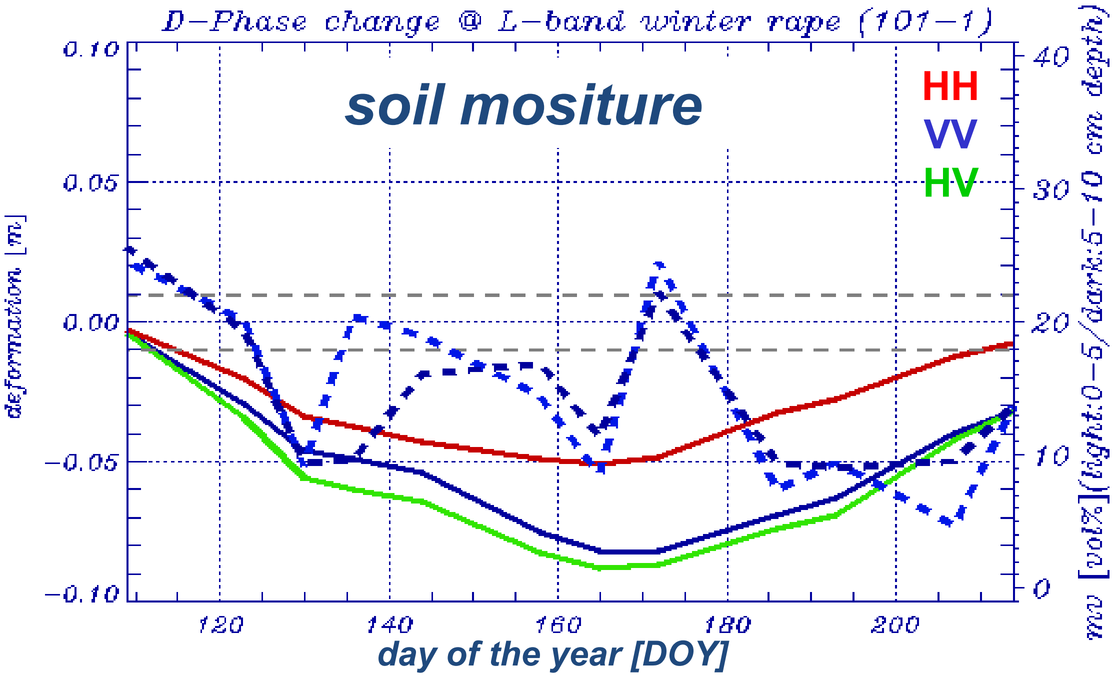

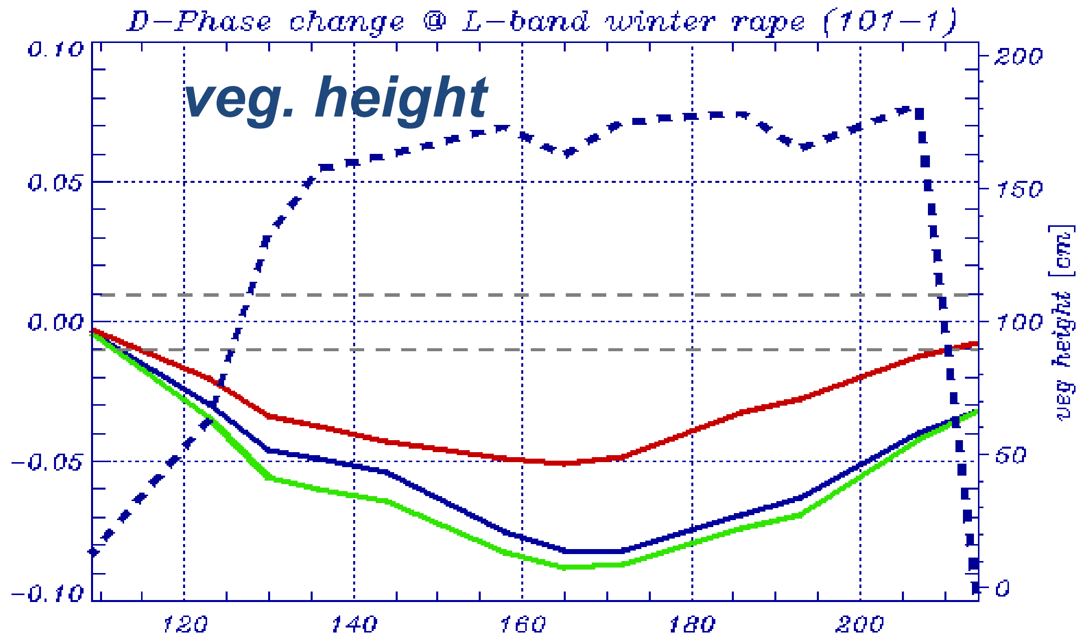

- Deformation up to 9 mm in VV & HV and up to 5 mm for HH
- Soil moisture: slight correlation over time – no correlation with local variation
- Veg. height: slight correlation in the beginning and no sensitivity in time
- Biomass: best correlation results over time

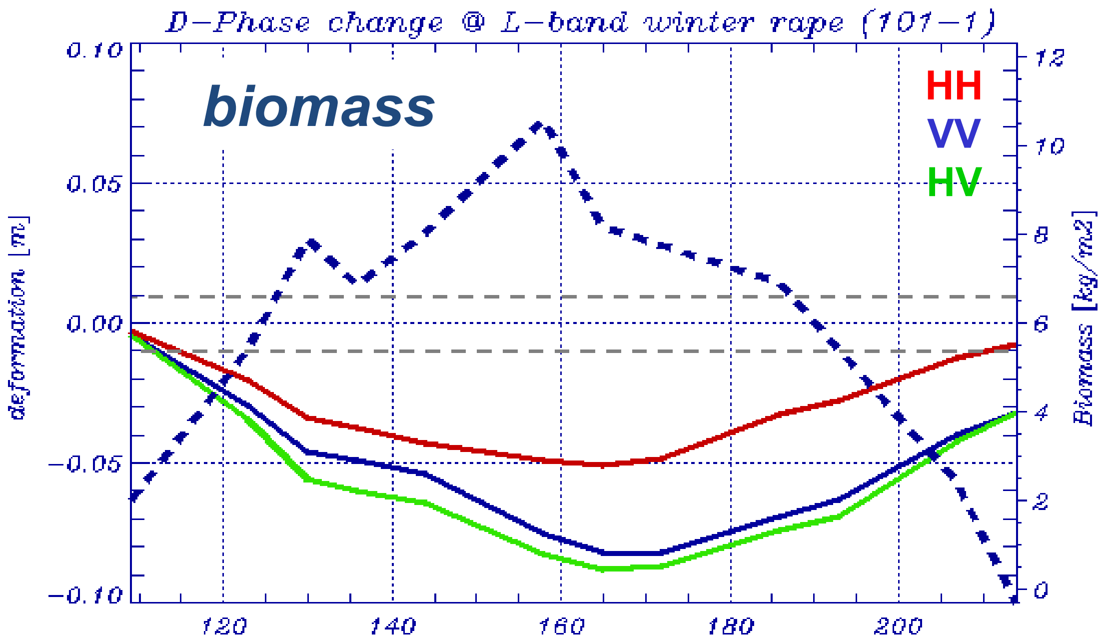

hajnsek@ifu.baug.ethz.
irena.hajnsek@dlr.de

Structure Parameters & Applications

Forest

- Forest Height
- Forest (Vertical) Structure
- Forest Biomass
- Underlying Topography

- Forest Ecology
- Forest Management
- Ecosystem Modeling
- Climate Change

Agriculture

- Underlying Soil Moisture
- Moisture of Vegetation Layer
- Height of Vegetation Layer
- Soil Roughness

- Farming Management
- Ecosystem Modeling
- Water Cycle / CC
- Desertification

Snow & Ice

- Ice Layer Structure
- Penetration Depth (Ice)
- Snow Layer Thickness
- Snow Water Equivalent

- Ecosystem Change
- Water Cycle
- Water Management

Snow

First Pol-InSAR Snow Experiment in Austria 2004

E-SAR: Kuehtai / Austria 2004 Cooperation with University of Innsbruck

Campaign Objectives:

Investigation of Pol-InSAR for snow characterisation

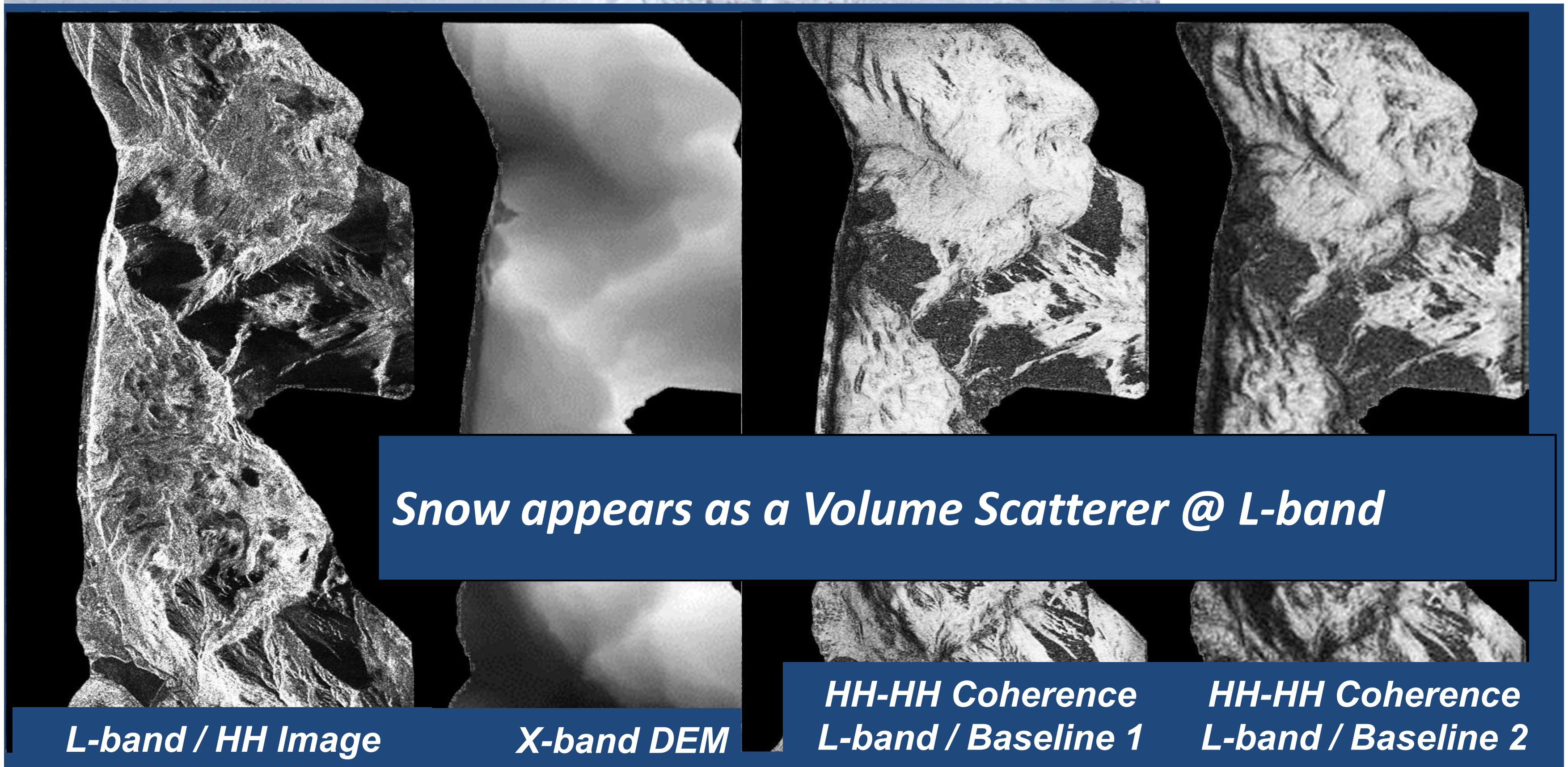

Snow Depth Estimation

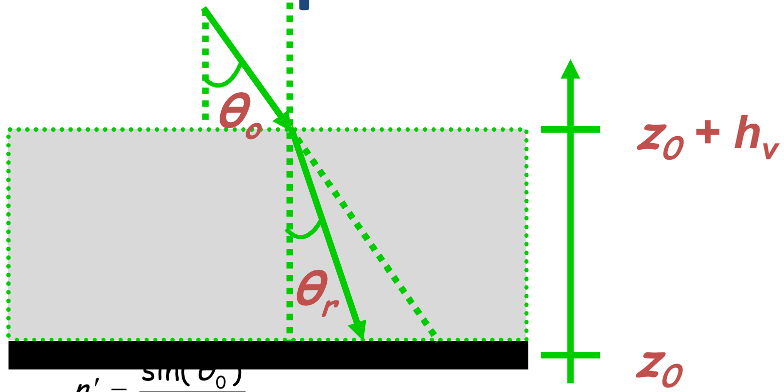

$$n' = \frac{\sin(\theta_0)}{\sin(\theta_r)}$$

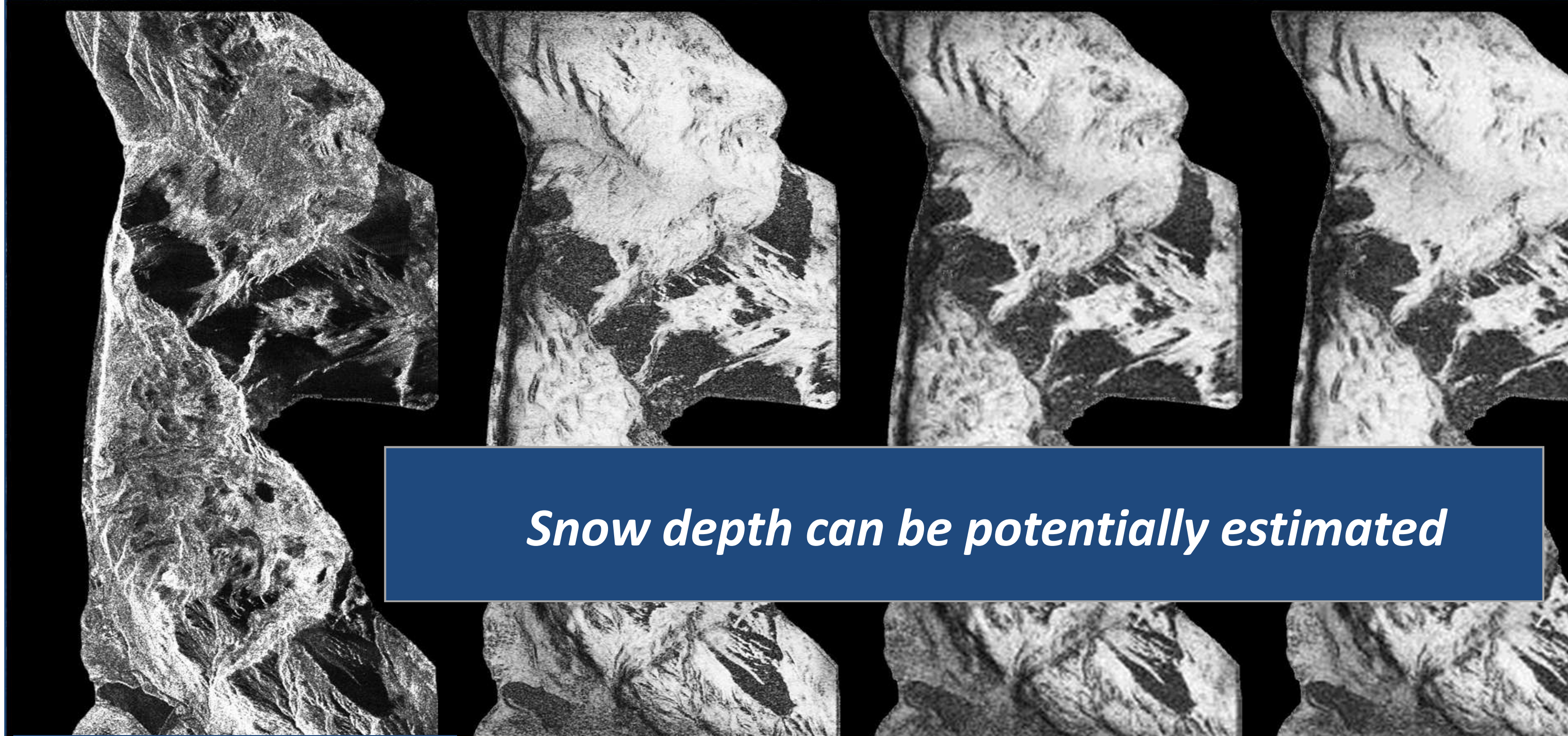

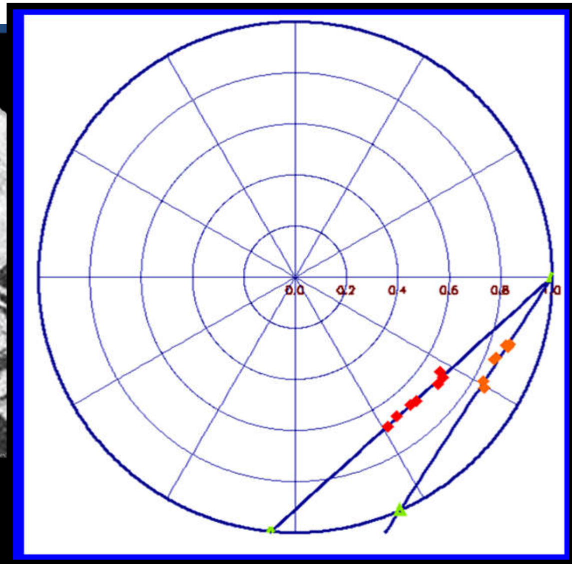

Snow depth can be potentially estimated

Baseline 1 (20M): Δφ=17° -> Δz=1.48m

Baseline 2 (40M): Δφ=28° -> Δz=1.22m

L-band / HH Image | ***HH-HH Coherence*** | ***XX-XX Coherence*** | ***VV-VV Coherence***

hajnsek@ifu.baug.ethz.ch
irena.hajnsek@dlr.de

IceSAR Campaign 2007 @ ~80°N

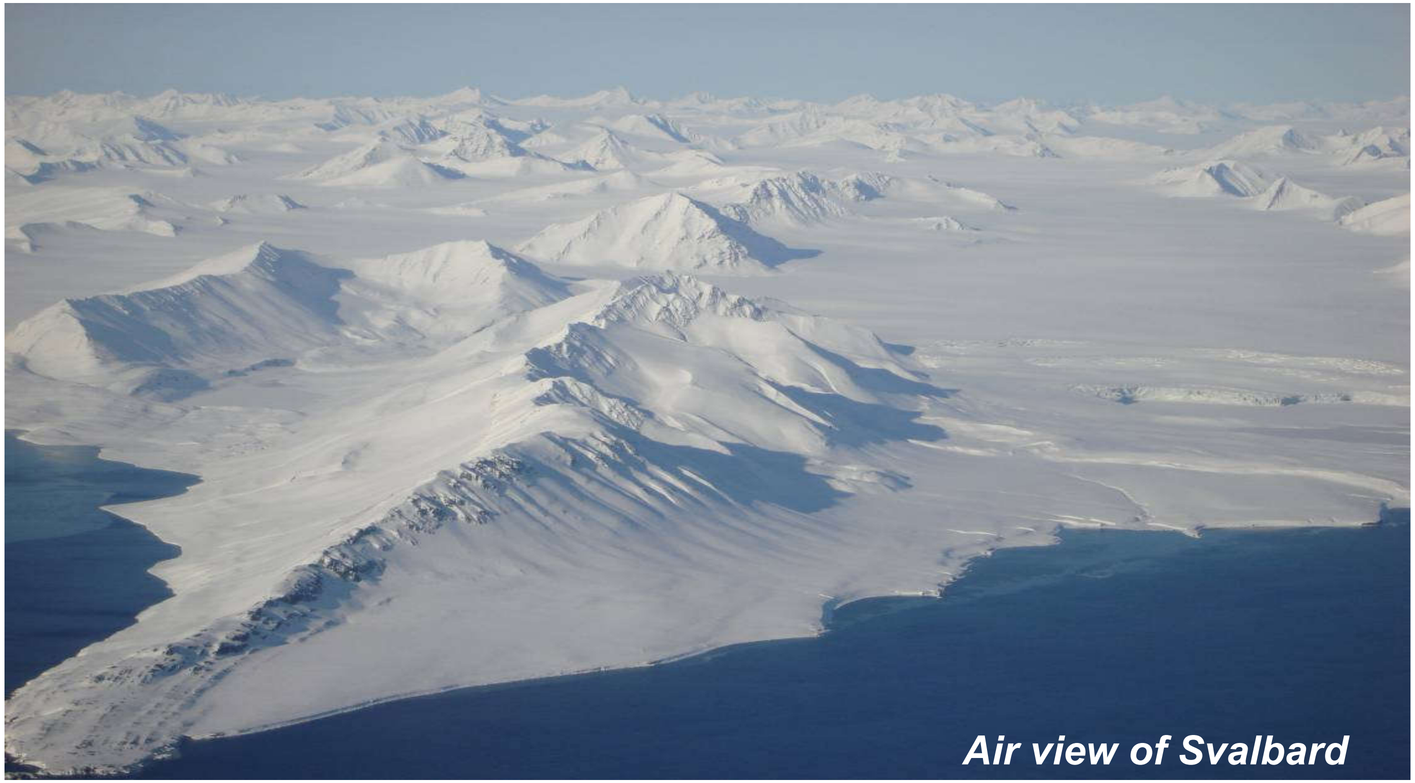
Air view of Svalbard


Base station Oxford


CR Installation


ICESAR Team

Austfonna: 2 Flight Tracks (~ 10km) @ CryoSAT

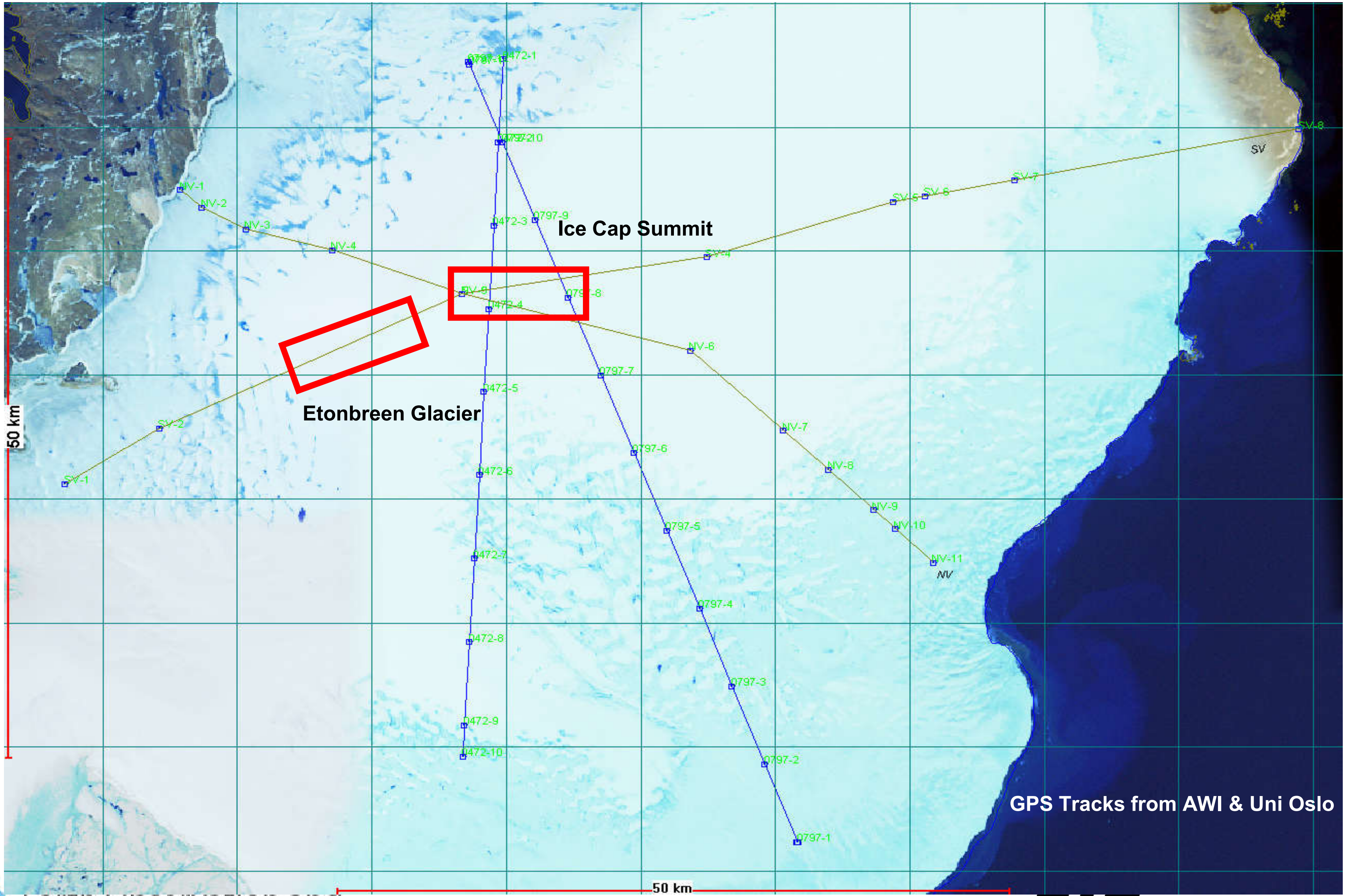

ICESAR Campaign 2007: InSAR Coherences

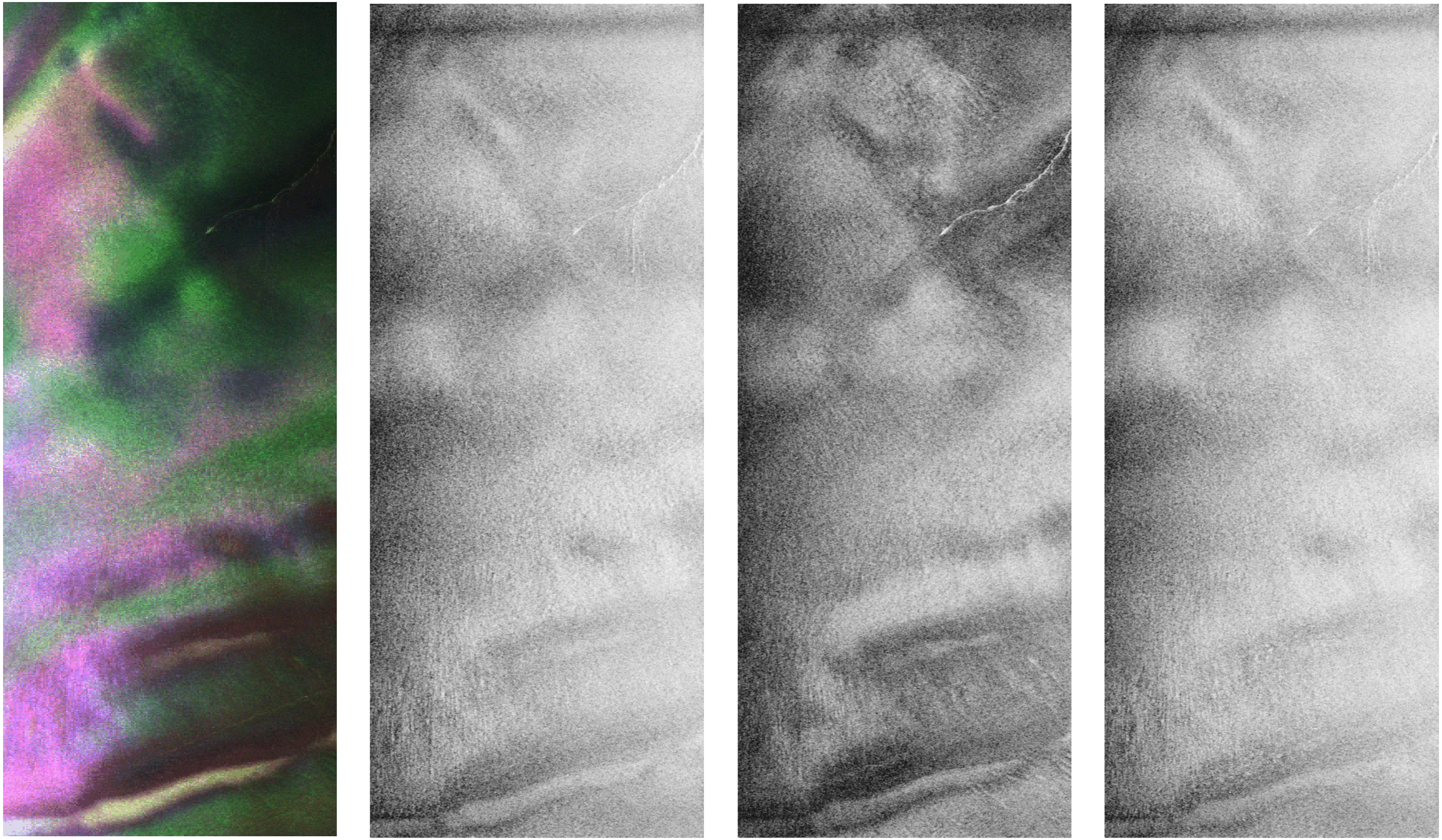

hajnsek@ifu.baug.ethz.ch
irena.hajnsek@dlr.de

Two Layer Ice Model: Ground + Infinite Volume

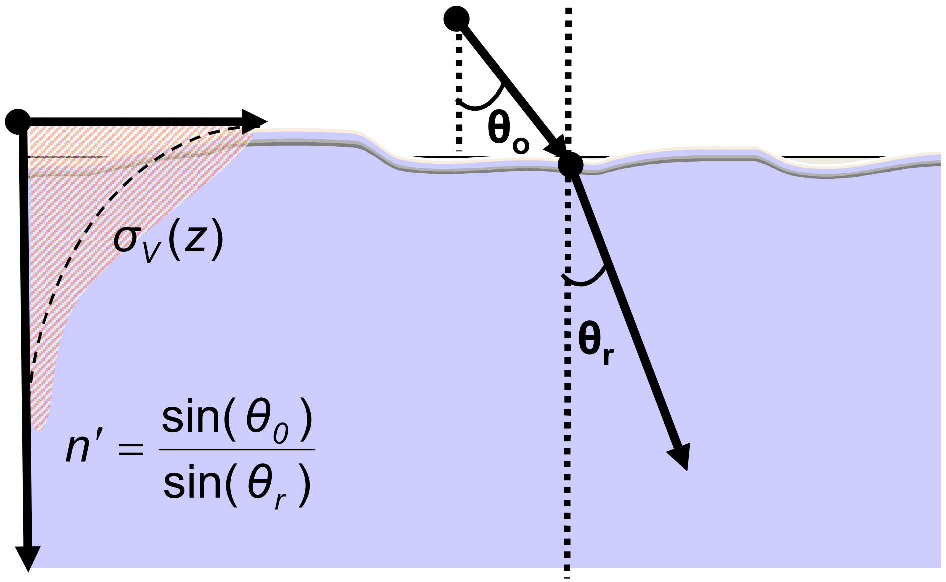

$$n' = \frac{\sin(\theta_0)}{\sin(\theta_r)}$$

Interferometric (Volume) Coherence:

$$\tilde{\gamma}(\vec{w}) = \exp(i\varphi_0)\frac{\tilde{\gamma}_V + m(\vec{w})}{1 + m(\vec{w})}$$

$$\tilde{\gamma}_V = \frac{I}{I_0} = \frac{2\sigma}{2\sigma - i\kappa_z \cos(\theta_r)} = \frac{1}{1 - i\kappa_z d_{2z}}$$

$$I = \int_0^\infty \exp(i\kappa_z z')\exp\left(\frac{2\sigma z'}{\cos\theta_0}\right)dz'$$

$$I_0 = \int_0^\infty \exp\left(\frac{2\sigma z'}{\cos\theta_0}\right)dz'$$

Penetration Depth: $d_{2z} = \frac{1}{2\sigma}\cos(\theta_r)$

G/V R: $m(\vec{w}) = \frac{m_G(\vec{w})}{m_V(\vec{w})T_{a-v}(\vec{w})}$

Vertical Wavenumber: $\kappa_z = \frac{\kappa\Delta\theta_r}{\sin(\theta_r)}$

Wavenumber: $\kappa = \frac{4\pi n'}{\lambda}$

4 Parameters:

Extinction	σ
Ref. Index	n'
Topography	φ_0
G/V Ratio	$m(\vec{w})$

hajnsek@ifu.baug.ethz.ch
irena.hajnsek@dlr.de

Extinction Inversion Results

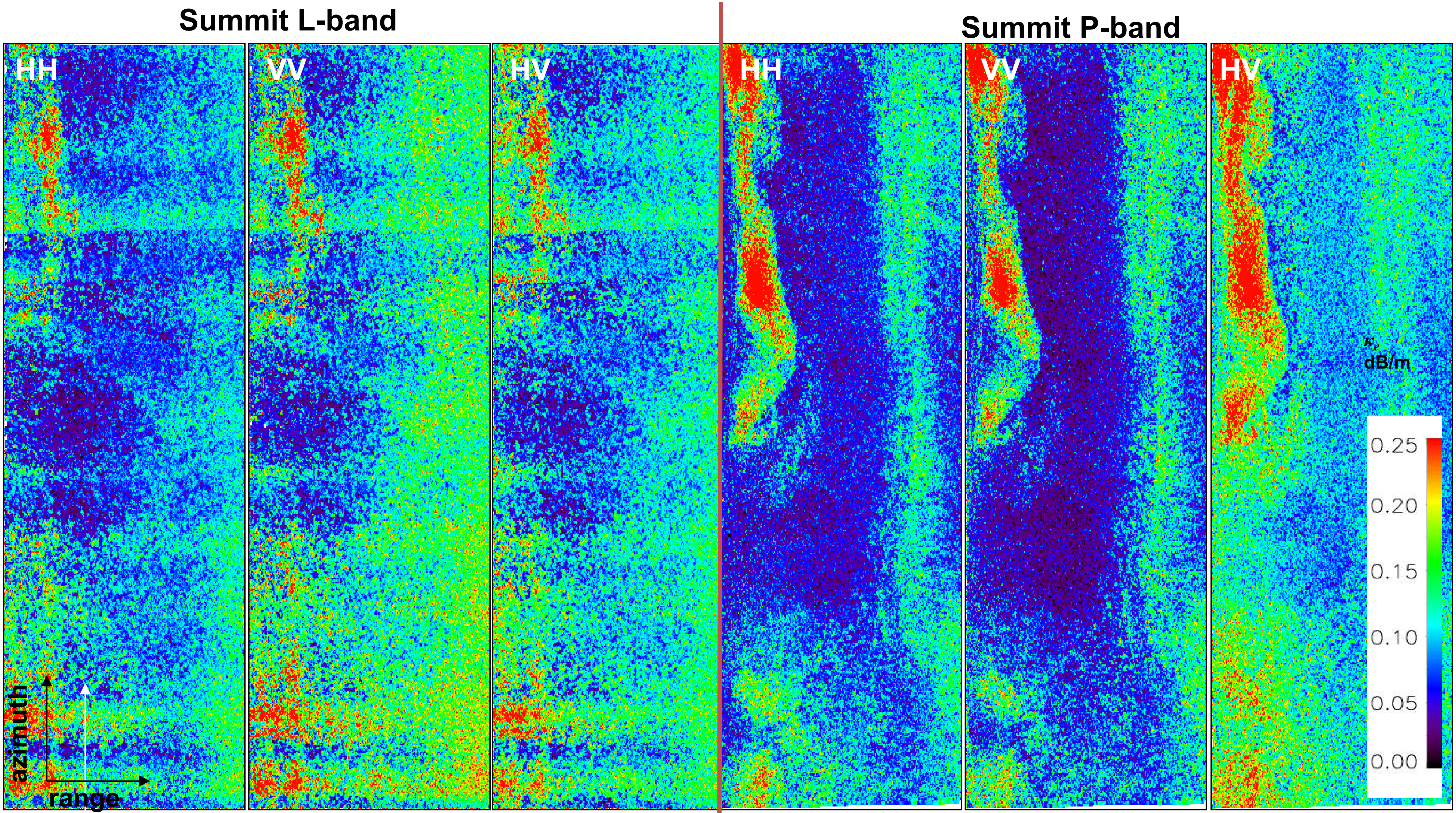

Extinction Inversion Stability

L-band $\sigma°$

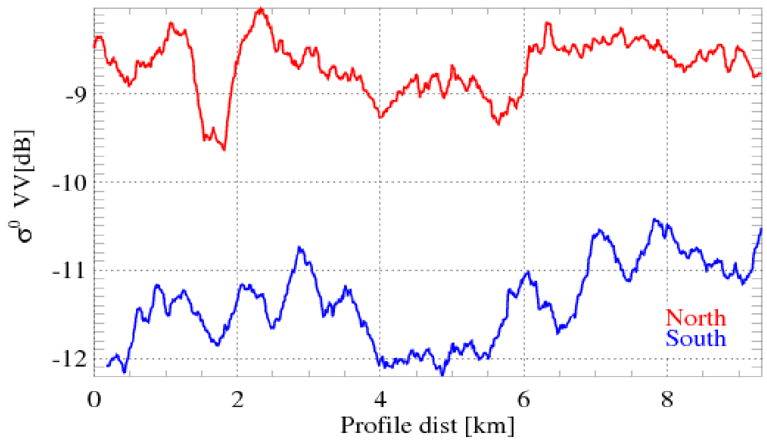

L-band κ_e

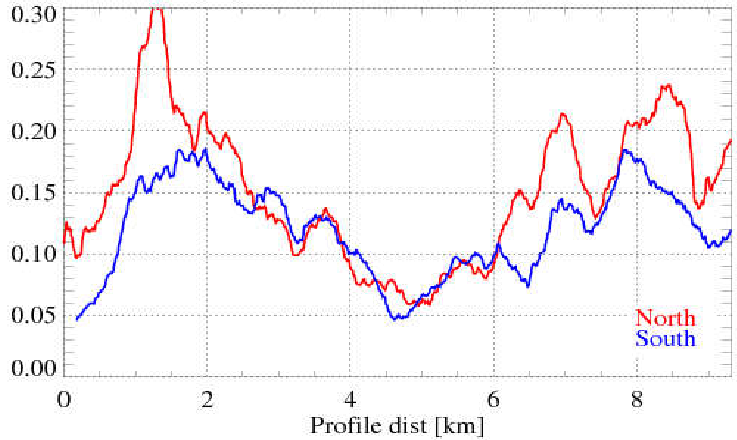

P-band $\sigma°$

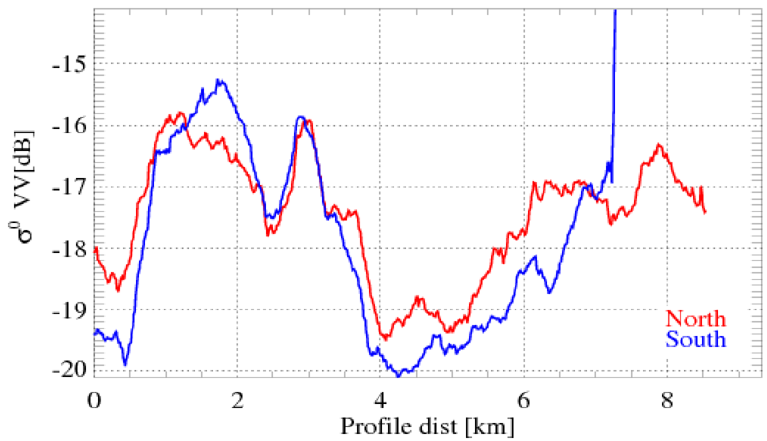

P-band κ_e

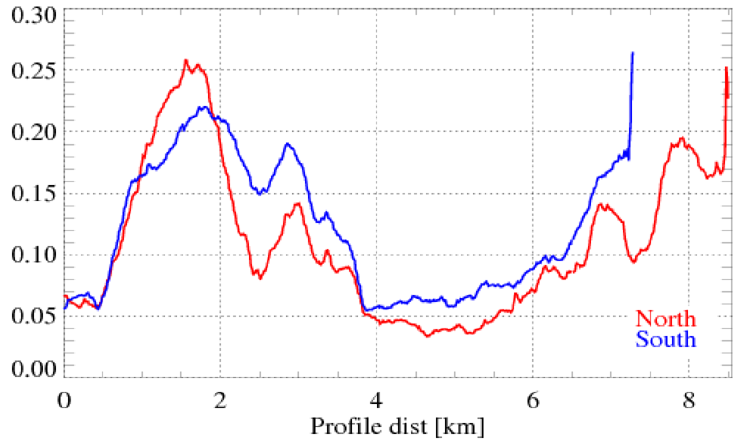

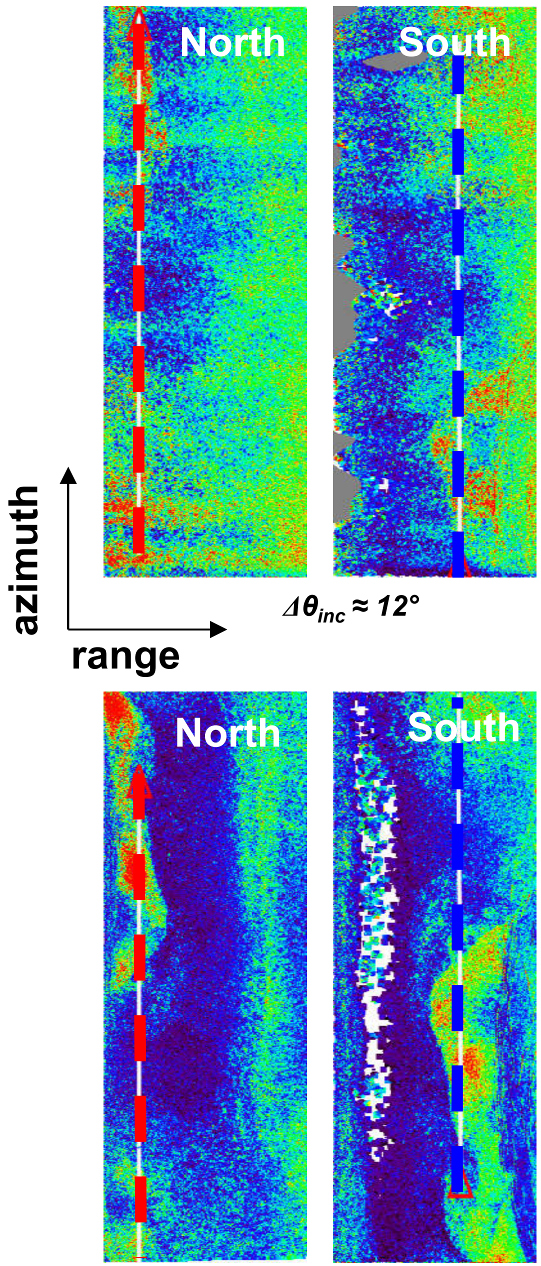

hajnsek@ifu.baug.ethz.ch
irena.hajnsek@dlr.de

First Validations of the Estimated Extinction Parameter

P-band Sounder vs. P-band Pol-InSAR (Summit)

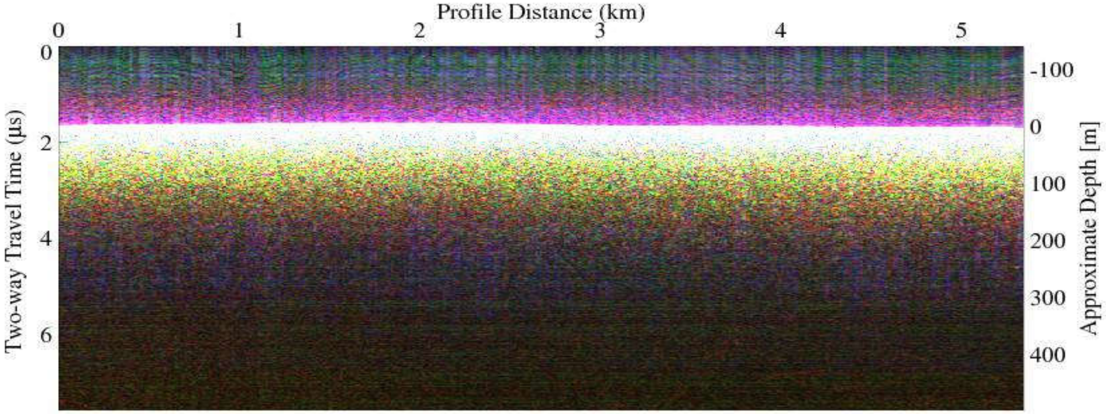

- σ^0_{SND} ***(sounder summed over depth)***
- κ_e ***(P-band Pol-InSAR extinctions)***

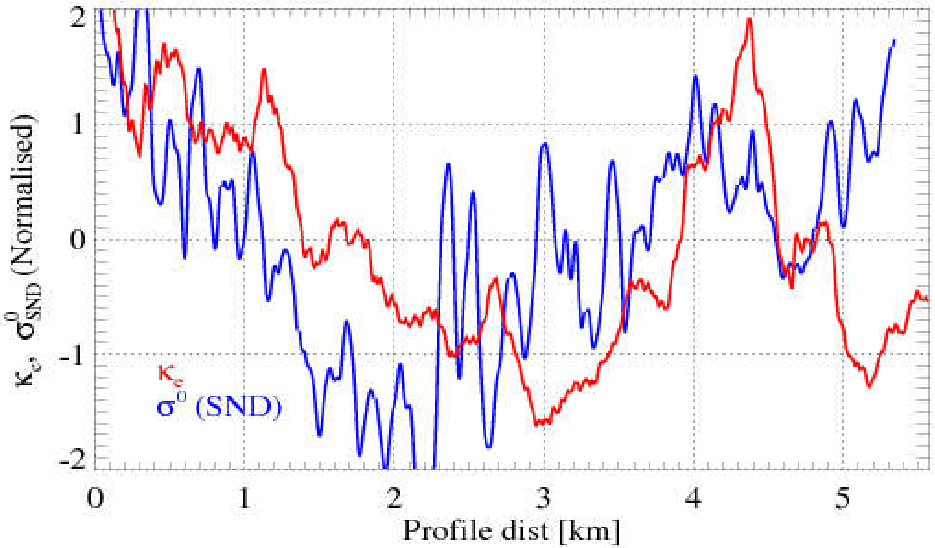

GPR (800 MHz) vs. L-band Pol-InSAR (Etonbreen)

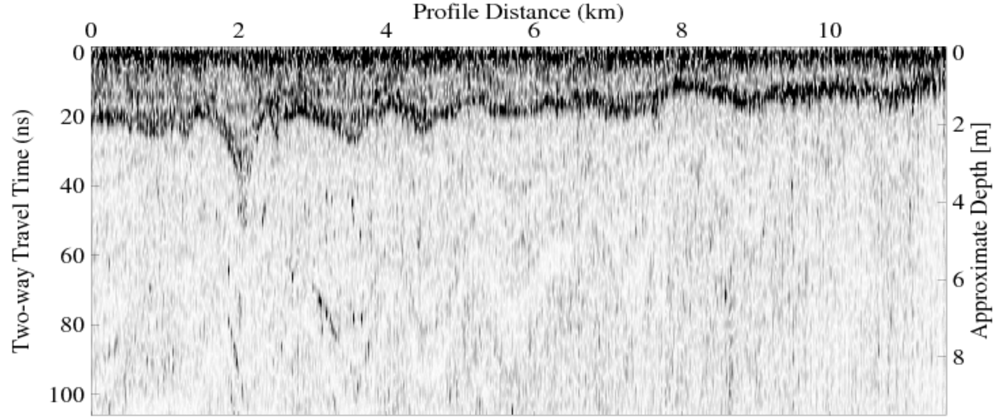

- σ^0_{GPR} ***(volume summed over depth)***
- κ_e ***(L-band Pol-InSAR extinctions)***